



THE HONG KONG
POLYTECHNIC UNIVERSITY

香港理工大學

Pao Yue-kong Library

包玉剛圖書館

Copyright Undertaking

This thesis is protected by copyright, with all rights reserved.

By reading and using the thesis, the reader understands and agrees to the following terms:

1. The reader will abide by the rules and legal ordinances governing copyright regarding the use of the thesis.
2. The reader will use the thesis for the purpose of research or private study only and not for distribution or further reproduction or any other purpose.
3. The reader agrees to indemnify and hold the University harmless from and against any loss, damage, cost, liability or expenses arising from copyright infringement or unauthorized usage.

IMPORTANT

If you have reasons to believe that any materials in this thesis are deemed not suitable to be distributed in this form, or a copyright owner having difficulty with the material being included in our database, please contact lbsys@polyu.edu.hk providing details. The Library will look into your claim and consider taking remedial action upon receipt of the written requests.

**EVALUATION OF THE EFFECT OF BEAM
ARRANGEMENTS AND ESTABLISHMENT OF
TREATMENT PLANNING MODELS IN INTENSITY
MODULATED RADIATION THERAPY OF HEAD AND
NECK CANCERS**

LEUNG WAN SHUN

PhD

The Hong Kong Polytechnic University

2021

The Hong Kong Polytechnic University

Department of Health Technology and Informatics

**Evaluation of the Effect of Beam Arrangements and
Establishment of Treatment Planning Models in Intensity
Modulated Radiation Therapy of Head and Neck Cancers**

Leung Wan Shun

A Thesis submitted in partial fulfilment of the requirements for the Degree of

Doctor of Philosophy

May 2020

CERTIFICATE OF ORIGINALITY

I hereby declare that this thesis is my own work and that, to the best of my knowledge and belief, it reproduces no material previously published or written nor material which has been accepted for the award of any other degree or diploma, except where due acknowledgement has been made in the text.

_____ (Signed)

Leung Wan Shun

(Name of student)

ABSTRACT

Introduction:

Intensity modulated radiotherapy (IMRT) has been the main treatment modality for many head and neck (H&N) cancers. This study aims to provide guidance for planners in the treatment planning of head and neck cancers treated by IMRT. The guidance refers to the suggestion of optimal beam arrangement, the feasibility to escalate tumour dose and the determination of reference dose to the organs at risk (OARs).

Methodology:

Study 1: 5 types of H&N cancers were included and a total 119 patients previously treated with IMRT were recruited. 5 plans of different beam arrangement methods were optimized for each case, including equal spaced beam (ESB), coplanar beam angle optimization (BAOc), non-coplanar beam angle optimization (BAOnC), 2 arcs volumetric modulated arc therapy (VMAT2) and 3 arcs volumetric modulated arc therapy (VMAT3). Apart from the dose volume parameters, a “figure-of-merit” known as uncomplicated target conformity index (UTCI) was used to rank the beam arrangement method in each type of cancers. ANOVA with repeated measures was used to rank the plans according to UTCI.

Study 2: 25 NPC cases (stage T3-4, N0-1) were recruited. With the same prescription of the planning target volumes (PTVs) and the planning goals of the OARs, 3 IMRT plans of different gross tumour volume (GTV) doses (76 Gy, 78 Gy and 80 Gy) were optimized using the BAOnC for each case. Paired sample T test was used to determine any statistical increase of OARs dose in the GTV dose between the dose escalated plans and the reference plan.

Study 3: 70 cases of NPC patients (45 in training dataset, 25 in validation dataset) were retrieved from the database of a local hospital and a hypothetical IMRT plan was computed for each patient. Multiple regression analysis was carried out using the OAR dose parameters as the dependent variables and the anatomical parameters such as the distance and the overlapping volume between the OARs and PTVs as the independent variables. External validity of the multiple regression models was evaluated using the validation dataset.

Results:

Study 1: All treatment plans met the dose requirements for the PTVs and OARs. The OARs for the evaluation included brain stem, spinal cord, lens, optic nerve, optic chiasm, eyeball, pituitary, parotid, cochlea, temporal lobe and brachial plexus. The UTICI favoured the use of BAO and VMAT methods. BAOnc offered the best chance for OARs sparing. However, if treatment time was included into consideration, VMAT plans would be recommended for cancers of nasopharynx (VMAT3), oral cavity and larynx (VMAT2).

Study 2: The dose to most OARs showed no statistical increase in the GTV dose escalated plans except lens, temporal lobe and pituitary. Despite the dose to temporal lobe and lens were increased, the dose did not exceed their tolerance even for the plans with GTV dose = 80 Gy. Only the pituitary gland demonstrated dose above its tolerance.

Study 3: A total of 11 multiple regression equations, one for each OAR dose parameter, were formulated. The adjusted R^2 value of the multiple regression models ranged from 0.916 for the brain stem to 0.436 for the lens. All multiple regression equations passed the validation to test the reliability of the standard error of the estimates except the eyeball and the lens.

Conclusion:

With regard to the optimal beam arrangement for H&N cancers treated by IMRT, VMAT was recommended for the cancer of nasopharynx, oral cavity and larynx; and BAOc for the cancer of maxillary sinus and parotid. In the dosimetric study for GTV dose escalation of NPC, most OARs tolerated the increased dose except the pituitary gland, which demonstrated dose beyond its tolerance in the GTV dose was escalated to 80 Gy. It is suggested that further study for more accurate case selection is needed, so that dose escalation will only be performed in those cases that weigh higher for the local control over the protection of pituitary gland. Lastly from the result of study 3, multiple regression models have been demonstrated to be able to determine reference OARs dose to guide the IMRT optimization.

PRESENTATIONS AND PUBLICATIONS

Conference Oral Presentations

1. Wan Shun Leung, Vincent Wing Cheung Wu. Dosimetric comparison of different beam arrangement in intensity modulated radiotherapy (IMRT) of maxillary sinus carcinoma. 20th Asia-Australasia Conference of Radiological Technologists, 2015. Singapore.
2. Wan Shun Leung, Vincent Wing Cheung Wu, Fuk Hay Tang, Ashley Chi Kin Cheng. Development of a model to produce reference parotid dose from anatomical parameters in IMRT of NPC. ESTRO 35, 2016. Turin, Italy.
3. Wan Shun Leung, Vincent Wing Cheung Wu, Clarie Yuen Wai Liu, Ashley Chi Kin Cheng. A Dosimetric Comparison of the Use of Equally Spaced Beam (ESB), Beam Angle Optimization (BAO) and Volumetric Modulated Arc Therapy (VMAT) in Head and Neck Cancers Intensity Modulated Radiotherapy. Hong Kong Radiographers and Radiation Therapists Conference, 2019. Hong Kong.

Paper Publications

1. Wan Shun Leung, Vincent Wing Cheung Wu, Clarie Yuen Wai Liu, Ashley Chi Kin Cheng. A dosimetric comparison of the use of equally spaced beam (ESB), beam angle optimization (BAO) and volumetric modulated arc therapy (VMAT) in head and neck cancers treated by intensity modulated radiotherapy. Journal of Applied Clinical Medical Physics. 20(11): 121-130; 2019.

ACKNOWLEDGMENTS

I would first like to thank my chief supervisor Dr Vincent Wu. Dr Wu is always helpful whenever I ran into a trouble spot or had a question about my research or writing. His every suggestion helped me to steer in the right direction, not only on the study but also in every aspect in the life of clinical practice and university teaching.

I would also like to thank the colleagues who were involved in the research project in the Department of Oncology, Princess Margaret Hospital: Dr Ashley Cheng, Chief-of-service; Ms Annie Yung, Department Manager; and Ms Clarie Liu, Senior Radiation Therapist. Without their passionate participation and the provision of treatment planning system for the radiotherapy planning, the project could not have been successfully conducted.

Finally, I must express my heartfelt gratitude to my parents and to my wife, Ellen, for providing me with unfailing support and continuous encouragement throughout my years of study and writing this thesis. This accomplishment would not have been possible without them. Thank you.

TABLE OF CONTENTS

CERTIFICATE OF ORIGINALITY	i
ABSTRACT	ii
PRESENTATIONS AND PUBLICATIONS	v
ACKNOWLEDGMENTS	vi
TABLE OF CONTENTS	vii
FIGURE LEGENDS	xiii
TABLE LEGENDS	xv
ABBREVIATIONS	xvii
Chapter 1 Literature Review	
1.1. Head and Neck Cancers	1
1.1.1. Statistics in Hong Kong	1
1.1.2. Investigations	2
1.1.2.1. Physical examination	2
1.1.2.2. Endoscopy	8
1.1.2.3. Medical imaging	9
1.1.3. Classification	12
1.2. Treatment of Head and Neck Cancers Using Radiotherapy	13
1.2.1. Nasopharynx	13
1.2.2. Oral Cavity	14

1.2.3.	Larynx	15
1.2.4.	Maxillary Sinus	16
1.2.5.	Parotid	17
1.3.	Intensity Modulated Radiotherapy (IMRT)	18
1.4.	IMRT Planning	19
1.4.1.	Target Delineation	21
1.4.2.	Organs at risk Delineation (OARs)	22
1.4.3.	Beam arrangement	23
1.4.3.1.	Equally Spaced Beams (ESB)	23
1.4.3.2.	Beam Angle Optimization (BAO)	23
1.4.3.3.	Volumetric Modulated Arc Therapy (VMAT)	25
1.4.4	Optimization Objectives and Procedures	26
1.4.5	Dose Constraints of Targets and OARs	27
1.4.6	Practical Difficulty of Optimizing a Radiotherapy Plan for Head and Neck Cancers	29

Chapter 2 Introduction

2.1	Treatment Planning of IMRT for Head and Neck Cancers	31
2.1.1	Challenges	31
2.1.2	Impact of Beam Arrangement	32
2.1.3	Dose Escalation in NPC	34
2.1.4	Organs at Risk (OARs) Dose Estimation	35

2.2	Figure of Merits in Plan Evaluation	36
2.3	Application of Regression Analysis in Radiotherapy Planning	43
2.4	Research Questions and Hypotheses	46
2.4.1	Research Questions	46
2.4.2	Research Hypotheses	46
2.5	Purpose of study	47
2.5.1	Aims	47
2.5.2	Objectives	47

Chapter 3 Study 1 – Dosimetric Evaluation of Beam Angles Arrangement Methods in IMRT of Head and Neck Cancers

3.1	Introduction	48
3.2	Materials and Methods	50
3.3	Results	55
3.4	Discussion	64
3.4.1.	Cancer of Nasopharynx	64
3.4.2.	Cancer of Oral Cavity	65
3.4.3.	Cancer of Larynx	66
3.4.4.	Cancer of Maxillary Sinus	66
3.4.5.	Cancer of Parotid Gland	67
3.4.6.	Comparison with Previous Literature	68
3.5	Conclusion	70

Chapter 4 Study 2 – Dosimetric Evaluation of Maximum Deliverable Dose to GTV in IMRT of Locally Advanced NPC using Non-coplanar Beam Arrangement

4.1	Introduction	71
4.2	Materials and Methods	73
	4.2.1. Patient Selection and Plan Specification	73
	4.2.2. Plan Evaluation and Statistical Analysis	76
4.3	Results	78
	4.3.1. Doses Delivered to PTVs, GTV, Spinal Cord and Brain Stem	78
	4.3.2. Doses Delivered to the Other OARs	79
4.4	Discussion	84
4.5	Conclusion	86

Chapter 5 Study 3 – Development of Regression Model to Determine Reference OARs Doses from Anatomical Parameters in IMRT Treatment Planning of Nasopharyngeal Cancer

5.1	Introduction	87
5.2	Materials and Methods	89
	5.2.1. Subjects Selection and IMRT Plans Specifications	89
	5.2.2. Generation of IMRT Plans	91
	5.2.3. Data Acquisition	93
	5.2.4. Multiple Regression Modelling	96
	5.2.5. Residuals Evaluation	97

5.2.6.	Model External Validation	98
5.3	Results	99
5.3.1.	Analysis of the Anatomical Parameters	99
5.3.2.	Establishment of Multiple Regression Models	101
5.3.3.	Parotid Gland	103
5.3.4.	Spinal Cord	103
5.3.5.	Brain Stem	103
5.3.6.	Optic Nerve	104
5.3.7.	Optic Chiasm	104
5.3.8.	Eyeball	104
5.3.9.	Lens	104
5.3.10.	Temporal Lobe	105
5.3.11.	Cochlea	105
5.3.12.	Brachial Plexus	105
5.3.13.	Residual Evaluation	105
5.3.14.	Model Validation	111
5.4	Discussion	112
5.5	Conclusion	115
Chapter 6	Discussion	
6.1.	Relationship and Novelty of the Studies	117
6.2.	Clinical Impacts and Practical Challenge in Implementation	119
6.3.	Limitations of the study	121

6.3.1. Exclusion of Partial-arc VMAT in the Beam Angle Arrangement	
Comparison	121
6.3.2. Lack of Clinical Results to Support the Suggested Dose Escalation	122
6.3.3. Clustering Feature in the Residuals of Multiple Regression	122
6.4. Future Directions	123
6.4.1. Evaluation of the Dosimetric Effect of 4pi VMAT in Head and Neck Radiotherapy Dose Escalation	123
6.4.2. Application of Radiomics to Selection of NPC Cases for Dose Escalation	124
6.4.3. Refinement of Models by LASSO Regression and Integration with Knowledge-based Radiotherapy Planning	125
Chapter 7 Conclusion	126
References	129
Appendices	141
Appendix 1. Ethics approval from the Hong Kong Polytechnic University	141
Appendix 2. Ethics approval from Princess Margaret Hospital, Kowloon West Cluster	142

FIGURE LEGENDS

Figure 1.1	Lateral view of the lymph node levels in the head and neck region.	3
Figure 1.2	Illustration of the technique and procedures of face and neck manual palpation.	4
Figure 1.3	Illustration of the relationship of beam intensity and target thickness.	19
Figure 1.4	Procedure of IMRT planning.	20
Figure 1.5	Part of the OAR delineation atlas.	22
Figure 1.6	User interface of BAO in Eclipse treatment planning system	24
Figure 1.7	User interface of Photon Optimizer.	26
Figure 1.8	Dose constraints setting of PTV.	28
Figure 1.9	Dose constraints setting of serial OARs	28
Figure 1.10	Dose constraints setting of parallel OARs	29
Figure 2.1	Field arrangement in 3DCRT affects the distribution of the prescribed dose.	33
Figure 2.2	Examples of different PTV coverage, homogeneity and conformity situations.	36
Figure 2.3	Classification of regression analysis	44
Figure 3.1	Diagram showing the dose distribution of the 5 types of H&N cancers using different beam arrangement methods.	56
Figure 3.2	Illustration of the coverage of tumour position variations by the five types of head and neck cancers.	69
Figure 4.1	Plan evaluation and statistical analysis procedure	78

Figure 5.1	Schematic diagram of the creation of pseudo-structures to optimize the dose to parotid glands.	93
Figure 5.2a	The normal probability plot for evaluation of residuals normality.	107
Figure 5.2b	The normal probability plot for evaluation of residuals normality.	108
Figure 5.3a	The scatterplot for evaluation of residuals homoscedasticity.	109
Figure 5.3b	The scatterplot for evaluation of residuals homoscedasticity.	110

TABLE LEGENDS

Table 1.1	Correlation of masses and their palpation characteristics.	5
Table 1.2	Name, function and foramina involved of cranial nerves.	7
Table 1.3	Part of TNM staging system for head and neck cancer.	12-13
Table 2.1	Components included in the calculation of different FOMs.	43
Table 3.1	The distribution of T and N stages of the selected patients.	51
Table 3.2	Comparison of PTVs, OARs dose parameters and integral dose between IMRT plans of 5 beam arrangements for cancer of nasopharynx (n = 25).	59
Table 3.3	Comparison of PTVs, OARs dose parameters and integral dose between IMRT plans of 5 beam arrangements for cancer of oral cavity (n=25).	60
Table 3.4	Comparison of PTVs, OARs dose parameters and integral dose between IMRT plans of 5 beam arrangements for cancer of larynx (n=25).	61
Table 3.5	Comparison of PTVs, OARs dose parameters and integral dose between IMRT plans of 5 beam arrangements for cancer of maxilla sinus (n=19).	62
Table 3.6	Comparison of PTVs, OARs dose parameters and integral dose between IMRT plans of 5 beam arrangements for cancer of parotid gland (n=25).	63
Table 4.1	Patient demographic.	74

Table 4.2	List of prescribed dose to the targets in the four hypothetical plans.	75
Table 4.3	Dose parameters for OARs and the local OARs tolerances guideline.	76
Table 4.4	GTV and PTV coverage, HI and CN.	80
Table 4.5	OARs dose parameters and integral dose between plans with different prescription.	81
Table 4.6	GTV minimum dose in all 25 recruited cases	82
Table 4.7	Paired sample t-test results.	83
Table 5.1	Subjects characteristics.	90
Table 5.2	Dose constraint protocol of PTV and OAR dose for IMRT of NPC.	91
Table 5.3	Dose parameters and anatomical parameters used for model training.	94
Table 5.4	Results of Pearson correlations between dose parameters and anatomical parameters	100
Table 5.5	Multiple Regression analysis	102
Table 5.6	Residual Independence evaluation	106
Table 5.7	Model Validation	111

ABBREVIATIONS

3DCRT	Three dimensional conformal radiotherapy
AAPM	Association of Physicists in Medicine
AJCC	American Joint Committee
API	Application programming interface
ASR	Age-standardized rate
BAO	Beam angle optimization
BAOc	Coplanar beam angle optimization
BAOnc	Non-coplanar beam angle optimization
BED	Biological equivalent dose
CN	Conformation number
CN I-XII	Cranial nerves
COSI	Critical organ scoring index
CT	Computed tomography
DVH	Dose-volume histogram
ESB	Equally spaced beam
FDG	Fluorodeoxyglucose
FOM	Figure of merit
GBM	Glioblastoma multiforme
gEUD	Generalized equivalent uniform dose
GTV	Gross tumour volume
H&N	Head and neck

HI	Homogeneity index
IMRT	Intensity modulated radiotherapy
LASSO	Least absolute shrinkage and selection operator
MLC	Multi-leaf collimator
MU	Monitor unit
NPC	Nasopharyngeal carcinoma
NTCI	Normal tissue sparing index
OARs	Organs at risk
PQI	Plan quality index
PTV	Planning target volume
PTVH	High risk planning target volume
PTVI	Intermediate risk planning target volume
PTVL	Low risk planning target volume
QA	Quality assurance
RFS	Relapse free survival
RMSE	Root mean squared error
ROI	Regions of interest
SE	Standard error
TCI	Target conformity index
TNM	Tumour/node/metastasis
UTCI	Uncomplicated target conformity index
VMAT	Volumetric modulated arc therapy

VMAT2	2 arcs volumetric modulated arc therapy
VMAT3	3 arcs volumetric modulated arc therapy

Chapter 1 Literature Review

This chapter aims to provide background information about the cancers included in this study, including their respective treatment options and radiotherapy techniques. It is divided into 4 parts. Part 1 summarizes the information about the head and neck cancers. Part 2 discusses the use of radiotherapy for the head and neck cancers. Part 3 introduces the intensity modulated radiotherapy (IMRT) which is commonly used in the treatment of head and neck cancers. Finally, part 4 reviews the planning techniques of IMRT.

1.1 Head and Neck Cancers

1.1.1 Statistics in Hong Kong

The head and neck cancers refer to the carcinomas that originate from any parts of the upper aero-digestive tract. They also include the cancers of the thyroid and salivary glands. Although head and neck cancers are no longer the top 5 leading cancers in Hong Kong in the most recent report (Hong Kong Cancer Registry, 2016), they are still regarded as major types of cancer in Hong Kong (Ng, Wong, Lee, Chan, & Lee, 2017). One of the main reasons for this recognition is that nasopharyngeal cancer (NPC) is ranked sixth in terms of the number of new cases in male population in Hong Kong (Hong Kong Cancer Registry, 2016). The NPC worldwide figures illustrated by the age-standardized rate (ASR) was 1.2 per 100,000 (Shield et al., 2017), which were much lower than the incidence in Hong Kong which was 7.4 per 100,000 in the year 2012 (Hong Kong Cancer Registry, 2016). The high incidence of NPC in Hong Kong is attributed to its special geographical epidemiology pattern that 76% of new cases were found in east and

south-eastern parts of Asia, in which Hong Kong is situated (Ferlay et al., 2018). Other head and neck cancers recorded in the Hong Kong Cancer Registry include cancers of lip, oral cavity, pharynx, nasal cavity, middle ear and accessory sinuses, larynx and thyroid gland. Altogether, There were 2617 new cases of head and neck cancers reported in 2016 in Hong Kong, which accounted for 8.3% of all cancer new cases (Hong Kong Cancer Registry, 2016). Among all the new cases of head and neck cancers, NPC was most common which accounted for 46.6%. It was followed by the cancer of tongue and larynx which accounted for 13.9% and 11.4% respectively (Hong Kong Cancer Registry, 2016). Although there were some variations in the trend of ASR of different sub-sites, the overall ASR of head and neck cancers in Hong Kong remained at about 21 per 100,000 in the past decade. Because of the relatively high incidence of head and neck cancers, their treatment remains as one of the major burdens in the health care services in Hong Kong (Ng et al., 2017).

1.1.2 Investigations

Diagnosis of head and neck cancers involves various investigation procedures including endoscopy, biopsy, blood test and imaging etc. (Chan et al., 2012). Among all these procedures, physical examination, endoscopy and medical imaging are most relevant to radiotherapy because they are important to confirm the extent of disease for the delineation of tumour and target volumes

1.1.2.1 Physical examination

Physical examination plays an important role in the investigation of head and neck cancer patients because it helps to detect superficial regional lymph nodes, abnormalities in the facial

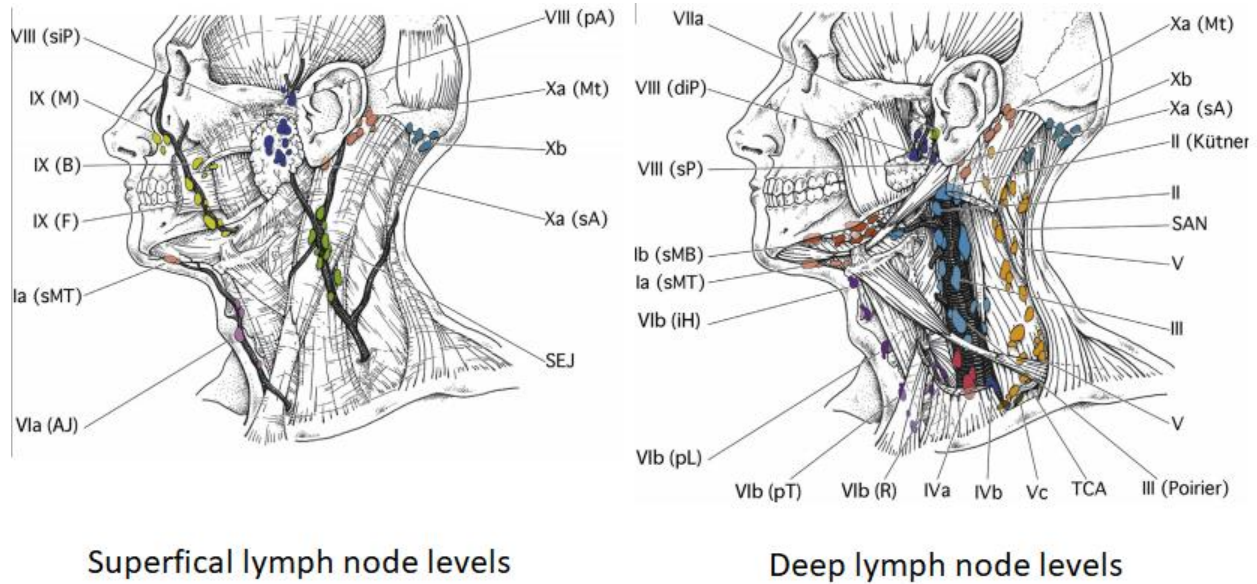


Figure 1.1. Lateral view of the lymph node levels in the head and neck region. Adapted from “Delineation of the neck node levels for head and neck tumors: A 2013 update. DAHANCA, EORTC, HKNPCSG, NCIC CTG, NCRI, RTOG, TROG consensus guidelines.” Copyright 2014 by Elsevier Ireland Ltd.

region and oral cavity. Superficial lesions and symptoms related to the cancer can be detected by visual inspection and manual palpation of the concerned anatomical regions (Hornig, Malin, & Oconnell, 2014). For example, physical examination of the neck can help to investigate the size, mobility and location of the involved lymph nodes. The palpated involved lymph nodes can be correlated with the lymph node levels as shown in Figure 1.1 (Gregoire et al., 2014).

In the facial region, the examination can look for gross asymmetry of facial structures, swelling and surface lesions (Hornig et al., 2014). Different types of palpable lesions have various palpation characteristics as listed in Table 1.1. These palpation characteristics can help the initial identification of the nature of any visualized swelling or masses (Eversole & Silverman, 2001). In addition, superficial organs including thyroid gland and salivary gland are also investigated in

the palpation process to look for any abnormalities. Procedures have been suggested for the comprehensive palpation of the superficial organs and lymph nodes as shown in Figure 1.2 (O'Donnell, 1962).

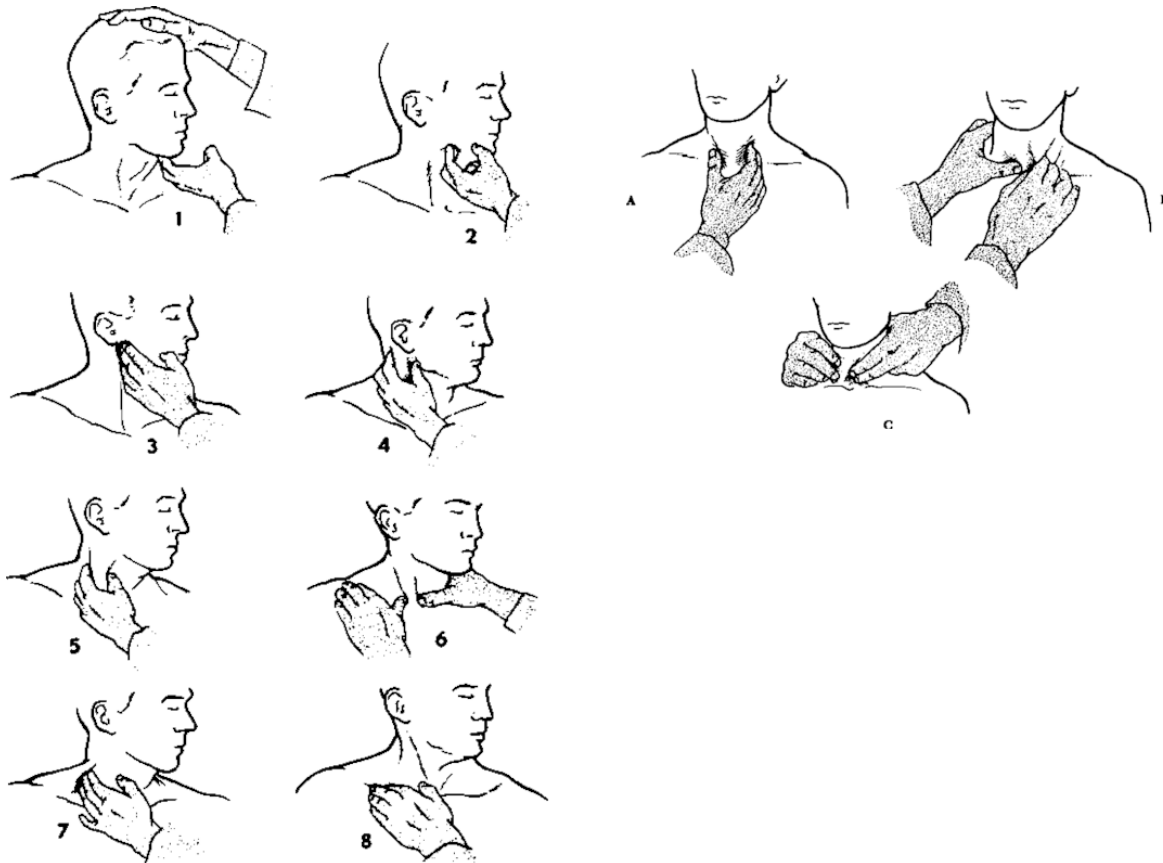


Figure 1.2. Illustration of the technique and procedures of face and neck manual palpation. 1-8: Palpation of superficial salivary glands and lymph nodes. A-C: Palpation of the thyroid gland. Adapted from "Early detection and diagnosis of cancer," by Walter E. O'Donnell, 1962. Copyright 1962 by C. V. Mosby Company.

Table 1.1. Correlation of masses and their palpation characteristics (Eversole & Silverman, 2001)

Palpation Characteristics	Mass
Soft, fluctuant	Mucocele, ranula Developmental cysts Sialocysts Gingival cysts Parulis Space infections and abscesses
Soft, nonfluctuant	Lipoma Fibroma Organized mucocele
Firm, movable	Mesenchymal tumours Granulomas Salivary adenomas Adnexal skin tumours
Firm fixed	Granular cell tumour Seborrheic keratosis Keratoacanthoma Fibromatosis
Indurated, fixed	Basal cell carcinoma Salivary adenocarcinomas Squamous cell carcinoma Melanoma Sarcomas lymphomas

Besides examination of the face and neck, intra-oral examination is another step in the physical examination. It involves the examination of a number of sub-sites in the oral cavity which includes the lips, buccal mucosa, alveoli, tongue, tonsils, roof and floor of mouth, and the visual inspection of the pharynx (Hornig et al., 2014; O'Donnell, 1962). Gross tumours or precancerous lesions can be found in the oral cavity mucosa in oral cavity cancer patients. Mucosal changes such as abnormal pigmentation, ulcerations and new growth are also investigated (Brockstein & Masters, 2003). The sub-sites in the oral cavity where these lesions mostly occur include the floor of mouth, buccal mucosa and tongue (Napier & Speight, 2008). To facilitate the visualization of

the oral cavity, tongue blades and head lights are usually used. The degree of trismus can also be assessed when patients are asked to open their mouths for examination.

Furthermore, physical examination can be used to detect the disease involvement of the cranial nerves (CN). CN examination is used to detect the symptoms of any CN palsy. It is important because cranial nerve involvement is common in locally advanced NPC, which accounted for 12-35% of all NPC patients (Turgut, Ertürk, Saygi, & Özcan, 1998). This occurs when the tumour invades the bony foramina in the skull base that the CN passes through. It was reported that the trigeminal nerve (CN V) and the abducent nerve (CN VI) were most frequently affected in these patients (S. F. Leung, Tsao, Teo, & Foo, 1990; J.-C. Li, Mayr, Yuh, Wang, & Jiang, 2006).

Different CNs serve different sensory or motor function, hence the cranial nerve examination aims to test their designated functions. Table 1.2 summarizes the names, functions and the clinical features involved of all cranial nerves.

Table 1.2. Name, function and foramina involved of cranial nerves.

Number	Name	Sensory Function	Motor Function	Clinical Features
CN I	Olfactory	Smell		Unilateral anosmia
CN II	Optic	Vision		Unilateral visual impairment
CN III	Oculomotor		Eyeball movement (up/down) & pupil contraction	Ptosis, eye deviated and diplopia due to muscle dysfunction; Dilated and irresponsive pupil
CN IV	Trochlear		Eyeball movement (infero-medial)	Eye motion disability and diplopia
CN V	Trigeminal	Sensory to lower 2/3 of face	Mastication	Partial facial numbness; Episodes of facial pain
CN VI	Abducent		Eyeball movement (lateral)	Eye motion disability and diplopia
CN VII	Facial	Sensory to cornea & taste	Facial expression	Hemifacial paresis; Abnormal taste
CN VIII	Vestibulocochlear	Hearing	Balance	Unilateral anosmia; Vertigo
CN IX	Glossopharyngeal	Taste	Pharynx & larynx	Loss of gag reflex; Abnormal taste
CN X	Vagus	Taste	Soft palate & vocal cords	Lass of soft palate elevation; Hoarseness of voice
CN XI	Spinal Accessory		Motor to trapezius & sternocleidomastoid muscle	Shoulder pain; Shoulder weakness
CN XII	Hypoglossal		Motor to tongue	Difficulty in speaking, chewing and swallowing due to tongue weakness

To test the CNs involvement based on their functions, clinical guidelines in the physical examination of cranial nerve involvement has been described (Damodaran, Rizk, Rodriguez, & Lee, 2014; Hurley, 2011). For example, the examination of the CN V involves the checking of both its sensory function and motor function. In general, the sensory response of the face is checked by comparing the sense of touch by cotton wool and pins in different parts of the face,

whereas the muscles of mastication are checked for their strength by the palpation of muscle bulk in contraction (Damodaran et al., 2014).

The findings in the physical examination contribute useful information in the diagnosis and staging of the disease. The results of physical examination can guide the oncologist to look for the relevant disease involvement regions in the medical images and therefore are supplementary to the results of medical images in making accurate diagnosis and staging for cancer patients.

1.1.2.2 Endoscopy

Endoscopy in the head and neck cancer investigations involves the use of fiberoptic instruments which pass through the nasal cavities into the airway. It is used to visualize the pharynx, larynx and any parts in the airway where physical examination cannot assess. It was reported in a study that more than 60% of the NPC patients employed endoscopy as the first diagnostic tool (K. H. Wang, Austin, Chen, Sonne, & Gurushanthaiah, 2017). It is because endoscopy has the benefit of short operation time and wide availability in clinics (M. Li et al., 2017). The reliability of the endoscopy is another reason for its wide application in which it was reported that the sensitivity, specificity and accuracy of endoscopy in the diagnosis of NPC were 88.7%, 97.5% and 93.3% respectively (Gao, Liu, Zhu, & Yi, 2014). Besides visualizing the airway, endoscopy is an important tool to obtain biopsy. In fact, it was suggested that the definitive diagnosis of NPC should be confirmed with the endoscopic biopsy in the primary tumour (Chan, Felip, & Group, 2008). The findings in the endoscopy contribute to the delineation of target volume because the gross tumour volume (GTV) should include all the macroscopic disease that is seen, palpated and imaged (Burnet, Thomas, Burton, & Jefferies, 2004). Although it has been suggested that the entire nasopharynx should be included in the high dose clinical target volume for the

radiotherapy of NPC regardless of the endoscopy findings (Sze, Ng, Yuen, Lai, & Ng, 2019), endoscopy remains to be the essential source of information in the GTV delineation of head and neck cancers (Mendenhall, Amdur, & Palta, 2006).

1.1.2.3 Medical Imaging

Many imaging modalities contribute to the diagnosis of head and neck cancers. In general, imaging in the head and neck cancers patients is important for the definition of tumour extent, the assessment of lymph nodes involvement and the evaluation of perineural spread (Rumboldt, Gordon, Bonsall, & Ackermann, 2006). These are important criterion for the delineation of target volume in radiotherapy. The common modalities include computed tomography (CT) and magnetic resonance imaging (MRI). Both CT and MRI are imaging modalities that provide sectional images with 3-dimensinal reconstruction. Each of them has their unique strengths and therefore can provide complementary information in the localisation of tumour and organs at risk.

Although both CT and MRI generate sectional images, their image generation mechanisms are not the same. The CT generates images using X-ray. By rotating the X-ray tube, a fan beam of X-ray is irradiated around the patients. After passing through the patient's body and being attenuated differentially by different body tissue with various densities, the X-ray detector receive many projections from the scanned body region. The computer then generates cross-sectional images based on the information gathered from the detected X-ray projections (Seeram, 1994). The resultant images are shown in grayscale according to the tissue density, which can be illustrated by appearing white for bone (high density), grey for soft tissue (medium density) and black for air (low density) (Seeram, 1994). In addition to the visualization of internal anatomy for

the diagnosis purpose, the grayscale which is derived from the CT numbers and the robust geometrical information make the CT images suitable to be used for the dose calculation in radiotherapy planning (R. P. Parker, 1979).

On the other hand, MRI works by detecting the reaction of the MR-active nuclei in different part of the body, mainly hydrogen, to the magnetic fields generated by the MRI machine (Grover et al., 2015). MR-active nuclei refer to the particles that have net spins of the protons and neutrons, which create magnetic fields on the nuclei (Bitar et al., 2006). These MR-active nuclei therefore react to the strong magnetic field applied by the MRI machine. The image formation is first done by the application of magnetic field to patients' body to align the spinning axis of the MR-active nuclei in the body tissue. Then, by the application of short pulses radiofrequency, the alignment is displaced and then relaxed. This procedure, called relaxation, leads to the release of energy detected by the receiver coil (Grover et al., 2015; Westbrook, 2019). The two main types of relaxation are longitudinal relaxation time (T1) and transverse relaxation time (T2). T1 determines the rate of the spinning axis of the MR-active nuclei to realign to the MRI machine magnetic field, while T2 determines the rate of the MR-active nuclei to lose phase from the alignment (Bitar et al., 2006). The detection of the energy released can then be processed by computers to generate the cross-sectional images. The differences of the relaxation time (T1 or T2) and the density of the nuclei contribute to the tissue contrast in MRI images (Bitar et al., 2006).

Utilization of both CT and MRI images in head and neck cancers is common because they are complementary to each other. In general, MRI is better in soft tissue contrast while CT is better in detecting bone erosion. For example, T1 weighted MRI images are the most suitable to

delineate NPC tumours because of better soft tissue contrast and more sensitive in detecting perineural extension of the tumour (Rumboldt, Castillo, & Smith, 2002). However, MRI images may fail to detect subtle skull base bone erosion, which can be complemented by coronary CT images in bone window (Sakata et al., 1999). Also, in the cancer of oral cavity, contrast enhanced T1 weighted MRI images are the best for the delineation of tumour margin (P. Lam et al., 2004), while CT images are useful for the detection of small lytic lesion in the cortical mandible (Mukherji et al., 2001).

Although being not a common modality in diagnosis of head and neck tumours due to its high cost, PETCT provides additional information to the commonly used CT and MRI images. The PETCT information is provided by the increase uptake of the fluorodeoxyglucose (FDG) in tumour cells than in normal cells because of their higher metabolic activity (Berger, 2003). The FDG uptake site can then be localized by scanners by detecting the radioactivity of the FDG. There are several circumstances that PETCT can provide supplementary information in addition to CT and MRI images. PETCT has been reported to have superior performance than CT and MRI in the detection of involved cervical lymph nodes. This is illustrated by the sensitivity of 90% and specificity of 94% in PETCT, compared with about 80% sensitivity and specificity in MRI and CT (Adams, Baum, Stuckensen, Bitter, & Hör, 1998). Also, PETCT is better in the detection of unknown primary tumour, which is essential to decide the treatment regimen (Kwee & Kwee, 2009). Furthermore, PETCT is useful in determining the presence of distant metastasis. It has the sensitivity and specificity of 89% and 95% respectively which indicates very accurate diagnosis of the metastatic stage of the disease (Xu, Guan, & He, 2011). In general, despite PETCT can provide supplementary information to the CT and MRI images, it is currently not

able to replace them in the target delineation in radiotherapy (Omami, Tamimi, & Branstetter, 2014).

1.1.3 Classification

The classification refers to the staging system of the head and neck cancers. The staging of the head and neck cancers is a very important guide to the treatment of choice for individual patients. The information from physical examination and image acquisition is incorporated to classify the disease into different stages. The staging system is commonly based on the American Joint Committee on Cancer (AJCC) (American Joint Committee on, 2017). The AJCC system classifies the cancer by the size, extent of the lymph node involvement and the status of distant metastasis by the tumour/node/metastasis (TNM) system. The definition of the TNM staging system is summarized in Table 1.3.

Table 1.3. Part of TNM staging system for head and neck cancer

Primary tumor (T)	
T1	≤ 2 cm in maximum dimension
T2	> 2 cm and ≤ 4 cm in maximum dimension
T3	> 4 cm in maximum dimension; or with minor bone erosion; or with perineural invasion / with deep invasion
T4a	With gross cortical bone; or marrow invasion
T4b	With skull base invasion; or with skull base foramen involvement
Clinical regional lymph nodes (N)	
NX	Cannot be assessed
N0	No regional lymph node involvement
N1	Single ipsilateral lymph node with greatest dimension ≤ 3 cm and no extranodal extension
N2a	Single ipsilateral lymph node with greatest dimension > 3 cm and ≤ 6cm and no extranodal extension
N2b	Multiple ipsilateral lymph node with greatest dimension ≤ 6cm and no extranodal extension
N2c	Single or multiple, bilateral or contralateral lymph node with greatest dimension ≤ 6cm and no extranodal extension
N3a	Any lymph node with greatest dimension > 6cm and no extranodal extension

N3b Any lymph node with extranodal extension

Distant metastasis (M)

cM0 No distant metastasis

cM1 With distant metastasis

cM1 Distant metastasis with pathology examination confirmation

1.2 Treatment of Head and Neck Cancers Using Radiotherapy

The role of radiotherapy in the radical treatment of five types of head and neck cancers including cancers of nasopharynx, oral cavity, larynx, maxillary sinus and parotid gland is discussed in this section. Intensity modulated radiotherapy is a standard radiotherapy technique used. The benefit of the use of IMRT is that it can deliver highly conformal dose to the target while spare the nearby organs at risk (OARs).

1.2.1 Nasopharynx

Radiotherapy is the main treatment modality for nasopharyngeal carcinoma (NPC). It is because the primary tumour site of NPC is difficult to be accessed by surgical intervention; and the tumour cells of NPC is sensitive to radiation (M. L. K. Chua, Wee, Hui, & Chan, 2016). The use of radiotherapy alone is effective to treat stage I to II NPC, while concurrent chemotherapy is added for higher stages disease to obtain better local regional control and survival outcome (A. W. Lee et al., 2015). IMRT is the preferred radiotherapy technique because it has shown to have better overall survival and less side effect when compared with the other conventional techniques in external beam radiotherapy such as the three dimensional conformal radiotherapy (3DCRT) (Zhang et al., 2015). This is concurred by the report stating that the overall survival has been improved from 81% in 3DCRT to 85% in IMRT (A. W. M. Lee et al., 2014), and the late side effect of xerostomia in patients receiving IMRT was significantly reduced (Kam et al., 2005).

The current standard of the prescribed total dose to the primary tumour is to give 70 Gy in 33 – 35 fractions (Sze et al., 2019). With the use of simultaneous integrated boost, the prophylactic dose which is lower than the dose to the primary tumour is prescribed for potential microscopic spread of the primary tumour and selected cervical lymph nodes regions. The prophylactic prescription can be varied in different local practices, it was reported that the prescriptions for the intermediate and low risk cervical lymph nodes were about 60 Gy and 50 Gy respectively (Chan et al., 2008; Sze et al., 2019).

1.2.2 Oral Cavity

The cancer of oral cavity includes various sub-sites such as the anterior tongue, buccal mucosa, hard palate, soft palate, alveolus and floor of mouth. The primary treatment of the cancer of oral cavity varied according to stage, which can be briefly divided into early and advanced. For early stage which refers to T1 and early T2 tumour, radiotherapy entirely or partly delivered by brachytherapy can result in similar local control as in surgery (Barrett & Dobbs, 2009; Mazeron et al., 2009). However, a recent retrospective study reported that primary radiotherapy to early stage oral cavity cancer patients resulted in higher mortality as compared with those who received primary surgery (M. A. Ellis et al., 2018). It has also been reported in the same article that majority (more than 95%) of early stage oral cavity cancer patients received primary surgery. The small proportion of patients receiving primary radiotherapy in this group of patients was attributed by the fact that brachytherapy services were not available due to lack of expertise and suitability of applicator for insertion (Barrett & Dobbs, 2009). Hence, most early stage oral cavity cancer patients receive surgery for primary treatment, although radiotherapy is also an

alternative. Post-operative radiotherapy is only indicated for positive or close margins after resection (Fridman et al., 2018). For advanced oral cavity cancer, surgery is often the standard primary treatment whenever resectable (Budach et al., 2016), and then followed by adjuvant radiotherapy or chemo-radiotherapy. For non-resectable advanced oral cavity cancer, radical radiotherapy is offered in conjunction with chemotherapy or targeted therapy to improve the disease control (S. H. Huang & O'Sullivan, 2013). IMRT is used in the radiotherapy of oral cavity cancer and has shown superior outcome over 3DCRT. It has been reported that the 2-year local control was improved from 70% (3DCRT) to 92% (IMRT) in the post-operative radiotherapy of advanced disease (Studer, Zwahlen, Graetz, Davis, & Glanzmann, 2007). The total prescribed dose is 70 Gy to the gross tumour or 66 Gy to the tumour bed after resection, delivered with 2 Gy per fraction. Similar to NPC, prophylactic irradiation to the cervical lymph nodes regions is also used, where 60 Gy and 54 Gy are prescribed to the intermediate risk and low risk regions respectively (Gomez et al., 2009)

1.2.3 Larynx

The specific consideration in the choice of treatment in the cancer of larynx is organ and function preservation. Radiotherapy alone or concurrent chemoradiotherapy is the most widely applied approach in organ preservation therapy (Pfister et al., 2006). Radical surgery is the rival choice for the patients, the outcome would lead to sub-optimal quality of life because it would result in loss of voice, swallowing problem and often a permanent tracheostomy. To achieve better quality of life after treatment, organ preservation therapy using radiotherapy or chemoradiotherapy is recommended for early stage disease and some advanced cases of T3 and T4 (Bhalavat, Fakhri, Mistry, & Mahantshetty, 2003; Pfister et al., 2006). The consideration of offering surgery instead

of radical chemoradiotherapy for advanced cases include patients' condition and the extent of the disease, and should be assessed by an expert panel of clinicians from different disciplines (Timme, Jonnalagadda, Patel, Rao, & Robbins, 2015). Even when surgery is chosen as the treatment option, radiotherapy still has the role in providing post-operative adjuvant treatment for high grade tumours, positive margins, cervical lymph nodes involvement and tumour invasion beyond larynx (Skora et al., 2015). IMRT is the preferred technique in the radiotherapy of laryngeal cancer, unless for cases of T1 and T2 glottic cancer when prophylactic irradiation to the neck is not indicated. In T1 and T2 glottic cancer, when the treatment target is limited to the primary tumour, the use of 3DCRT can achieve 5-year local control of more than 95% with limited toxicity (Jones et al., 2010). However, in more advanced disease, IMRT is advocated for better local control and less severe toxicity such as xerostomia (Daly et al., 2011). The prescribed dose ranged from 66 Gy to 76 Gy to the primary tumour site and involved lymph node; and the prescription for the selective lymph node with suspected microscopic involvement is at least 50 Gy (Anonymous, 1991).

1.2.4 Maxillary sinus

Although the primary treatment of the cancer of maxillary sinus is surgery, post-operative radiotherapy is indicated for stage 2 and stage 3 disease, and for stage 1 disease when the surgical margin is insufficient (Bristol et al., 2007). For locally advanced disease, induction chemotherapy and then concurrent chemoradiotherapy have been suggested for non-resectable patients (Won et al., 2009). The treatment outcome for these patients would be better if the tumour can be down-staged and subsequent resection is possible (Won et al., 2009). The concern

of the radiotherapy to the maxillary sinus includes the preservation of the optic apparatus which are near to the tumour (Bristol et al., 2007). It has been reported that the radiotherapy induced blindness in 37% of the patients who received conventional radiotherapy (Katz et al., 2002). IMRT is the preferred technique because it has been reported to be significantly better in sparing the nearby organs than those in 3DCRT. This was demonstrated by the report that the dose to the optic chiasm can be significantly decreased from over 60 Gy in 3DCRT to less than 40 Gy in IMRT (D. Huang et al., 2003), while the tumour coverage by the prescribed dose is increased from 83% in 3DCRT to 95% in IMRT. The prescribed dose to the primary tumour site ranged from 66 to 70 Gy.

1.2.5 Parotid gland

The primary treatment for the cancer of parotid gland is surgical resection. Radiotherapy is used for adjuvant post-operative treatment except in small and low histological risk tumour with clear surgical margins (Adelstein, Koyfman, El-Naggar, & Hanna, 2012). In addition, radiotherapy is also indicated as radical treatment in advanced parotid gland cancer cases when resection of the tumour is not possible (Spratt et al., 2014). The prescribed dose to the primary site is about 66 Gy. IMRT is advocated as the treatment technique to improve OARs sparing (Schoenfeld et al., 2012). Although study on the comparison of IMRT and 3DCRT in terms of treatment outcome is limited, report has suggested that the 3-year local control of the post-operative adjuvant IMRT to be 92%, while acute grade 3 mucositis occurred only in 8% of the cohort (Schoenfeld et al., 2012).

1.3 Intensity Modulated Radiotherapy

As discussed in the previous section, IMRT is commonly used for radiotherapy of head and neck cancers because of its superior dosimetric outcome, as compared to conventional treatment, to deliver conformal and homogeneous dose to the targets while sparing the OARs. The concept of IMRT has been introduced as early as thirty years ago (Anders Brahme, 1988), when the method of optimizing the intensity distribution of the incident beams with the purpose to achieve the required dose distribution in the targets was described. The following points summarize the concept of the delivery of IMRT: 1. There are multiple radiation beams with specially decided non-uniform intensity in beamlets, also known as intensity modulation. 2. The multiple radiation beams are applied from different directions, and the region of the convergence of the beams can achieve the desired dose distribution based on the modulated beam intensity. 3. Calculation of the modulated beam intensity usually follows an inverse approach, in which the final dose distribution indicated by planners is used by the computer to calculate the intensity of each beamlets in the treatment field of IMRT plan.

The delivery of intensity modulated beams is largely contributed by the dynamic multi-leaf collimator (MLC). The MLC can change the field shape automatically and the summation of numerous sub-fields in different shapes then generate a field with intensity modulation. A simplified rationale of intensity modulation is illustrated in Figure 1.3. Assume there is no OAR surrounding the target, the intensity of the beam should be proportional to the target thickness from the perspective of each beam. Although beam modifying devices such as wedges and compensators have been used in 3DCRT, their flexibility of beam intensity modification is far less than that in the IMRT. This is best illustrated by the fact that IMRT can produce concave

shape isodose distribution which 3DCRT can hardly generate. The freedom of intensity modulation has great impact on the dosimetric superiority of IMRT, in which better target coverage and less dose to the OARs can be achieved.

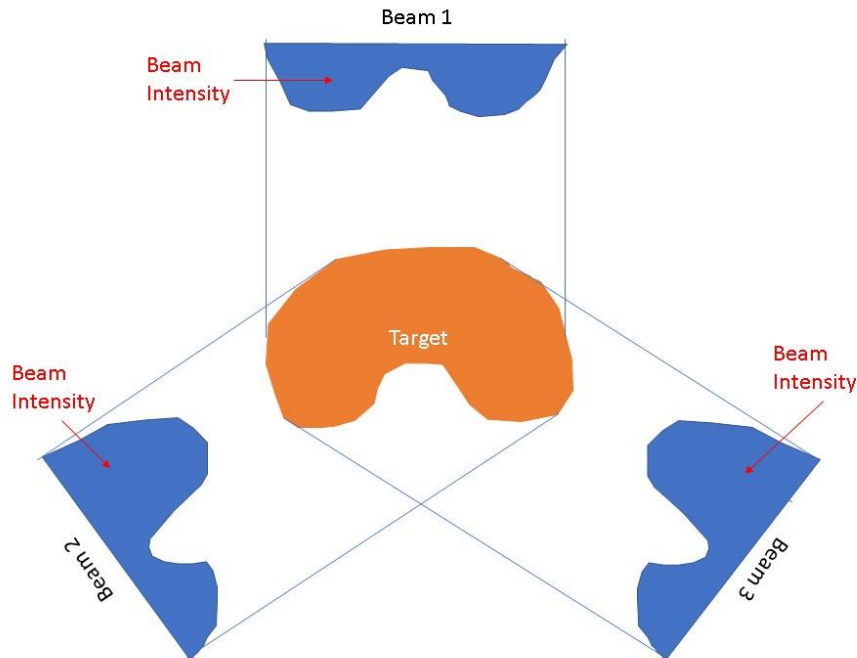


Figure 1.3 Illustration of the relationship of beam intensity and target thickness.

1.4 IMRT Planning

To achieve the dosimetric superiority of IMRT described in the last section, the planning procedure adopts an inverse approach. The inverse planning is a process to determine the optimal beam intensity. Numerous inverse planning approaches have been proposed and they can be classified as dose-volume based or biological index based (Chui & Spirou, 2001). In this study, the dose-volume based approach of the inverse planning is used and is the focus in this section. The inverse planning procedure starts with the delineation of the regions of interest (ROI) which

includes the PTV and OAR, followed by the beam configuration, objective function setting and computer optimization. The workflow of IMRT planning is illustrated in Figure 1.4.

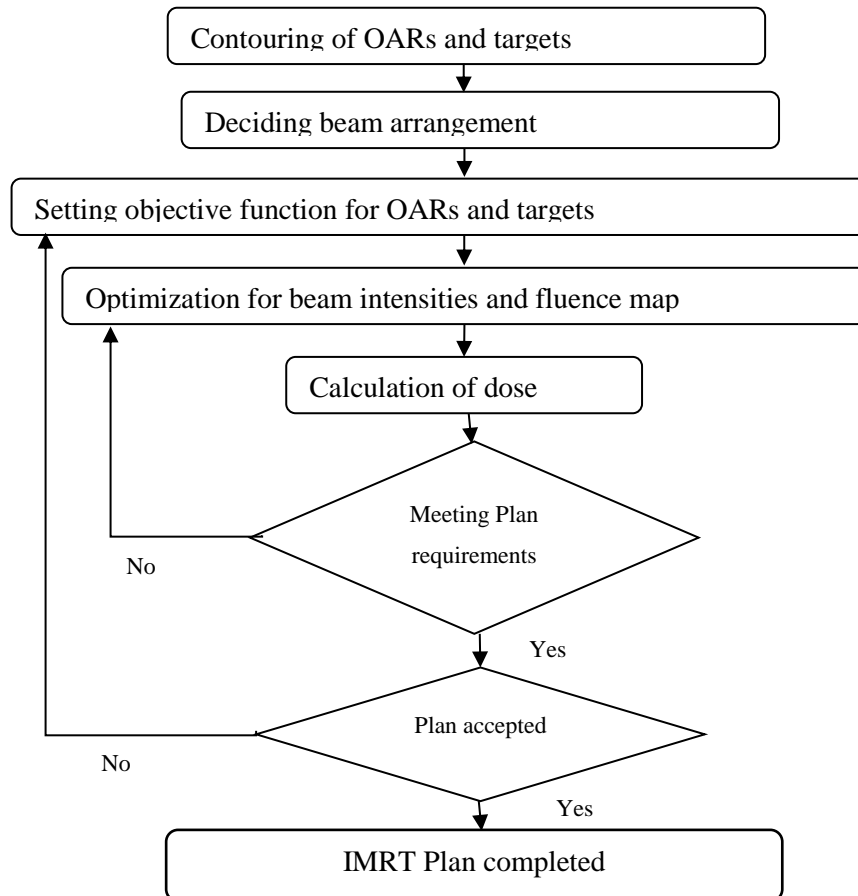


Figure 1.4. Procedure of IMRT planning

The procedures which require human input, including the setting of ROI delineation, beam configuration and objective function, and evaluation of the plan are further discussed in the following sections.

1.4.1 Target Delineation

The delineation of targets in head and neck cancers includes the high-risk, intermediate-risk and low-risk planning target volume (PTV) (Elicin et al., 2017). The intermediate-risk PTV refers to the regional lymph nodes and the isotropic margins of the high risk PTV, the low-risk PTV refers to selective negative lymph nodes for prophylactic treatment, and the high risk PTV encompasses the primary tumour or tumour bed and the positive lymph nodes. The consensus guideline on the delineation of elective lymph nodes levels is well-established (Gregoire et al., 2014). The guideline classifies the regional lymph nodes in the head and neck region into 10 levels and defines their anatomical boundaries. While the selection of lymph nodes levels to be treated largely depends on different oncologists' judgement and individual patients' condition, there has been published guidelines to review the criteria for the lymph nodes levels selection for treatment in different types of head and neck cancers (Eisbruch, Foote, O'Sullivan, Beitler, & Vikram, 2002; Gregoire et al., 2014). Contrary to the well-established consensus in the delineation of PTV for the regional lymph nodes, the high risk PTV delineation technique varies among oncologists. It can either be based on isotropic expansion of the gross tumour volume or inclusion of anatomical sub-sites (Elicin et al., 2017). The method of isotropic expansion to form PTV and the margins needed has been described (Antolak & Rosen, 1999). The aim of the margins is to account for the uncertainties in the delivery of radiation to avoid target miss. On the other hand, the aim of the inclusion of anatomical sub-sites in the high risk PTV in addition to the gross tumour volume is to include regions with possible microscopic extension (Eisbruch et al., 2002). Due to the high level of variability, the target delineated by oncologist in this study was reviewed by at least one other oncologist to obtain consensus.

1.4.2 Organs at Risk Delineation

Inverse planning of IMRT involves the estimation of OAR dose for the calculation of the beam modulated intensity. The accuracy of the OARs delineation is crucial for the estimation of OARs dose, and hence the inverse planning procedure. There has been consensus guideline on the OARs delineation in the head and neck regions (Brouwer et al., 2015). This guideline listed the anatomical boundaries of 25 OARs in the head and neck region for the purpose of consistency in the delineation. Detailed atlas has also been supplemented for reference. Figure 1.5 shows part of the atlas provided by the guideline

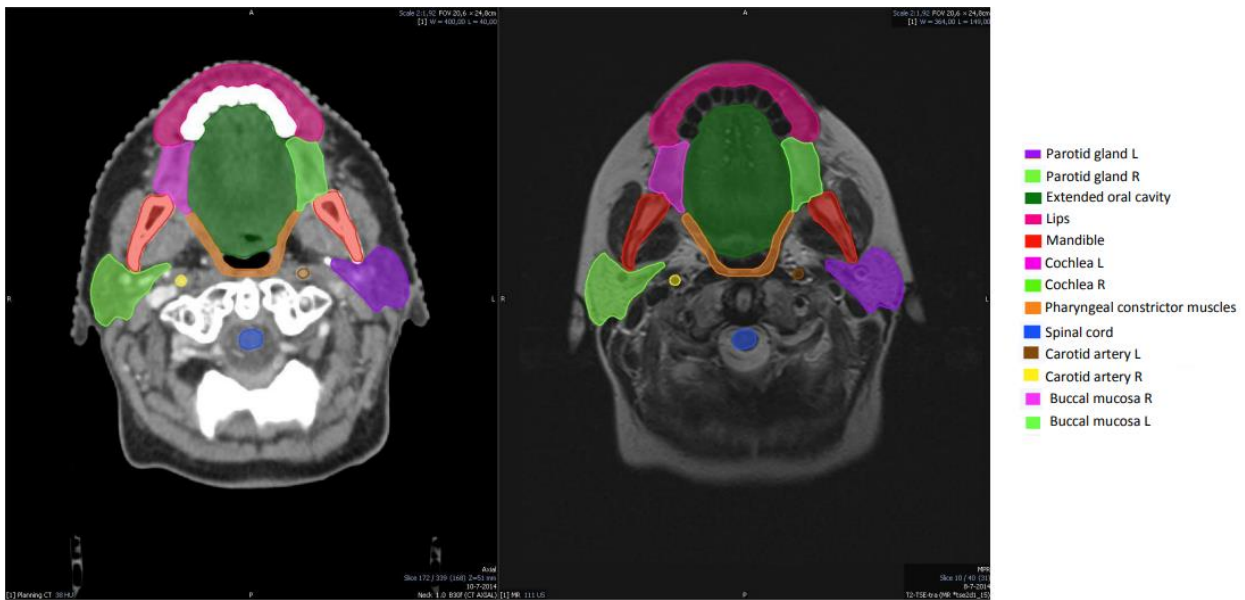


Figure 1.5. Part of the OAR delineation atlas. Adapted from “CT-based delineation of organs at risk in the head and neck region: DAHANCA, EORTC, GORTEC, HKNPCSG, NCIC CTG, NCRI, NRG Oncology and TROG consensus guidelines” by Brouwer et al., 2015. *Radiotherapy and Oncology*, 117 (1), 83-90. Copyright 2015 The Authors

1.4.3 Beam Arrangement

In the early application of IMRT, equally spaced beam arrangement was commonly used (Gupta et al., 2012; Vlachaki, Teslow, Amosson, Uy, & Ahmad, 2005). There are two other beam arrangement options available in the Eclipse treatment planning system (Varian Medical System, Palo Alto, USA). These include volumetric modulated arc therapy (VMAT) that enables rotational beams, and beam angle optimization (BAO) that automatically chooses optimal static beam angles in either coplanar or non-coplanar beam arrangements.

1.4.3.1 Equally Spaced Beams (ESB)

The delivery of IMRT requires several beams to achieve the assigned dose distribution (Anders Brahme, 1988). It has been a common practice to use the 5-9 beams arrangement in IMRT for head and neck cancer (Ahmed, Hansen, Harrington, & Nutting, 2009; Gupta et al., 2012).

Although theoretically greater number of beams can have higher chance to achieve the planned dose distribution, it increases the time for delivery and quality assurance. Hence, effort should be put to minimize the number of beams to use. Another concern in the beam placement is that opposing beam should be avoided in IMRT because it reduces the effectiveness of the optimization (Soyfer et al., 2012). Furthermore, it has been calculated that the optimal number of beams is 7 – 9 after striking a balance between the gain in dose distribution and the expenses of treatment time in further addition of beams (Webb, 1994).

1.4.3.2 Beam Angle Optimization (BAO)

Selecting optimal beam orientations can help to improve the dose distribution in complex plans (Stein et al., 1997). BAO is a function available in the Eclipse treatment planning system that a built-in algorithm can automatically choose the optimal beam arrangements in static beam IMRT.

The mechanism of selecting the beams is by elimination of beams from up to 400 pre-assigned beams orientations. Then, the calculation of fluence optimization iterations can help to eliminate the beams that cause the least contribution to the pre-set objective functions until the number of desired beams is reached. Planners must customize the resulting number of beams, coplanar or non-coplanar arrangement and the number of initial beams. Also, objective functions for each target volumes and OARs must be set beforehand for the purpose of fluence optimization in the beam elimination process. The user interface of BAO is shown in Figure 1.6.

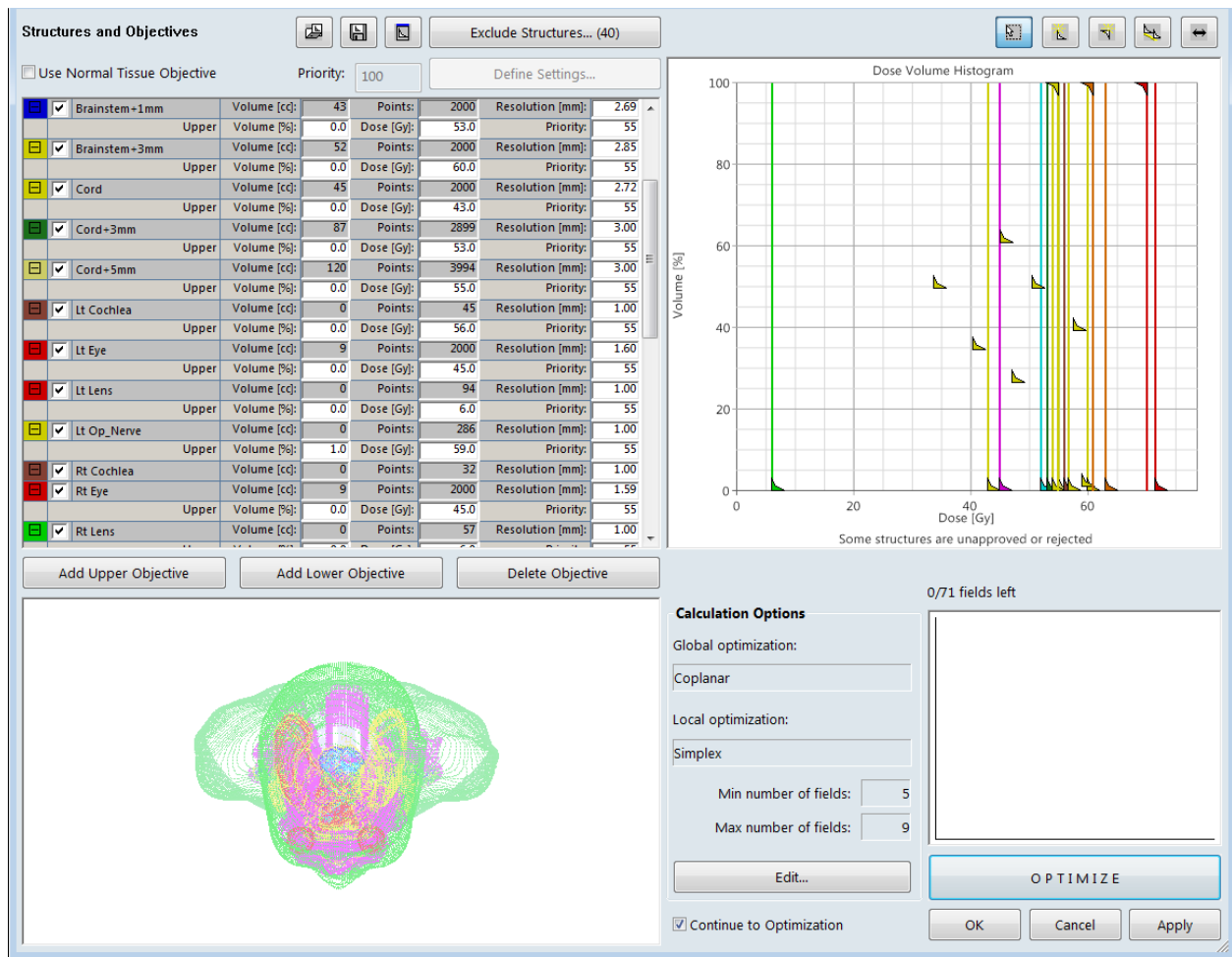


Figure 1.6 User interface of BAO in Eclipse treatment planning system

1.4.3.3 Volumetric Modulated Arc Therapy (VMAT)

VMAT is a technique that enables delivery of IMRT in one or more rotations of the linear accelerator gantry. The delivery time is shorter than static gantry methods while maintaining at least comparable dosimetric quality (Vanetti et al., 2009). It is done by simultaneous modulation of gantry speed, dose rate and position of multi-leaf collimator (MLC) while the gantry is rotating round the patient during treatment. The optimization of VMAT plan is done on the same user interface as fixed beam IMRT plan, which is the Photon Optimizer in the Eclipse treatment planning system. While individual fluence map for the beam intensity modulation is optimized for the fixed beam IMRT, the VMAT optimization considers the full rotation of the gantry by dividing into 178 equally spaced control points (Vanetti et al., 2011). Assuming that the radiation from each control points is delivered from a static gantry, the optimizer then generates the information of the gantry speed, MLC position and dose rate altogether for the dose distribution calculation. The Photon Optimizer user interface for the optimization of IMRT in Eclipse treatment planning system is shown in Figure 1.7.

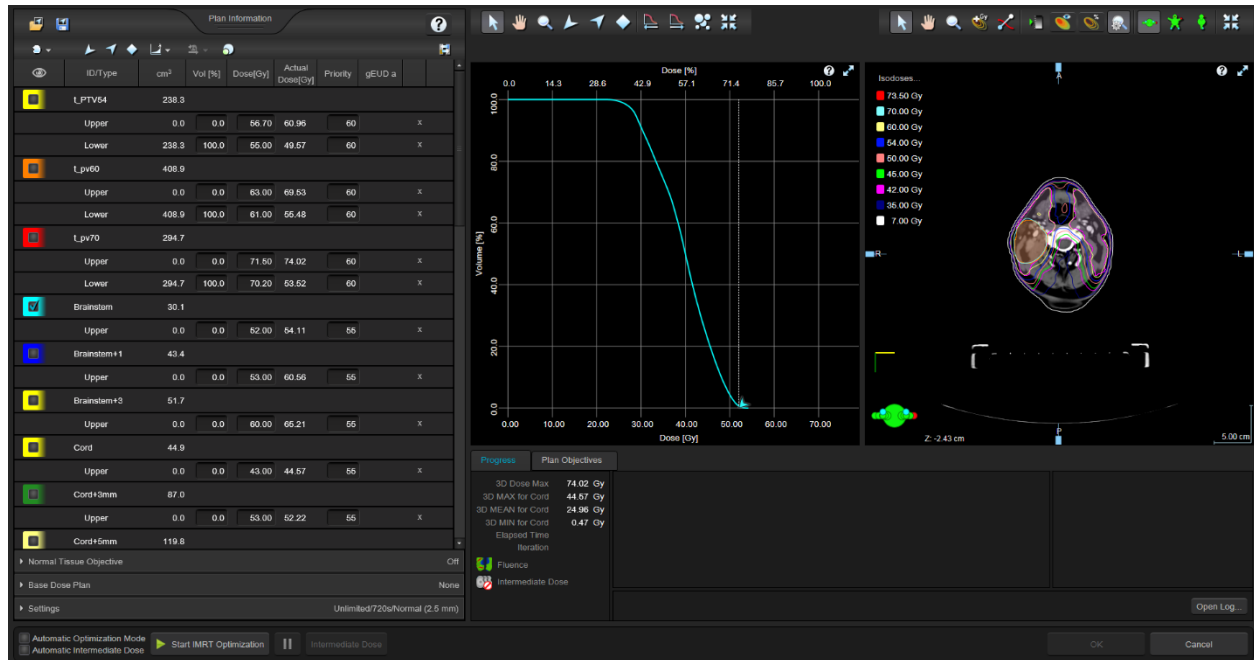


Figure 1.7. User interface of Photon Optimizer.

1.4.4 Optimization Objectives and Procedures

Setting of dose objective is a crucial step in inverse planning because it defines the doses to be delivered to various delineated structures. The computer then calculates the intensity modulation of the treatment field based on the definition of dose objectives (Cho, 2018). While both dose-volume based objectives and biological objectives can be input in current commercially available system, only dose-volume based objectives were used in this study. This is because it has been demonstrated that the use of generalized equivalent uniform dose (gEUD) objectives would lead to poorer homogeneities (Qiuwen, 2003). Inverse planning was first proposed in 1982 (A. Brahme), in which the dose distribution was defined by planners for the calculation of beam intensity to deliver the desired dose. It is an “inverse” process when compared with the conventional “forward” approach, in which the planners define beam parameters for the calculation of dose distribution (Cho, 2018). There are upper objective, lower objective and mean

objective in the definition of dose-volume based objectives for a structure. A priority number is assigned for each objective to indicate their relative importance. Because the objectives to achieve target dose coverage and to avoid dose to OARs sometimes oppose to each other, the setting of priority provide information for the computer system to decide the “trade-off” between conflicting objectives.

1.4.5 Dose Constraints of Targets and OARs

In general, there are 3 types of dose constraints settings before the optimisation. They are the PTVs, serial OARS and parallel OARs respectively. For the PTV, it requires the setting of at least one upper objective and one lower objective as shown in Figure 1.8. The resultant dose-volume histogram (DVH) should show that the majority of the PTV receives the desired dose with little volume receive the higher dose, and the shape should look like a plateau at 100% volume with an extremely steep cliff at the end when it reaches the prescribed dose.

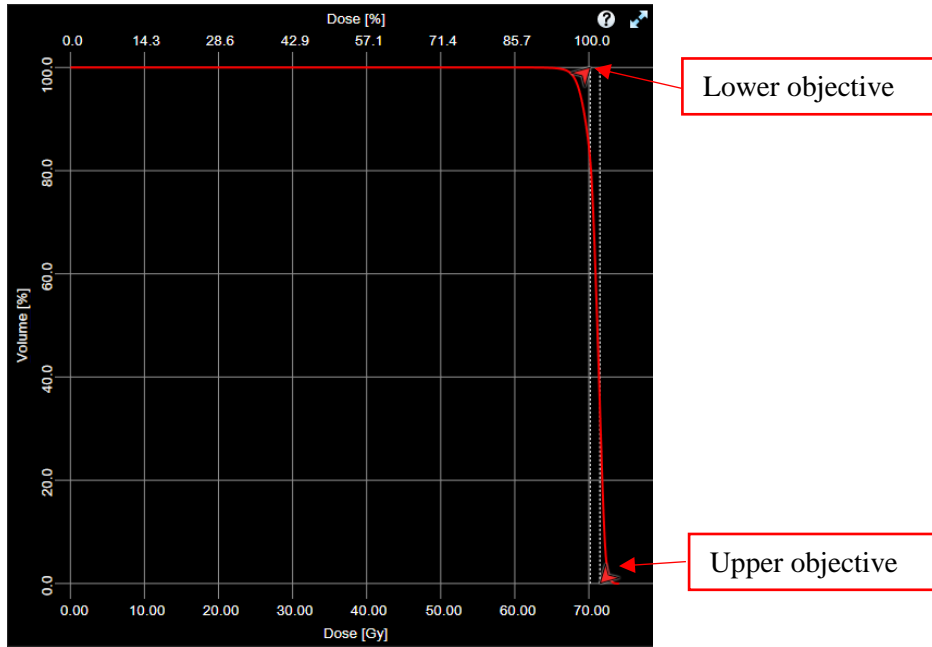


Figure 1.8 Dose constraints setting of PTV

The dose constraints setting for serial OARs only requires an upper objective to limit its maximum dose, as shown in Figure 1.9.

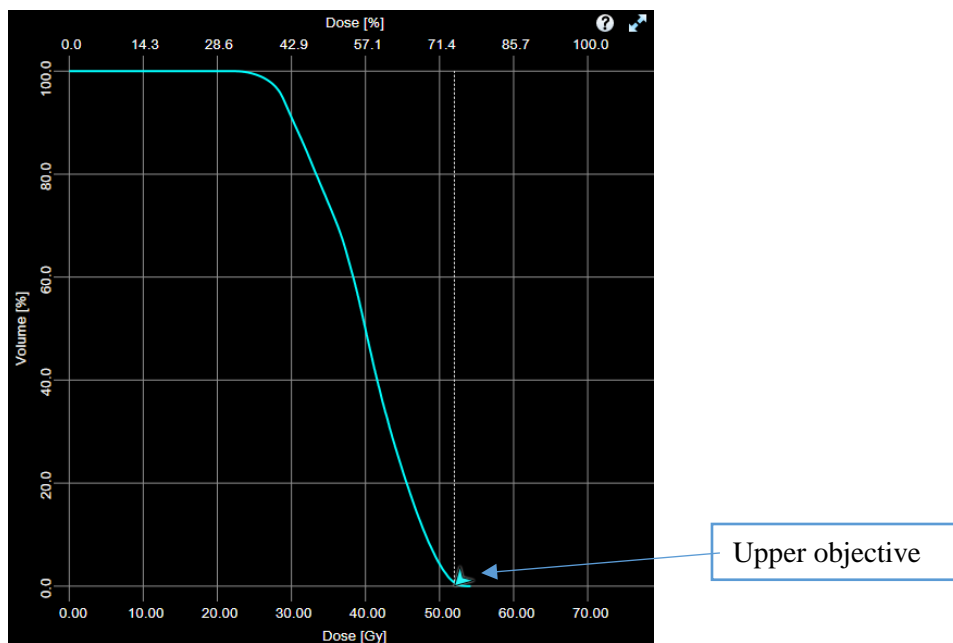


Figure 1.9 Dose constraints setting of serial OARs

For parallel OARs, since the dose received by various proportion of volume is the concern for late side effects, setting of upper objectives to limit the maximum dose is not enough. It can be done by setting multiple upper objectives at different dose volume levels or setting the mean objectives. The purpose is to limit the received dose at all volume level and to push the DVH to its left end as much as possible. A sample objective setting for a parallel OAR is shown in Figure 1.10.

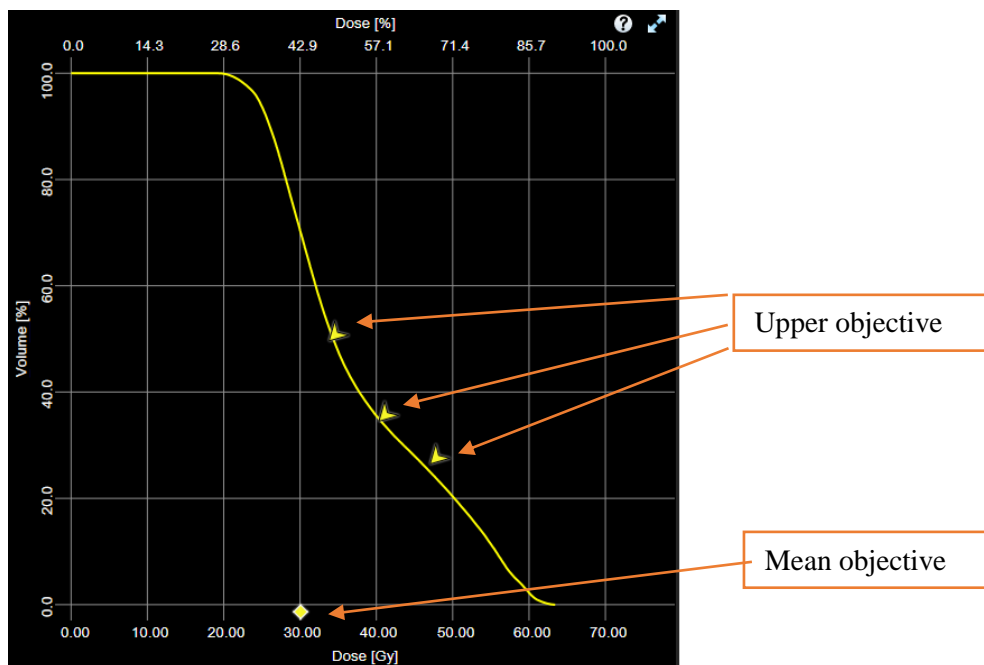


Figure 1.10 Dose constraints setting of parallel OARs

1.4.6 Practical Difficulty of Optimizing a Radiotherapy Plan for Head and Neck Cancers

Although the planning procedures are driven by treatment planning computer calculations in an inverse planning process, it is not a completely automatic procedure and there are difficulties in the planning. The difficulties in planning is largely related to the number of OARs and the geometric relationship between the PTVs and the OARs. In the optimization process of the inverse planning, it is usually not possible to achieve all the lower objectives for the PTVs while

fulfilling all the upper and mean objectives for the OARs because they naturally contradict each other when the PTVs and OARs are in vicinity (Tanaka, Fujimoto, & Yoshinaga, 2015). In head and neck cancers, there are many OARs near to the PTVs including but not limited to the brain stem, the spinal cord, the parotid gland and the optic nerves. Because of this, the treatment planning system optimization usually has no optimal solution that can fulfil all the set objective functions. Therefore, planners need to intervene the procedure by evaluating the optimized treatment plans using their own experiences, and to balance the trade-off among all the non-optimal objective functions of the PTVs and OARs.

Chapter 2 Introduction

It has been discussed in Chapter 1 that IMRT is the main treatment modality for head and neck cancers. To maximize the benefit of IMRT in which cancericidal dose can be delivered to the targets while sparing the OARs, challenges including target and OAR delineation, treatment planning and quality assurance should be addressed. Treatment planning is the focus of this study, in which the issues of beam arrangement, tumour dose and OARs dose are discussed. This chapter aims to introduce the purposes of conducting this study to address these aforementioned issues.

2.1 Treatment Planning of IMRT for Head and Neck Cancers

2.1.1 Challenges

As illustrated in the previous chapter, IMRT offers the opportunity for better treatment outcome and less side effects in radiotherapy of head and neck cancers when compared with 3DCRT. This is based on the advantages of IMRT that it can increase the dose conformity and homogeneity to the PTV while better spare the OARs (Daly et al., 2011; Zhang et al., 2015). To achieve this advantage, effort needs to be made to address the challenges of optimal target and OAR delineation, treatment planning and quality assurance (QA) (Gomez-Millan, Fernandez, & Medina Carmona, 2013). For the target and OAR delineation, comprehensive guidelines have been established (Brouwer et al., 2015; Gregoire et al., 2014; Gregoire et al., 2018; Sze et al., 2019). Also, techniques and tools for the QA of IMRT has been suggested by the American Association of Physicists in Medicine (AAPM) (Low, Moran, Dempsey, Dong, & Oldham, 2011). These guidelines are fundamental guidance for the standard of practice to maximize the

benefits of IMRT on cancer patients. In terms of treatment planning, however, there are currently no comprehensive guidelines, and it was suggested that planners should put effort to learn the relationship between the controlling the planning parameters and the changes in optimized dose (Ezzell et al., 2003). The controlling planning parameters refer to the beam arrangement, planning goals, dose constraints, priorities and margins/overlap regions between delineated structures (Ezzell et al., 2003). Manipulation of various controlling parameters to achieve the planning goals of the IMRT plans depends on planners' preferences and the characteristics of different treatment planning systems (Bohsung et al., 2005). Studies are needed to provide objective evidence to help in the decision making in the concerned aspects during treatment planning process so that it would not need to rely only on the planner's personal preferences. The improvement of treatment planning, therefore, is the focus of this study to provide guidance for planners. The areas of interest are further discussed in the following sections.

2.1.2 Impact of Beam Arrangement

Beam arrangement refers to the number of beams and the beam angles employed in the treatment planning of radiotherapy. This has been one of the main parameters which affects the dose to the PTV and OARs in the treatment planning (W. Parker & Patrocinio, 2005), although it is more difficult for planners to appreciate the dosimetric effect of beam angles selection in IMRT. In 3DCRT, planners need to decide the beam arrangement for the purpose of target coverage and OAR sparing (Funk, Stockham, & Laack, 2016). For example, wedged pair beams are used in treating the parotid glands and parallel opposed beams are used in treating the larynx as illustrated in Figure 2.1 (Mayles, Nahum, & Rosenwald, 2007). The considerations in the beam arrangement include the avoidance of direct incidence at critical OARs such as

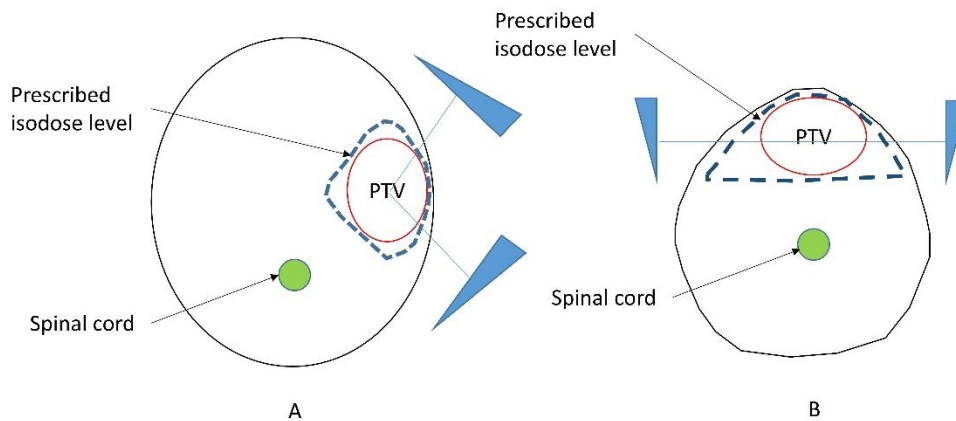


Figure 2.1. Field arrangement in 3DCRT affects the distribution of the prescribed dose. A: a typical wedged pair arrangement for treatment of the parotid gland. B: A pair of parallel opposed wedged field arrangement for treatment of the larynx.

the spinal cord. Also, the employed beam angles affects the shape of the high dose volume distribution. These considerations, however, are not applicable in the treatment planning of IMRT. One of the reasons for this is that the intensity modulation in IMRT can overcome the effect of the sub-optimal beam arrangement as in the case of 3DCRT (Stein et al., 1997). This is because theoretically, homogeneous prescribed dose distribution within the PTV and rapid dose falloff gradient outside the PTV can be achieved with the intensity modulation by optimization and increasing number of beams (Rehman et al., 2019). As a routine practice, planners usually use five to nine equally spaced beams (ESB) in the beam configuration of IMRT (Cheung et al., 2010; X. Wang et al., 2005). Nevertheless, in actual implementation, beam arrangement including beam angle selection has been reported to have significant dosimetric effect in IMRT of many cancers including oesophagus (Fu et al., 2017), lung (Fitzgerald et al., 2016), pharynx and larynx (Vanetti et al., 2009), and nasopharynx (Budrukkar, Hope, Cramb, Corry, & Peters, 2004). Also, it has been suggested that steep dose gradient between PTV and OARs can be better

achieved by increasing the number of beams (Hunt & Burman, 2003). These indicate that beam arrangement, although being overlooked due to the less significant impact in the dosimetric outcome in IMRT, can influence the IMRT plan quality. Furthermore, ESB, beam angle optimization (BAO) and volumetric modulated arc therapy (VMAT) are the available choices of beam arrangement methods in the Eclipse treatment planning system. Guidance is needed so that planners can choose the optimal beam arrangement methods in the treatment planning of IMRT.

2.1.3 Dose Escalation in NPC

IMRT offers the possibility to escalate the dose to the tumour because of its better ability to spare the OARs. In fact, dose escalation has already been implemented in IMRT in the treatment of NPC when the gross tumour dose was raised from 66 Gy in conventional radiotherapy to about 70 Gy (Kam et al., 2004). NPC is known for its radio-sensitivity and the existence of dose-tumour-control relationship beyond routine cancericidal dose (Teo, Leung, Lee, & Zee, 2000), hence increasing the dose to the tumour volume is able to increase the local control rate. It has been reported that in the group of predominantly locally advanced NPC (T3-4 N0-1), 61.8% of the failure was caused by local relapse (D. T. T. Chua, Sham, Wei, Ho, & Au, 2001). Another study also revealed that 80% of the recurrent cases had the relapse sites at the region delivered with the median dose of 70.4 Gy in the previous treatment (Dawson et al., 2000b). Clinical investigations on the dose escalation in the treatment of NPC using external beam radiotherapy (Kwong et al., 2006) and brachytherapy have been reported (Chao et al., 2017). Although it has shown good local control and survival in both reports, treatment side effects were the concern. For example, grade 3 mucositis were observed in about 80% of the cases (Kwong et al., 2006). Also, by assessing the acute toxicity, it has been suggested that the maximal tolerable dose in

IMRT of head and neck cancers was 2.36 Gy per fraction to a total of 70.8 Gy (Lauve et al., 2004). With our part one study on the evaluation of an optimal beam arrangement method for IMRT of NPC, more effective sparing of OARs might be possible. It is worth to conduct dosimetric study to review the maximum deliverable doses to the gross tumour of NPC with consideration to keep the doses of the OARs below their tolerance.

2.1.4 Organs at Risk (OARs) Dose Estimation

In the treatment planning of IMRT, the inverse planning process requires planners to define the dose limits of various PTVs and OARs for the optimization of the beam intensity modulation. This process is regarded as the setting of objective function, which includes the dose constraints and priority of the PTVs and OARs as discussed in section 1.4.5. In general, the setting of PTVs objective functions are guided by the prescription whereas those for the OARs are set according to their dose tolerance (Brodin & Tome, 2018). In practice, however, the objectives for OARs sparing are often in conflict with the objectives to achieve PTV dose coverage (Banaei, Hashemi, Bakhshandeh, & Mofid, 2019). This is because OARs and PTVs are often in close proximity and sometimes may even overlap one another. In this condition, we may have to deliver OARs doses that are close to or even higher than their dose tolerance in order to achieve PTV adequate dose coverage. On the contrary, when the OARs are far from the PTV, the actual OARs dose would be well below their tolerance. It is logical to deduce that the OARs dose is related to their anatomical relationship with PTVs, and this relationship varies greatly among different patients. It is worth to conduct studies to address the relationship of the OARs dose and the anatomical parameters, so that we can identify the specific anatomical parameters that affect the doses to

individual OARs. Also, the OAR doses can be estimated for the purpose of guiding initial setting of OARs objective functions before optimization in the inverse planning of IMRT.

2.2 Figure of Merits in Plan Evaluation

In the evaluation of radiotherapy plan dosimetric quality, there are four main parameters to be evaluated: 1. PTV coverage, 2. OAR dose, 3. PTV homogeneity and 4. PTV conformity (Funk et al., 2016). PTV coverage refers to the minimum proportion of PTV covered by the prescribed dose. OAR dose is to see whether it is within the organ tolerance. PTV homogeneity is used to assess the dose uniformity within the PTV whereas PTV conformity is to evaluate whether the prescribed dose level encompass and follow the shape of the PTV. Examples of different PTV coverage, homogeneity and conformity situations are illustrated in Figure 2.2.

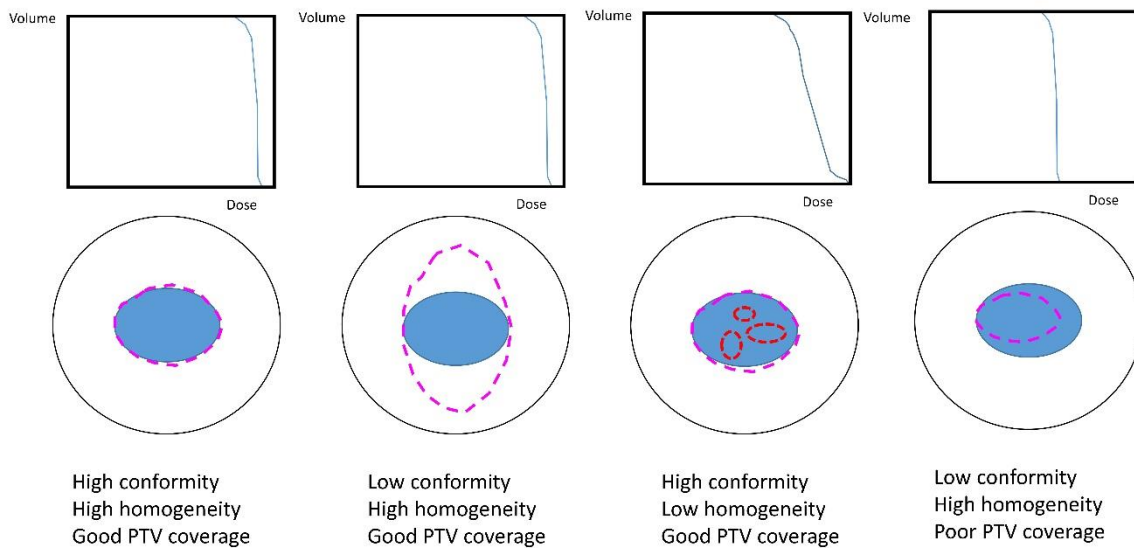


Figure 2.2. Examples of different PTV coverage, homogeneity and conformity situations. The PTV is in blue solid lines and the body is in black solid lines. The purple dashed lines are the prescribed isodose and the red dashed lines are the hot spots isodose. Their respective dose volume histograms are shown above.

The evaluation of PTV coverage and OAR dose is conducted using the dose volume histogram (DVH). PTV homogeneity and conformity are assessed by indices known as the homogeneity index (Grégoire & Mackie, 2011) and conformity index respectively (Riet, Mak, Moerland, Elders, & van der Zee, 1997). These dosimetric evaluation parameters are discrete and may not indicate the overall plan quality. Figure of merit (FOM) aims to incorporate the necessary parameters into a single score to represent the overall quality of radiotherapy plans. It is useful in the current study for evaluating the overall dosimetric quality in the treatment planning of head and neck cancers.

Various FOMs for the purpose of radiotherapy plan dosimetric evaluation have been developed (Jain & Kahn, 1992; L. H. Leung, Kan, Cheng, Wong, & Yau, 2007; Menhel, Levin, Alezra, Symon, & Pfeffer, 2006; Meyer et al., 2007; Miften, Das, Su, & Marks, 2004). A review was conducted which helped to provide the suitable FOM for this study.

FOM by Jain & Kahn (1992)

The FOM was calculated by:

$$\text{FOM} = \prod_i^{\text{issues}} (1 - \text{probability}_i * f(\text{prototypical weight, modifier}))$$

This FOM is calculated by the product of the weighted uncomplicated probability of various issues. The issues in the equation refers anything that needs to be considered in the evaluation of plans, which includes PTV coverage, OAR dose and anything that planners concern. On top of the probability, a prototypical weight addressed the relative importance of the issues and a modifier addressed the patient specific relative importance of the issue.

This FOM provided a framework of a possible way to construct a single score, which incorporated various dosimetric requirements, for the evaluation of radiotherapy plan. Because the authors intended to allow users to specify the FOM based on their own focus, the calculation details including the issues, probability and modifier were not specified.

Critical Organ Scoring Index by Menhel et.al.(2006)

The critical organ scoring index (COSI) was suggested to include target coverage and excessive dose to OAR in a FOM using the following equation:

$$COSI=1 - \frac{V(OAR)_{>tol}}{TC_v}$$

$V(OAR)_{>tol}$ is the proportion of volume of OAR which receives more than the tolerance dose and TC_v was the proportion of volume of target covered by prescribed dose. There is one COSI for each OAR in a radiotherapy plan, and the summation of all calculated COSI gives the overall plan dosimetric quality. As noticed in the calculation formula, the conformity and homogeneity are not addressed. Also the calculation of OAR dose that focuses on the volume which exceeds the tolerance dose is not relevant to serial organ.

Composite Criteria by Meyer et. al. (2007)

The Composite Criteria (C) is calculated as follow:

$$C = \sum x_i f_i(p_i - t_i)$$

Where x is a user-defined weight, f is a linear or quadratic function, p is the dosimetric parameter in the plan and t is the planning goal. The composite criteria is the sum of the weighted

difference between the planning goals and the corresponding actual dosimetric parameters in the plan. There was no concrete suggestion of what planning goals to be included in the calculation of the Composite Criteria.

Plan Quality Index by Leung et.al. (2007)

Plan quality index (PQI) is calculated by:

$$PQI = \sqrt{(1 - H)^2 + (1 - M)^2 + (1 - P)^2}$$

In which H, M and P represented healthy tissue conformity index, target coverage and normal tissue sparing respectively. They are calculated by separate equations.

$$H = \frac{1}{r} \times \sum_{i=1}^r \left(\frac{TV_{RI,i}}{V_{RI,i}} \right)$$

In the above equation, r represents the number of targets, $TV_{RI,i}$ represents the target volume covered by the prescribed dose and $V_{RI,i}$ represents the total volume of the prescribed dose. It is a modification of the conformity index proposed by Lomax and Scheib (2003) to calculate the score for radiotherapy plans with multiple targets.

$$M = \frac{1}{r} \sum_{j=1}^r \left\{ \frac{\sum_{i=1}^p \left(\frac{V_{Tj, Di}}{V_{Tj, RDi}} \right) + \sum_{i=1}^q \left(1 - \frac{V_{Tj, Di}}{V_{Tj, ADi}} \right)}{\sum_{i=1}^p \left(\frac{100}{V_{Tj, RDi}} \right) + q} \right\}$$

The target coverage (M) is calculated to monitor the hot spot and cold spot within the targets. In the above equation, p is the number of cold spot checks, q is the number of hot spot checks, r is the number of targets with different prescribed doses, $V_{Tj, Di}$ is the volume of target which received the prescribed dose, $V_{Tj, RDi}$ is the minimum allowable volume of target to receive the

prescribed dose for cold spot checks, $V_{Tj, ADi}$ is the maximum allowable volume of target to receive a specific dose for hot spot checks.

For example, suppose there is a one-target-radiotherapy plan in which the cold spot check is minimum 95% of target volume receiving 95% of the prescribed dose and the hot spot check is maximum 10% of the target volume receiving more that 99% of the prescribed dose, the actual plan is that 100% of the target received 95% of the prescribed dose and 5% of the target received more than 110% of the prescribed dose. By substitution, the M value can be calculated by the

equation:

$$M = \frac{\left(\frac{100}{95}\right) + \left(\frac{5}{10}\right)}{\left(\frac{100}{95}\right) + 1} = 0.75$$

$$P = \frac{1}{n} \times \sum_{j=1}^n \left\{ \frac{1}{m} \times \sum_{i=1}^m \left[1 - \frac{V_{Oj, Di}}{V_{Oj, ADi}} \right] \right\}$$

In the above equation, n represents the number of OARs, m represents the number of dose check points, $V_{Oj, Di}$ is the volume of the OAR which received a specific dose for dose check point, $V_{Oj, ADi}$ is the allowable volume of OAR which receive the specific dose for dose check point. For example, there is a radiotherapy plan with one organ at risk, the two dose check points are: No more than 35% of the volume of the organ receive more than 40 Gy, and no more than 17% of the volume of organ received more than 65 Gy. Whereas in the actual plan 5% of the volume of organ received 40 Gy and 0% of the volume of organ received 65 Gy. The P value can then be calculated by the equation: $P = \frac{1}{1} \times \left\{ \frac{1}{2} \times \left[1 - \frac{5}{35} \right] + \left[1 - \frac{0}{17} \right] \right\} = 0.93$.

Uncomplicated Target Conformity Index by Miften et.al. (2004)

Uncomplicated target conformity index (TCI+) consists of target conformity index (TCI) and normal tissue sparing index (NTSI).

$$TCI+ = \prod_{i=1}^{N_T} TCI_i \prod_{j=1}^{M_{NT}} NTSI_j$$

In which N_T is the total number of PTVs and M_{NT} is the number of OARs.

The equation for the calculation of TCI is:

$$TCI = P_{ptv} \left(\frac{PTV_{td}}{PTV} \right)$$

An individual TCI score is calculated for each PTV, where PTV_{td} is the volume of PTV covered by a specified therapeutic dose and PTV is the volume of PTV. P_{ptv} is a penalty function that is used to penalize overdose or underdose of the PTV, which should be rare in a completed plan because this is the main goal to achieve in the treatment planning of IMRT.

$$NTSI = P_{ntv} \left(\frac{NTV_{td}}{NTV} \right)$$

For each OAR of the plan, an NTSI score is calculated. In the equation, NTV is the normal tissue volume and NTV_{td} is the volume of normal tissue volume which received the PTV prescribed dose. P_{ntv} is the penalty function which penalized the NTSI score when the OAR received dose exceeding the tolerance.

The equation for the penalty function is:

$$P_{ntv}(V_i, D_i) = \begin{cases} 1 & \text{for } D_i \leq D_{tol} \\ e^{-\gamma(D_i - D_{tol})} & \text{for } V_i > V_{max} \text{ and } D_i > D_{tol} \end{cases}$$

D_{tol} is the tolerance dose by a maximum volume V_{max} of the OAR. If the dose does not exceed D_{tol} ; or the OAR is intentionally sacrificed by oncologists, no penalty will be imposed and the penalty will be equal to 1. γ value defined the seriousness of penalty depending on the type of OAR. For a serial organ 0.25 will be used as γ value and 0.05 will be used for parallel organ.

Components included in the calculation of FOMs

A very important criteria of a FOM is to incorporate sufficient information into the calculation equation so that the final score can represent the overall quality of the radiotherapy plan. The information is regarded as sufficient when the four items of plan evaluation, i.e. target coverage, OAR dose, conformity and homogeneity, are addressed in the calculated FOMs.

Table 2.1 summarizes the components included in the five FOMs. It was noted that the FOM suggested by Leung et.al. and Miften et.al. includes all the four components of plan evaluation. These two FOMs were better than the others because they could account for the plan quality more comprehensively.

Table 2.1. Components included in the calculation of different FOMs.

	Target coverage	OAR dose	Conformity	Homogeneity
<i>Jan & Kahn, 1992</i>	Depend on user	Depend on user	Depend on user	Depend on user
<i>Meyer et.al., 2007</i>	Depend on user	Depend on user	Depend on user	Depend on user
<i>Menhel et.al., 2006</i>	✓	✓		
<i>Leung et.al., 2007</i>	✓	✓	✓	✓
<i>Miften et.al., 2004</i>	✓	✓	✓	✓

*There was one condition that the target coverage could not be addressed in the FOM.

2.3 Application of Regression Analysis in Radiotherapy Planning

Regression analysis is a statistical tool for the investigation of relationships between variables, in which it can specify how the dependent variable changes when the independent variables are varied. It is an important tool for modelling and analyzing data for the estimation of the dependent variable out of a given set of independent variables. There are different types of regression analysis and they can be classified based on three factors (Pardoe, 2012): 1. The number of independent variables, 2. The shape of the regression line and 3. The data type of dependent variable as illustrated in Figure 2.3.

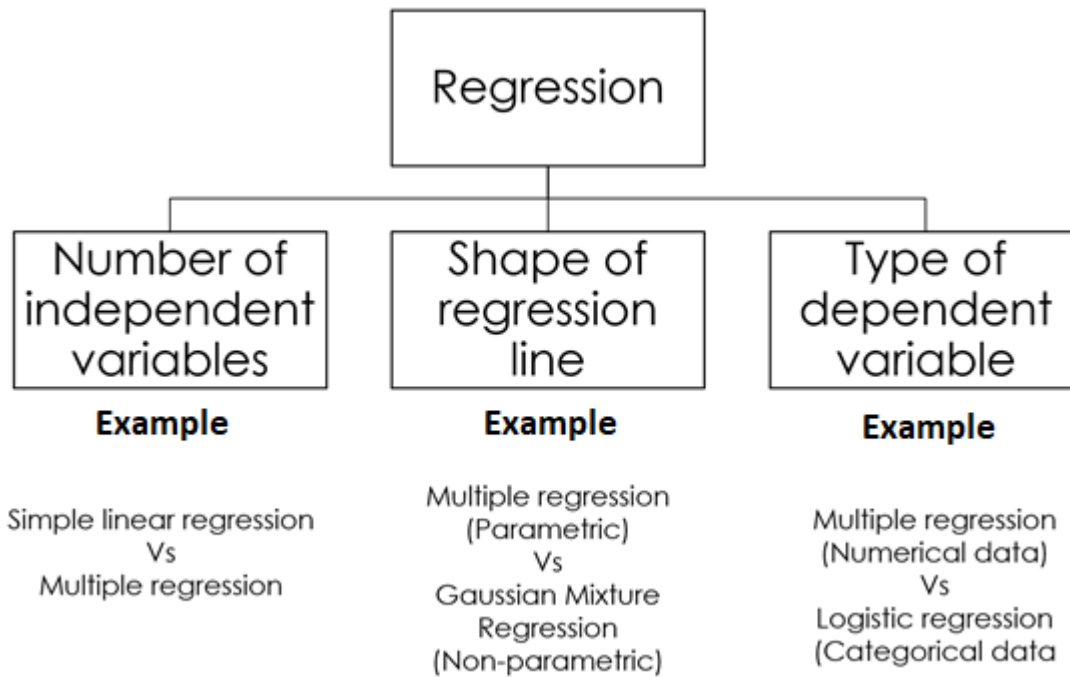


Figure 2.3. Classification of regression analysis

The OAR dose is likely to be influenced by a number of anatomical parameters in terms of volume and distance as illustrated in section 2.1.4. Multiple regression, which can be used to establish models to correlate multiple independent variables to a dependent variable, is proposed to be used in our study.

Multiple regression is a kind of linear regression in which the relationship between dependent variable and independent variables is established using an equation in the form of $Y = b_0 + b_1X_1 + b_2X_2 + \dots + b_kX_k$, where Y is the dependent variable, X_k is the independent variable and b_k is the coefficient estimate (Pardoe, 2012). When constructing the multiple regression model, there are two important points which could affect the outcome of the model. They are the multicollinearity and model selection methods.

Multicollinearity is a term to describe the situation when two or more independent variables are highly correlated (Farrar, 1967). The effect of multicollinearity to the regression model is that it increases the variance of the coefficient estimates. Therefore, the coefficient estimates are very unstable as they are very sensitive to minor change in the model. This makes the specification of the regression model, in terms of the selection of the model components, to be less accurate (Farrar, 1967). Multicollinearity should be checked by collinearity statistics, such as the variance inflation factor, before the regression generation process (R. G. Lomax, 2012).

Model selection of multiple regression refers to the method to incorporate the independent variables into the regression models. There are four types of methods, namely: 1. enter, 2. forward selection, 3. backward selection and 4. stepwise (Pardoe, 2012). The “enter” method is to enter all the selected independent variables into the regression models regardless of their contribution to the models, while the other methods employ measures to select independent variables based on their contribution. The “forward” method starts with a model with no variable. It then adds variables one at a time in a sequence per the amount of contribution of the variables to the regression model. The “backward” method starts with a model with all the independent variables. It then removes variable one at a time in a sequence that the variable with the least contribution to be removed first. Stepwise-entering method is an automatic process through step-by-step consideration of each independent variable until all independent variables had gone through the process. During each step, independent variables’ contribution to the regression model are considered for inclusion or exclusion into the final model. The process could eliminate the independent variables with the least contribution to the model, and therefore resulted in a simplified but valid model.

There are several limitations in multiple regression models. First, the regression model does not imply a cause-and-effect relationship between the dependent variables and the independent variables. It only shows the correlation between them (R. G. Lomax, 2012). Second, prediction of the dependent variables using the extra-large/extra-small values of independent variables is possible but not necessarily accurate because it involves extrapolation of the model (R. G. Lomax, 2012). The limitations will be addressed in the discussion of the study in this thesis which involves the use of regression analysis.

2.4 Research Questions and Hypotheses

2.4.1 Research Questions

- 4.2.1. Does the use of ESB, BAO and VMAT have impact on the dosimetric outcome in the treatment planning of IMRT in head and neck cancers?
- 4.2.2. Does the use of the optimum beam arrangement method, which shows higher capability in sparing OAR dose, increase the maximum deliverable dose in NPC treated with IMRT?
- 4.2.3. Does the use of multiple regression help to give a better estimation of the OAR dose from the anatomical parameters in the IMRT plan of NPC?

2.4.2 Research Hypotheses

1. There are significant differences in the mean dosimetric parameters and FOM in the IMRT plans among the ESB, BAO and VMAT beam arrangement methods.
2. There is no significant difference in the OAR dose and normal tissue integral dose in the NPC IMRT plans with increased gross tumour dose compared with the reference IMRT plans.

3. There are significant relationships of OARs dose parameters and anatomical parameters in the IMRT plans of NPC.

2.5 Purpose of Study

2.5.1 Aims

The purpose of this study is to provide evidence-based guidance in the treatment planning of IMRT, which is currently more based on planners' preferences. The guidance refers to the use of beam arrangement methods in head and neck cancers, the maximum allowable dose to the gross tumour in locally advanced NPC and the estimation of OARs doses in NPC.

2.5.2 Objectives

1. To evaluate the PTVs and OARs dosimetric outcome in five types of head and neck tumours, including cancers of the NP, larynx, oral cavity, maxilla and parotid gland, treated by intensity modulated radiation therapy (IMRT) using different beam arrangements.
2. To evaluate the maximum deliverable dose to the gross tumour volume (GTV) in non-coplanar IMRT of nasopharyngeal carcinoma (NPC) using beam angle optimization (BAO).
3. To develop a model to address the relationship between the OAR dose parameters and anatomical parameters in the IMRT of NPC.

Chapter 3

Study 1 – Dosimetric Evaluation of Beam Angles

Arrangement Methods in IMRT of Head and Neck Cancers

This study was conducted to determine the optimal beam arrangement methods for different head and neck cancers, in correspondence to objective 1. This study has been published in the Journal of Applied Clinical Medical Physics (Volume 20: 121-130).

3.1 Introduction

Head and neck cancer is one of the most complicated sites in the body for radiotherapy planning because the planning target volume (PTV) is usually irregular in shape and surrounded by many important organs. Over irradiation of the organs at risk (OARs) may cause irreversible side effects such as xerostomia, cataract, hearing loss and trismus that degrade the patient's quality of life (Dijkstra, Kalk, & Roodenburg, 2004; Eisbruch et al., 2001; Pan et al., 2005). Furthermore, head and neck cancers at different sub-sites such as nasopharynx and larynx may lead to different considerations in treatment planning because of their variations in anatomy, body contour and tissue density combinations.

Intensity modulated radiotherapy (IMRT) has been the main treatment modality for many head and neck cancers due its relatively high target dose conformity and steep dose gradient at target-normal tissue interfaces compared with the conventional 3-dimensional conformal radiotherapy (3DCRT). While the dose distribution in IMRT is largely controlled by the beam modulation using dynamic multi-leaf collimators (MLC), the beam arrangement including beam number and

beam angle employed in the treatment plan have been reported to have significant dosimetric influence in the plan quality in IMRT of many cancers including oesophagus (Fu et al., 2017), lung (Fitzgerald et al., 2016), pharynx and larynx (Vanetti et al., 2009), and nasopharynx (Budrukkar et al., 2004).

Equally spaced beam (ESB) arrangement has been commonly used in the early application of IMRT in head and neck cancers after replacing 3DCRT in the early nineties (Ahmed et al., 2009; Gupta et al., 2012; Vlachaki et al., 2005). Volumetric modulated arc therapy (VMAT) and beam angle optimization (BAO) in the Eclipse treatment planning system (Varian Medical System, Palo Alto, USA) are the two more recent options in assigning IMRT beams. VMAT is the delivery of IMRT using rotating arc beams (Earl, Shepard, Li, & Yu, 2001; Mackenzie & Robinson, 2002), while BAO is the use of a specific optimization algorithm to select the optimum angles of static beams, either coplanar or non-coplanar.

Previous dosimetric studies on the applications of VMAT and ESB in head and neck cancers (Tsai, Wu, Chao, Tsai, & Cheng, 2011; Verbakel et al., 2009) reported that dual arc VMAT improved the target coverage and OARs sparing in cancers of oropharynx, hypopharynx and larynx (Clivio et al., 2009; Vanetti et al., 2009) and VMAT produced similar plan quality as ESB arrangement with marked reduction of monitor unit (MU) and shorter treatment delivery time (Tsai et al., 2011; Verbakel et al., 2009). Studies on BAO are limited. Some of them reported that coplanar BAO arrangement when applied to glioblastoma, prostate and pancreatic cancers resulted in similar plan quality as ESB arrangement with reduced MU and number of fields (Craft, Hong, Shih, & Bortfeld, 2012; Srivastava, Das, Kumar, & Johnstone, 2011). Apart from coplanar beams in IMRT, BAO can also generate non-coplanar beam arrangement. Although

non-coplanar IMRT has been reported to reduce the doses to OARs and normal tissues in prostate cancer patients (Tran et al., 2017), its use in the clinical department is uncommon mainly due to the treatment setup inconvenience. However, with the recent emergence of 4Pi radiotherapy with compatible linear accelerators (Rwigema et al., 2015), it is expected that the use of non-coplanar IMRT will be increased and its potential advantages can be better exercised.

To date, studies on IMRT beam arrangement for head and neck cancers have been limited to specific sites or just any two of the beam arrangement techniques. The optimum beam arrangement, in terms of dosimetric quality, for individual sites of head and neck cancers remains uncertain. Therefore we have conducted a more comprehensive study that evaluated the dosimetric performance of five main IMRT beam arrangement methods on five types of common head and neck cancers that covered the various sub-sites of this body region.

3.2 Materials and Methods

A total of 119 adult head and neck cancer patients treated by radical IMRT were randomly selected. They included cancers of the nasopharynx, oral cavity, larynx, parotid gland and maxillary sinus. Each cancer type consisted of a sample size of 25 except for maxillary sinus, which had 19 due to the limited number of cases available in the clinical department. Using G*Power software (Heinrich Heine University, version 3.1.9.4) with an effect size of 0.25 and an alpha value of 0.05, the power of 0.888 and 0.767 were calculated for a sample size of 25 and 19 respectively. It showed that with the sample size, the statistical test had 88.8% and 76.7% chance to detect the effect if the differences of dose parameters among plans of different beam arrangement were true (Type II error), while there was a 5% chance to detect the effect where the

differences were untrue (Type I error). The distributions of the T and N stages of the patients in each cancer group are summarized in Table 3.1. Ethical approval was obtained from the Hong Kong Polytechnic University and the Princess Margaret Hospital. To ensure confidentiality of the selected patients, the patient identifiers, such as name and registration number, were completely removed by an assigned study number and requirements of the Personal Data (Privacy) Ordinance was adhered to.

Table 3.1. The distribution of T and N stages of the selected patients

		Nasopharynx (n=25)	Oral cavity (n=25)	Larynx (n=25)	Maxillary sinus (n=19)	Parotid (n=25)
T-stage	T1	2	2	0	0	7
	T2	3	10	0	0	7
	T3	15	11	16	12	8
	T4	5	2	9	7	3
N-stage	N0	8	3	5	3	10
	N1	11	15	17	16	6
	N2	6	7	3	0	9

All patients' planning CT data with contoured structures were retrieved from the treatment plan database of a local oncology department. Five hypothetical plans, one for each beam arrangement

method, were computed for each patient using the Eclipse treatment planning system Version 13.6 (Varian Medical System, Palo Alto, US) by the same planner. The 5 beam arrangement methods were: equally spaced beams (ESB), coplanar beam angle optimisation (BAOc), non-coplanar beam angle optimisation (BAOnc), 2 volumetric modulated arcs (VMAT2) and 3 volumetric modulated arcs (VMAT3). The ESB arrangement employed 9 equally spaced beams at 40° apart as suggested by previous literature (Q. Wu, Manning, Schmidt-Ullrich, & Mohan, 2000). BAO was performed using Plan Geometry Optimizer (Version 13.6.23) in the Eclipse treatment planning system. BAOc used only coplanar beams while BAOnc included non-coplanar beams. The total number of beams used in both methods ranged between 5 and 9 depending on the beam selection process by the optimization algorithm. In addition, for the BAOnc, the maximum elevation angle of the non-coplanar fields from the principal plane was set at no larger than 30 degrees. This ensured that there would not be any vertex field in the BAOnc field arrangement, because vertex field would deliver substantial radiation dose that could cause damage to the gonad of the patients (Das et al., 1997). VMAT2 consisted of two full arcs whereas VMAT3 consisted of three full arcs. All treatment plans were planned with 6 MV photon and Millennium MLC. The PTVs were delineated by the oncologist in-charge. The prescription was 66-70Gy in 30-35 fractions for high risk PTV (PTVH) involving primary tumour or tumour bed and positive nodal involvement. The other two PTVs were intermediate risk PTV (PTVI) and low risk PTV (PTVL) in the nodal region with prescriptions of 60 Gy and 54 Gy respectively. The PTVs were treated using simultaneously integrated boost method. The Anisotropic Analytical Algorithm (Version 13.6.23) was used for volume dose calculation and the Photon Optimizer (Version 13.6.23) was used for optimization. For each patient, all the plans

were planned using the same prescribed dose and same set of dose objectives for the target volumes and OARs.

Plans were evaluated by the dose parameters generated from the dose volume histogram (DVH) of each structure. For the target volumes, the dose parameters were the homogeneity index (HI) and conformation number (CN). The HI was calculated according to the equation 1 as reported in ICRU 83 (Grégoire & Mackie, 2011) , while the calculation of CN as shown in the equation 2 was adopted from the equation suggested by Riet et al (1997).

$$HI = (D_{2\%} - D_{98\%}) \div D_{50\%} \quad (1)$$

$$CN = \frac{V_{T,ref}}{V_T} \times \frac{V_{T,ref}}{V_{ref}} \quad (2)$$

where $V_{T,ref}$ = volume of target receiving a dose equal to or greater than the reference dose,

V_T = volume of target,

V_{ref} = volume receiving a dose equal to or greater than the reference dose.

The OARs considered for dosimetric comparison were the spinal cord, brain stem and parotid glands (contralateral only for the parotid cancer group) as they were the relatively more critical organs and small changes in dose level would affect the risk of complications. For other OARs such as the cochlea and pituitary gland, it was expected that they received relatively lower doses, slight differences would not have clinical significance and therefore were not included in this study. In NPC IMRT planning, the optic nerves and optic chiasm are also considered critical OARs as they are in close proximity to the PTVs, however they are not as important for the other more inferior situated head and neck cancers such as the cancer of the larynx and the parotid. In

addition, the sparing of the optic nerves and optic chiasm from their tolerance dose mainly depends on whether they are overlapping with the PTVs (Niu, Chang, Gao, Hu, & Kong, 2013). Hence optic nerves and optic chiasm were not included in the dosimetric comparison. For the spinal cord and brain stem, $D_{2\%}$ was used for dose recording, whereas for the parotid gland, $D_{50\%}$ and D_{mean} were used. $D_{2\%}$ is a recommended dose parameter to replace the use of maximum dose by the ICRU report 83 (Grégoire & Mackie, 2011). The aim of the use of $D_{2\%}$ is to avoid reporting the received dose by a single point which can be susceptible to errors. In terms of the evaluation of near-maximum dose, $D_{2\%}$ is considered to be comparable to other dose-volume metrics such as $D_{0.5\text{cc}}$ (Grégoire & Mackie, 2011) and $D_{2\%}$ has been widely used in other IMRT dosimetric studies (Vanetti et al., 2009). The normal tissue dose, which was expressed as the integral dose (in $\text{Gy}\cdot\text{cm}^3$), was calculated by multiplying the D_{mean} of the patient body included in the planning CT scan excluding PTVs with the volume of this body region (normal tissue) (Aoyama et al., 2006). In addition, a “Figure of merit”, also known as uncomplicated target conformity index (UTCi), was used to rank the overall plan quality (Miften et al., 2004). It was calculated by $\text{CN} \times \text{Penalty of organs at risk (P}_{\text{OAR}}) \times \text{Penalty of integral dose (P}_{\text{ID}}$). The higher the score, the better was the overall plan quality. The CN component of the UTCi was adopted from the Riet study (1997). The P_{OAR} and P_{ID} were calculated by $e^{-0.05(D_i - D_{\text{tol}})}$ with D_i representing the actual received dose and D_{tol} representing the tolerance dose. Since there was no established tolerance for integral dose, the D_{tol} in the calculation of P_{ID} was taken as the lowest achieved integral dose within the group of the same cancer. The role of P_{OAR} and P_{ID} in the equation was to penalize the UTCi score when the actual OARs dose exceeded their tolerance dose.

Statistical analysis was performed using the SPSS version 20 (IBM Corp, Armonk, NY). All the dose parameters and the UTCI scores were first tested for normality using the Shapiro-Wilk test. The mean values of the dose parameters and UTCI scores for each beam arrangement group were calculated and compared. One-way Repeated Measures ANOVA test was used to analyze the differences among the five beam arrangement methods. When there was significant difference among them, post hoc Tukey test was applied to further determine the ranking of each method.

3.3 Results

All treatment plans met the pre-set dose requirements for the target volumes and OARs. Examples of dose distribution for the five beam arrangement methods for each of the five cancers are shown in Figures 3.1.

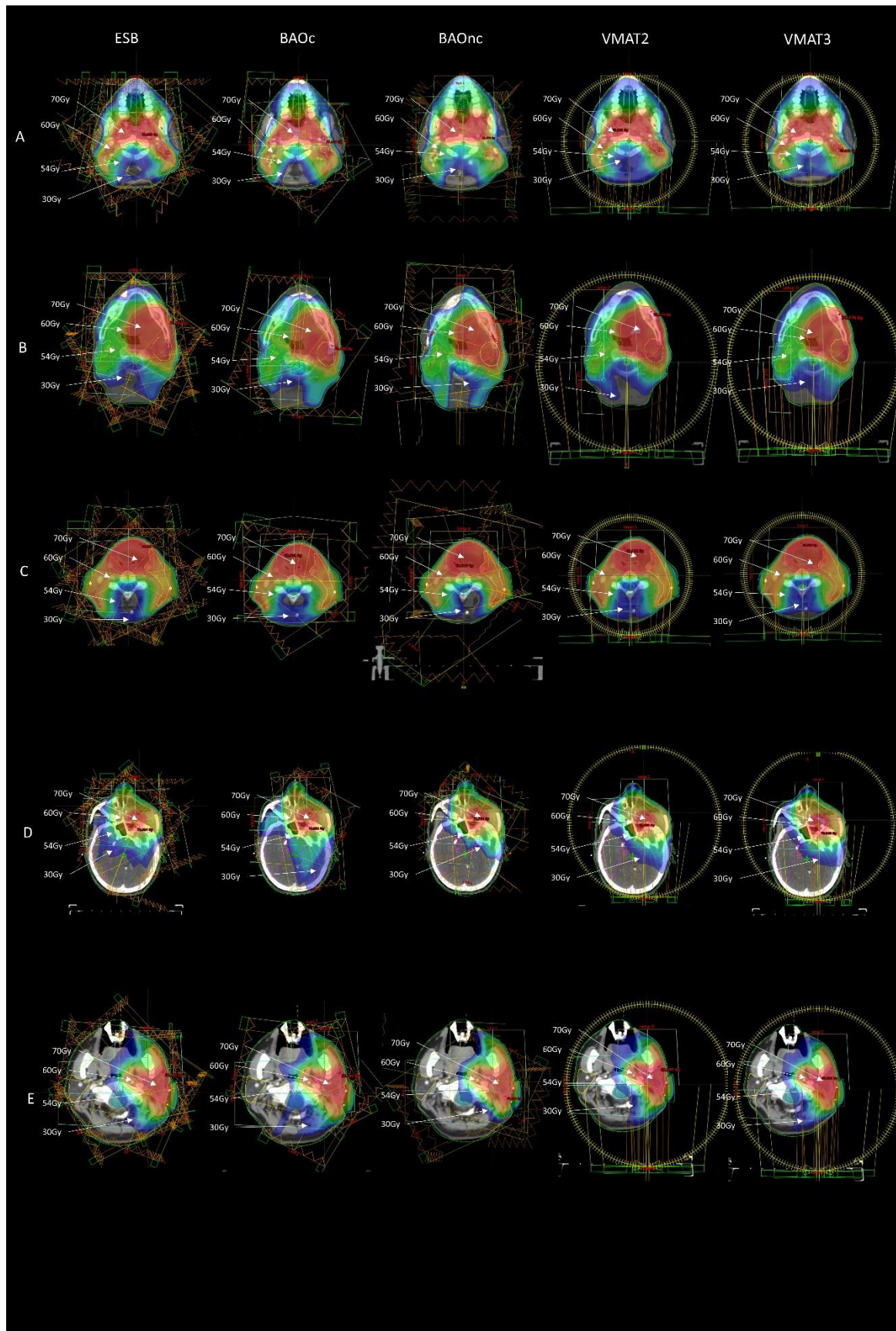


Figure 3.1. 5 types of H&N cancers. Diagram showing the dose distribution of the 5 types of H&N cancers using different beam arrangement methods. (A) Nasopharynx; (B) Oral cavity; (C) Larynx; (D) Maxilla; (E) Parotid.

Cancer of nasopharynx

For PTVH, ESB demonstrated the lowest HI and highest CN (Table 3.2 in P.57). ESB and VMAT3 performed relatively better in PTVI, in which ESB showed the highest CN, and VMAT3 showed the lowest HI. For PTVL, VMAT3 showed the lowest HI, whereas both VMAT2 and VMAT3 showed the highest CN. Comparing between BAOc and BAOnc, the later produced higher CN. In addition, VMAT2 and VMAT3 also showed similar target dose distributions. For the OARs and normal tissues, BAO methods delivered relatively lower doses, with BAOnc being the lowest. On the contrary, ESB delivered the highest dose to all OARs and normal tissues. In terms of overall plan quality, BAOnc and VMAT3 demonstrated significantly higher UTICI than the other three beam arrangement methods.

Cancer of oral cavity

For the target volume doses, VMAT3 in general performed better as it achieved lower HI in PTVH and PTVL, highest CN in PTVI and PTVL, and lowest $D_{2\%}$ in PTVH and PTVL (Table 3.3 in P.58). The rest of the parameters showed relatively small differences and did not reach statistical significance. For the OARs, there was no significant difference in the spinal cord and brain stem doses. For the parotid gland and normal tissues, the two BAO methods (BAOc and BAOnc) gave relatively lower doses and the difference between them was minimal. With regard to UTICI, BAOc, BAOnc, VMAT2 and VMAT3 achieved similar scores, which were higher than that of the ESB.

Cancer of larynx

There was no significant difference in most of the dose parameters for the target volumes except VMAT2 and VMAT3 gave a relatively higher CN in the PTVH (Table 3.4 in P.59). Similar

results were demonstrated in the OAR doses in which no significant difference was observed. For the normal tissues, the two BAO methods showed the lowest dose. However, there was no significant difference in UTICI among the five beam arrangement methods.

Cancer of maxillary sinus

In general, little difference was observed in PTVs except the two BAO methods showed relatively higher CN in PTVH and PTVI, and VMAT3 demonstrated the lowest HI for PTVL (Table 3.5 in P.60). There was no significant dose difference for the OARs among the five beam arrangement methods except for the mean parotid dose, in which the two VMAT plans were relatively higher. For the normal tissues, the two BAO methods demonstrated relatively lower doses. Furthermore, the UTICIs of the two BAO methods were significantly higher than the other three methods.

Cancer of parotid gland

There was no significant difference among the five beam arrangement methods for dose parameters of the PTVs and OARs (Table 3.6 in P.61). The two BAO methods delivered the lowest doses to the normal tissues and achieved the highest UTICI.

Table 3.2. Comparison of PTVs, OARs dose parameters and integral dose between IMRT plans of 5 beam arrangements for cancer of nasopharynx (n = 25)

Structure	Dose Parameter	ESB (mean±SD)	BAOc (mean±SD)	BAOnc (mean±SD)	VMAT2 (mean±SD)	VMAT3 (mean±SD)	Repeated ANOVA P-Value	Post hoc test
PTVH	HI	0.06 ± 0.01	0.08 ± 0.01	0.08 ± 0.02	0.06 ± 0.01	0.06 ± 0.01	<0.001	BAOc, BAOnc > ESB, VMAT3, VMAT2
	CN	0.93 ± 0.03	0.82 ± 0.03	0.83 ± 0.03	0.92 ± 0.03	0.91 ± 0.20	<0.001	ESB, VMAT2, VMAT3 > BAOnc, BAOc
PTVI	HI	0.08 ± 0.01	0.07 ± 0.01	0.09 ± 0.01	0.07 ± 0.01	0.06 ± 0.01	<0.001	BAOnc> BAOc, ESB> VMAT2> VMAT3
	CN	0.90 ± 0.03	0.79 ± 0.04	0.84 ± 0.03	0.89 ± 0.03	0.89 ± 0.03	<0.001	ESB, VMAT2, VMAT3> BAOnc> BAOc
PTVL	HI	0.07 ± 0.01	0.10 ± 0.01	0.10 ± 0.01	0.06 ± 0.01	0.06 ± 0.01	<0.001	BAOc, BAOnc > ESB> VMAT2, VMAT3
	CN	0.84 ± 0.42	0.83 ± 0.52	0.85 ± 0.41	0.86 ± 0.43	0.86 ± 0.47	0.024	VMAT2, VMAT3, BAOnc, ESB> BAOc
Spinal cord	D _{2%} (Gy)	43.8 ± 1.2	41.9 ± 0.9	41.5 ± 0.8	43.5 ± 1.1	43.7 ± 0.9	<0.001	ESB, VMAT3, VMAT2 > BAOc, BAOnc
Brain stem	D _{2%} (Gy)	51.7 ± 1.8	50.3 ± 1.9	50.2 ± 2.0	51.8 ± 1.8	51.8 ± 2.0	<0.001	VMAT3, VMAT2, ESB> BAOc, BAOnc
Parotid	D _{mean} (Gy)	32.4 ± 5.6	29.9 ± 5.7	29.4 ± 6.1	30.8 ± 5.3	30.7 ± 5.3	<0.001	ESB> VMAT2, VMAT3> BAOc, BAOnc
	D _{50%} (Gy)	29.9 ± 5.3	28.4 ± 4.8	27.9 ± 5.2	29.1 ± 5.1	28.9 ± 5.1	0.003	
Normal Tissue	D _{int} (x10 ⁴ Gy _{cm} ³)	9.5 ± 0.7	7.5 ± 0.7	7.4 ± 0.7	8.4 ± 0.7	8.4 ± 0.7	<0.001	ESB> VMAT2, VMAT3> BAOc, BAOnc
	UTCI	0.39 ± 0.15	0.41 ± 0.16	0.48 ± 0.20	0.46 ± 0.16	0.49 ± 0.18	<0.001	VMAT3, BAOnc> VMAT2> BAOc, ESB

HI = homogeneity index, CN = conformity number, D_{int} = integral dose, UTCI = uncomplicated target conformity index

Table 3.3. Comparison of PTVs, OARs dose parameters and integral dose between IMRT plans of 5 beam arrangements for cancer of oral cavity (n=25)

Structure	Dose Parameter	ESB (mean±SD)	BAOc (mean±SD)	BAOnc (mean±SD)	VMAT2 (mean±SD)	VMAT3 (mean±SD)	Repeated ANOVA P-Value	Post hoc test
PTVH	HI	0.07 ± 0.01	0.08 ± 0.02	0.08 ± 0.02	0.06 ± 0.01	0.06 ± 0.01	<0.001	BAOc, BAOnc> ESB, VMAT2, VMAT3, VMAT2, VMAT3> ESB> BAOc, BAOnc
	CN	0.84 ± 0.04	0.80 ± 0.04	0.80 ± 0.04	0.88 ± 0.03	0.88 ± 0.30	<0.001	
PTVI	HI	0.10 ± 0.02	0.10 ± 0.02	0.10 ± 0.02	0.10 ± 0.02	0.10 ± 0.02	0.378	VMAT2, VMAT3> ESB> BAOc, BAOnc
	CN	0.84 ± 0.04	0.80 ± 0.04	0.80 ± 0.04	0.86 ± 0.04	0.86 ± 0.04	<0.001	
PTVL	HI	0.10 ± 0.01	0.11 ± 0.01	0.11 ± 0.01	0.10 ± 0.02	0.10 ± 0.02	<0.001	BAOnc, BAOc, > ESB, VMAT2, VMAT3 VMAT3, ESB, VMAT2> BAOc, BAOnc
	CN	0.84 ± 0.45	0.81 ± 0.56	0.80 ± 0.44	0.84 ± 0.53	0.84 ± 0.36	<0.001	
Spinal cord	D _{2%} (Gy)	40.3 ± 2.5	39.8 ± 2.8	39.4 ± 2.6	39.1 ± 2.9	39.0 ± 3.1	0.088	
Brain stem	D _{2%} (Gy)	46.2 ± 6.3	46.4 ± 5.2	46.8 ± 5.8	45.7 ± 6.0	45.9 ± 6.2	0.425	
Parotid	D _{mean} (Gy)	28.1 ± 4.7	26.0 ± 5.8	26.0 ± 5.1	28.2 ± 4.6	28.0 ± 4.8	<0.001	VMAT2, ESB, VMAT3> BAOc, BAOnc ESB> VMAT3, VMAT2, BAOnc, BAOc
	D _{50%} (Gy)	28.7 ± 4.8	26.9 ± 5.9	27.2 ± 4.6	27.8 ± 4.8	28.0 ± 5.0	0.002	
Normal Tissue	D _{int} (x10 ⁴ Gy·cm ³)	9.7 ± 0.4	8.0 ± 0.6	8.0 ± 0.6	8.7 ± 0.5	8.8 ± 0.5	<0.001	ESB> VMAT2, VMAT3> BAOc, BAOnc BAOc, BAOnc, VMAT2, VMAT3> ESB
	UTCI	0.63 ± 0.45	0.77 ± 0.48	0.74 ± 0.48	0.70 ± 0.42	0.70 ± 0.44	0.003	

HI = homogeneity index, CN = conformity number, D_{int} = integral dose, UTCI = uncomplicated target conformity index

Table 3.4. Comparison of PTVs, OARs dose parameters and integral dose between IMRT plans of 5 beam arrangements for cancer of larynx (n=25)

Structure	Dose Parameter	ESB (mean±SD)	BAOc (mean±SD)	BAOnc (mean±SD)	VMAT2 (mean±SD)	VMAT3 (mean±SD)	Repeated ANOVA P-Value	Post hoc test
PTVH	HI	0.06 ± 0.01	0.08 ± 0.02	0.07 ± 0.01	0.06 ± 0.03	0.06 ± 0.02	0.100	
	CN	0.88 ± 0.05	0.88 ± 0.04	0.88 ± 0.05	0.90 ± 0.04	0.90 ± 0.40	0.013	VMAT2, VMAT3 > BAOc, ESB, BAOnc
PTVI	HI	0.12 ± 0.02	0.12 ± 0.02	0.13 ± 0.04	0.11 ± 0.03	0.11 ± 0.02	0.040	
	CN	0.82 ± 0.07	0.82 ± 0.08	0.84 ± 0.06	0.86 ± 0.05	0.86 ± 0.05	0.034	
PTVL	HI	0.08 ± 0.03	0.08 ± 0.04	0.08 ± 0.03	0.08 ± 0.03	0.07 ± 0.03	0.482	
	CN	0.84 ± 0.07	0.86 ± 0.05	0.86 ± 0.06	0.84 ± 0.81	0.86 ± 0.06	0.692	
Spinal cord	D _{2%} (Gy)	41.0 ± 2.1	42.2 ± 1.5	42.2 ± 1.8	42.2 ± 1.8	42.3 ± 1.9	0.222	
Brain stem	D _{2%} (Gy)	35.9 ± 19.4	35.1 ± 19.0	35.8 ± 19.5	35.1 ± 19.7	35.1 ± 19.9	0.554	
Parotid	D _{mean} (Gy)	28.5 ± 4.6	27.4 ± 5.1	26.4 ± 4.5	28.2 ± 4.8	27.4 ± 4.2	0.147	
	D _{50%} (Gy)	22.8 ± 4.9	20.3 ± 5.3	20.1 ± 5.5	22.0 ± 6.1	22.2 ± 7.1	0.040	
Normal Tissue	D _{int} (x10 ⁴ Gy·cm ³)	8.0 ± 0.4	7.3 ± 0.6	7.2 ± 0.6	8.1 ± 0.6	8.3 ± 0.6	<0.001	VMAT3, ESB, VMAT2, > BAOc, BAOnc
	UTCI	1.80 ± 1.61	1.73 ± 1.48	1.99 ± 1.47	1.81 ± 1.87	1.73 ± 1.94	0.527	

HI = homogeneity index, CN = conformity number, D_{int} = integral dose, UTCI = uncomplicated target conformity index

Table 3.5. Comparison of PTVs, OARs dose parameters and integral dose between IMRT plans of 5 beam arrangements for cancer of maxilla sinus (n=19)

Structure	Dose Parameter	ESB (mean±SD)	BAOc (mean±SD)	BAOnc (mean±SD)	VMAT2 (mean±SD)	VMAT3 (mean±SD)	Repeated ANOVA P-Value	Post hoc test
PTVH	HI	0.06 ± 0.01	0.07 ± 0.02	0.07 ± 0.02	0.07 ± 0.02	0.07 ± 0.02	0.206	
	CN	0.87 ± 0.03	0.90 ± 0.02	0.90 ± 0.03	0.87 ± 0.03	0.88 ± 0.03	0.003	BAOc, BAOnc, VMAT3> VMAT2, ESB
PTVI	HI	0.08 ± 0.01	0.09 ± 0.02	0.09 ± 0.01	0.08 ± 0.03	0.08 ± 0.03	0.286	
	CN	0.79 ± 0.04	0.83 ± 0.06	0.83 ± 0.03	0.81 ± 0.03	0.79 ± 0.03	<0.001	BAOnc, BAOc, VMAT2> VMAT3, ESB
PTVL	HI	0.09 ± 0.01	0.10 ± 0.01	0.10 ± 0.01	0.09 ± 0.02	0.08 ± 0.02	0.001	BAOnc> BAOc, ESB, VMAT2 > VMAT3
	CN	0.77 ± 0.04	0.79 ± 0.05	0.79 ± 0.03	0.79 ± 0.05	0.78 ± 0.04	0.046	
Spinal cord	D _{2%} (Gy)	41.6 ± 2.2	40.7 ± 2.6	40.9 ± 2.7	41.7 ± 2.5	41.7 ± 2.7	0.044	
Brain stem	D _{2%} (Gy)	51.1 ± 2.1	51.6 ± 1.4	51.6 ± 1.4	50.9 ± 1.7	50.2 ± 3.7	0.266	
Parotid	D _{mean} (Gy)	25.7 ± 5.9	23.9 ± 6.4	23.6 ± 6.7	26.2 ± 6.0	26.3 ± 6.0	<0.001	VMAT3, VMAT2 > ESB, BAOc, BAOnc
	D _{50%} (Gy)	25.7 ± 6.2	25.0 ± 5.7	24.0 ± 6.2	26.6 ± 5.3	26.2 ± 5.7	0.008	
Normal Tissue	D _{int} (x10 ⁴ Gy·cm ³)	7.5 ± 0.8	6.6 ± 0.8	6.6 ± 0.8	7.3 ± 0.8	7.2 ± 0.8	<0.001	ESB> VMAT2, VMAT3> BAOnc, BAOc
	UTCI	0.74 ± 0.43	0.99 ± 0.62	1.10 ± 0.72	0.71 ± 0.40	0.71 ± 0.40	<0.001	BAOnc, BAOc> ESB, VMAT2, VMAT3

HI = homogeneity index, CN = conformity number, D_{int} = integral dose, UTCI = uncomplicated target conformity index

Table 3.6. Comparison of PTVs, OARs dose parameters and integral dose between IMRT plans of 5 beam arrangements for cancer of parotid gland (n=25)

Structure	Dose Parameter	ESB (mean±SD)	BAOc (mean±SD)	BAOnc (mean±SD)	VMAT2 (mean±SD)	VMAT3 (mean±SD)	Repeated ANOVA P-Value	Post hoc test
PTVH	HI	0.06 ± 0.01	0.06 ± 0.01	0.06 ± 0.01	0.07 ± 0.02	0.07 ± 0.01	0.296	
	CN	0.86 ± 0.04	0.88 ± 0.04	0.87 ± 0.4	0.86 ± 0.03	0.86 ± 0.03	0.263	
PTVI	HI	0.07 ± 0.03	0.07 ± 0.02	0.07 ± 0.02	0.09 ± 0.01	0.08 ± 0.02	0.070	
	CN	0.83 ± 0.05	0.87 ± 0.04	0.85 ± 0.03	0.84 ± 0.02	0.82 ± 0.03	0.090	
PTVL	HI	0.09 ± 0.02	0.09 ± 0.03	0.09 ± 0.04	0.10 ± 0.02	0.11 ± 0.03	0.045	
	CN	0.83 ± 0.05	0.84 ± 0.03	0.85 ± 0.04	0.82 ± 0.05	0.84 ± 0.03	0.242	
Spinal cord	D _{2%} (Gy)	34.5 ± 9.4	33.9 ± 8.3	34.2 ± 9.1	34.9 ± 8.9	34.5 ± 9.0	0.319	
Brain stem	D _{2%} (Gy)	35.7 ± 13.4	35.5 ± 12.9	35.5 ± 12.9	36.1 ± 13.2	36.5 ± 11.9	0.390	
Parotid	D _{mean} (Gy)	7.0 ± 3.3	6.5 ± 2.3	6.1 ± 2.4	6.9 ± 3.0	6.8 ± 3.2	0.274	
	D _{50%} (Gy)	8.0 ± 6.2	6.9 ± 4.0	6.8 ± 4.0	7.3 ± 4.4	7.5 ± 4.8	0.051	
Normal Tissue	D _{int} (x10 ⁴ Gy·cm ³)	8.7 ± 0.7	7.6 ± 1.1	7.7 ± 0.9	8.2 ± 1.1	8.3 ± 0.9	0.002	ESB > VMAT3, VMAT2, BAOnc, BAOc
	UTCI	4.55 ± 1.68	5.66 ± 1.72	5.68 ± 1.81	4.80 ± 1.53	4.88 ± 1.89	<0.001	BAOnc, BAOc, VMAT3, VMAT2 > ESB

HI = homogeneity index, CN = conformity number, D_{int} = integral dose, UTCI = uncomplicated target conformity index

3.4 Discussion

Each of the beam arrangement methods had their uniqueness in delivering the tumoricidal dose to the tumour. The equally spaced beam in the ESB method directed the IM beams evenly from all angles around the patient and was best in treatment of central uniform-shaped tumours. The VMAT methods shared similar characteristics but employed more beams from all angles round the patients and reduced the treatment time (Verbakel et al., 2009). Because of this, they were expected to deliver higher integral dose to normal tissues (Higby et al., 2016). The VMAT3 had the potential to produce more conformal dose distribution than VMAT2 but required one additional gantry rotation and therefore increased the treatment time. In this study, the BAO methods used 5-9 beams directed from selected angles. Beams that did not have contribution to the plan were eliminated and the beam angles could be tailor made for individual patients. As a result, the integral dose and total monitoring units (MU) were lower (Shukla et al., 2016). BAOnc had greater freedom to direct the beams to the patient compared with BAOc, but in the expense of longer treatment set up time. Overall, the clinical merit of the current study is that it provides evidence-based recommendations on the beam arrangement for planners to use in the 5 types of head and neck cancers.

3.4.1 Cancer of Nasopharynx

With regards to the target conformity and homogeneity, ESB performed better in PTVH and PTVI. This could be due to the fact that these target volumes were relatively less irregular in shape than the PTVL and, being more centrally situated at the skull, the evenly distributed intensity-modulated IM beams were able to produce relatively more conformal dose distribution.

Whereas for PTVL which extended to both sides of the neck, and was more irregular with an inverted U-shape (Figure 3.1), the BAOnc and VMAT plans demonstrated relatively better dose coverage. The main reason was that with the use of non-coplanar beams in BAO and the greater number of effective beam angles from VMAT, they were both more effective in creating conformal high dose volumes covering the irregular target. By the same argument, the OARs were better spared by these two beam arrangement methods (Tran et al., 2017). By combining the performance in the target volumes and OARs, it was logical to see BAOnc and VMAT3 achieved the relatively better plans among the five beam arrangement methods. Overall, however, the VMAT3 would be recommended because it would have a much shorter treatment delivery time compared to BAOnc.

3.4.2 Cancer of Oral Cavity

In terms of dose coverage to the target volume, VMAT plans in general performed better among the five beam arrangement methods as it demonstrated the highest CN in all the PTVs. Since the oral cavity was a relatively large structure, tumours could arise from different locations in the oral cavity ranging from periphery to centre. The results showed evidence that the VMAT beam arrangement was more flexible to deal with target volume location variation, and its average performance on target coverage was better than the other beam arrangements. Regarding the OARs, the spinal cord and brain stem were located at some distance from the target volume, their doses were relatively low and therefore their differences were small. For the parotid gland, BAO plans provided relatively better sparing and were able to keep the average mean dose below 26 Gy, which was reported to be within the acceptable range of tolerance dose (mean dose 25-30 Gy) (Ortholan, Benezery, & Bensadoun, 2010). Since the VMAT plans and BAO plans

performed better in target volume coverage and parotid gland sparing respectively, it was logical to see their plans achieve similar rank in the UTCI scores. Furthermore, since there was no significant difference between VMAT3 and VMAT2, the addition of extra arc in VMAT3 did not bring any dosimetric advantage and therefore was not necessary. Moreover, BAOc was adequate when compared with BAOnc as including non-coplanar beams did not significantly improve the plan quality. Taking the treatment time into consideration, VMAT2 would be recommended as it shared similar plan quality as the BAOc plans but offered shorter treatment time.

3.4.3 Cancer of Larynx

Target volumes in laryngeal cancer were more regular in shape and further away from OARs. All five beam arrangement methods performed well on this relatively simple target volume geometry. This was the reason why there was no significant difference in most of the dose parameters of the target volumes, OARs and UTCI scores. This implied that any one of the beam arrangement methods was effective in treating this cancer. It was worth noting that since the BAO plans restricted the number of beams to below 9, it delivered relatively lower integral dose which might reduce of risk of secondary cancer when compared to the VMAT plans. However, in terms of treatment delivery time, the VMAT plans would have the advantage.

3.4.4 Cancer of Maxillary Sinus

Since tumour of the maxillary sinus was usually located at one side of the head, the evenly distributed beams in ESB and VMAT would irradiate the contralateral structures such as the parotid gland. This phenomenon was reflected in the dosimetric results of the VMAT plans that delivered higher mean parotid gland doses. Besides, the BAO plans which allowed beams mainly

directed from the ipsilateral side performed better overall plan quality with the UTICI scores significantly higher than the other three methods. It is logical to consider whether the use of the partial arc VMAT which could also avoid the direct beam entry from the contralateral side could be comparable to the BAO plans. Unfortunately, it was one of the limitations of the current study that the use of the partial arc VMAT was not included, because it was intended to include only the beam arrangements that were applicable to all the types of head and neck cancer in the study. In the current study, VMAT has shown to have comparable results with BAO in the HI and CN of PTV and in the dose to brain stem and spinal cord. Although the advantage of the use of the partial arc VMAT in the cancer of maxillary sinus was not explicitly deduced, the use of partial arc VMAT could possibly achieve the comparable results as in the full arc VMAT while reducing the disadvantages attributable to the beam entry from the contralateral side. Therefore, the current results were not against the use of partial arc VMAT in the cancer of maxillary sinus.

3.4.5 Cancer of Parotid Gland

Target volumes of the parotid gland tumour usually followed a triangular shape and would not pose great difficulty to the various beam arrangements. This was reflected in the dosimetric results of the target volumes in which there was no significant difference in all the dosimetric parameters among the five beam arrangement methods. Similar to the maxillary sinus cancer, parotid tumour is situated at the lateral aspect of the head, this would be a disadvantage for the ESB and VMAT beam arrangement. Relatively higher doses were found in the contralateral parotid gland in these plans although the differences did not reach statistical significance. With the same reason as for the maxillary sinus cancer, the integral dose in the BAO plans were significantly lower, and this also led to an overall better UTICI scores in these two plans. This

was echoed the study by Yirmibesoglu et al (2011) who reported that 4-field ipsilateral IMRT techniques provided excellent coverage while maximally sparing the contralateral parotid gland and submandibular gland. As a result, BAOc plans would be recommended as it achieved the same plan quality as the BAOnc but offered simpler treatment setup procedure. Furthermore, by the same argument as stated for the cancer of maxillary sinus, the current study results were not against the use of partial arc VMAT in the cancer of parotid gland.

3.4.6 Comparison with Previous Literature

Compared with previous similar dosimetric studies, the current study is unique in the methodology by 1) inclusion of five beam arrangement methods, 2) grouping of head and neck cancers and 3) the use of UTCI for plan ranking. Firstly, previous studies either compared ESB with VMAT (Vanetti et al., 2009; Verbakel et al., 2009) or ESB with BAO (Rowbottom, Nutting, & Webb, 2001; Srivastava et al., 2011). Without the inclusion of the all three beam arrangement methods in one study, their results could not be used to interpret the relative strengths and weaknesses between VMAT and BAO. Secondly, previous studies either included only one type of head and neck cancer (Rowbottom et al., 2001) or mixing several types of head and neck cancers together in the comparison (Vanetti et al., 2009). In contrast, the current study classified the subjects into 5 types of head and neck cancers. The classification of samples into five types of cancers contributed to more clinically useful results. The five types of head and neck cancers represented major variation of the target position in terms of lateral-medial and supero-inferior within the head and neck region as illustrated in Figure 3.2. Because body profile, adjacent OARs and tissue density inhomogeneity are varied across the different sub-sites in the head and neck regions, it is logical to expect different performance of beam arrangement methods in these

selected cancers. Thirdly, the UTCI allowed the ranking of beam arrangement methods whereas previous studies which reported only on the dose parameters comparison could not achieve an overall ranking for recommendation.

There were similarities and differences between our results and the previous studies. Two studies reported that VMAT2 resulted in better PTV homogeneity than ESB in head and neck cancers (Vanetti et al., 2009; Verbakel et al., 2009) where in the current study, similar results were only found in PTVI and PTVL of NPC. In addition, it was reported that VMAT provided better sparing of the parotid gland (Johnston et al., 2011; Verbakel et al., 2009), brain stem (Johnston et al., 2011; Vanetti et al., 2009) and spinal cord (Vanetti et al., 2009) while the current study only obtained similar results in the parotid dose of the NPC and oral cavity cases. These discrepancies could possibly be attributed by the classification of cases in the current study, instead of grouping all head and neck cancers together for IMRT planning.

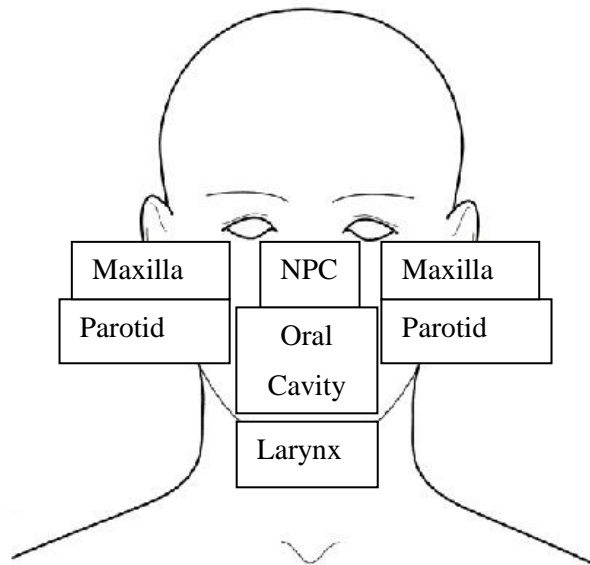


Figure 3.2. Illustration of the coverage of tumour position variations by the five types of head and neck cancers.

3.5 Conclusion

The five beam arrangement methods produced acceptable plans for all the five groups of head and neck cancer patients. Partial arc VMAT was not included in the beam arrangement methods because it was not commonly applied in centrally located cancers, therefore it could not be used in comparison among the five groups of head and neck cancers. The results showed that individual methods showed dosimetric advantages on certain aspects, and the UTCL scores were marginally greater in the BAO method in the cancers of the maxillary sinus and the parotid gland. However, if treatment time was included into consideration, VMAT plans would be recommended for cancers of nasopharynx (VMAT3), oral cavity and larynx (VMAT2).

Chapter 4

Study 2 – Dosimetric Evaluation of Maximum Deliverable Dose to GTV in IMRT of Locally Advanced NPC using Non-coplanar Beam Arrangement

This study was conducted to determine the maximum deliverable dose to GTV in radiotherapy of locally advanced NPC, in correspondence to objective 2 of the thesis.

4.1 Introduction

Radiotherapy treatment planning of locally advanced NPC is challenging because the disease is usually presented with base of skull, cranial nerve and/or intracranial involvements (Kwong et al., 2006). This means that the tumour is very close to critical OARs such as brain stem, temporal lobe, spinal cord and optic nerves. Hence, it is difficult to deliver enough dose to the tumour because it is limited by the dose tolerance of these OARs. This challenge has been reflected by the clinical outcome. In a local clinical study, the five-year relapse free survival (RFS) for stage I was as high as 95.7%, but it quickly dropped to 64.7% in stage II; and 54.5% and 41.1 % in stage III and IV respectively (D. T. T. Chua et al., 2001). Although there has been an improvement in survival by new radiation therapy techniques such as IMRT (A. W. M. Lee et al., 2014), local failures of treatment still occurred. When investigating the pattern of the relapse, it was reported that in the group of predominantly advanced local disease (T3-4 N0-1), the major cause was local relapse, which accounted for 61.8% of all failures (D. T. T. Chua et al., 2001). In this type of failure, the site of relapse was often at the area where the prescribed dose was delivered. This result was echoed

by another study which revealed that 80% of the recurrent cases had the relapse sites at the region of median dose 70.4 Gy in the previous treatment (Dawson et al., 2000a). A more recent study also reported that 78.4% of the recurrent NPC cases occurred in the nasopharynx (Zhao et al., 2016). These reports suggested the need of GTV dose escalation to tackle the problem of local relapse. Currently, NPC patients receive the radiotherapy dose of about 70 Gy to the PTV which involves gross tumour volume (GTV) and the dose of more than 50 Gy to the potential microscopically involved cervical lymph node regions (A. W. Lee et al., 2015). Despite not being a general clinical practice, escalation of radiation dose to the GTV is practiced in a few clinical centres (A. W. Lee et al., 2015). Clinical study has demonstrated that the dose-tumour control relationship existed when the GTV dose was above the current prescribed dose of 70 Gy (Teo et al., 2000). In fact, clinical report of dose escalation to GTV of NPC using brachytherapy (Chao et al., 2017) or IMRT (Kwong et al., 2006) has been reported to achieve better local control. However, the major limitation of dose escalation using IMRT is that it may exceed the tolerance doses of OARs and lead to more severe side effects. For example, it was reported that 80% of the patients developed grade 3 mucositis and 42% had hearing loss (Kwong et al., 2006). Nevertheless, the clinical result of good local control and the improved disease-free survival warranted the practice of dose escalation of radiotherapy in NPC.

Because it has been shown in study 1 that IMRT using BAOnC could achieve better OAR sparing in IMRT of NPC, it is worth to conduct a study to evaluate whether the use of BAOnC can overcome the limitation of increasing OAR dose in GTV dose escalation plans. In this study, the aim is to evaluate the capability of IMRT using BAOnC to escalate the dose to GTV of NPC cases. The capability is quantified by deducing the maximum deliverable dose to the GTV, which in turn is

determined by comparing the dosimetric outcome of the plans with escalated GTV dose a to the plan with the original prescription.

4.2 Materials and Methods

4.2.1 Patient Selection and Plan Specification

A total of 25 locally advanced NPC patients treated by IMRT were randomly selected. Using G*Power software (Heinrich Heine University, version 3.1.9.4) with an effect size of 0.6 and an alpha value of 0.05, the power of 0.821 was calculated for a sample size of 25. It showed that with the sample size, the statistical test had 82.1% chance to detect the effect if the differences of dose parameters among plans of different GTV dose were true (Type II error), while there was a 5% chance to detect the effect where the differences were untrue (Type I error). All the retrieved patients were locally advanced NPC with AJCC staging of T3 to T4 and N0 to N1. The patient demographics are listed in Table 4.1 (P. 72). Ethical approval was obtained from the Hong Kong Polytechnic University and the Princess Margaret Hospital. To ensure confidentiality of the selected patients, the patient identifiers, such as name and registration number, were completely removed by an assigned study number and requirements of the Personal Data (Privacy) Ordinance was adhered to.

Table 4.1 Patient demographics

Patient demographics	Number of patients
Gender	
Male	19
Female	6
Age	
0-34	0
35-64	21
65-84	2
>84	2
Tumour classification	
T1	0
T2	0
T3	19
T4	6
Lymph node status	
N0	18
N1	7
N2	0

The original prescription of the plans was 70 Gy to high risk PTV (PTVH), 60 Gy to intermediate risk PTV (PTVI) and 54 Gy to low risk PTV (PTVL), delivered using simultaneous integrated boost over 33 fractions. The PTVH encompassed the GTV and involved lymph nodes, whereas the PTVI and the PTVL involved the selective nodal regions and the isotropical expansion of the PTVH respectively. The PTVs were contoured by the oncologist in-charge and the OARs were contoured by the planner. Three hypothetical plans were computed for each patient using the Eclipse treatment planning system Version 13.6 (Varian Medical System, Palo Alto, US) by the same planner to compare with the original plans. The Anisotropic Analytical Algorithm (Version 13.6.23) was used for volume dose calculation and the Photon Optimizer (Version 13.6.23) was used for optimization. Among the four plans for comparison (3 hypothetical plans and 1 original plan), the original plan (GD₇₀) had the prescription of 70 Gy for the GTV whereas the others were GTV dose escalated plans. While keeping the dose to the PTVs and the number of fractions

unchanged, the escalated GTV dose of the three GTV dose escalated plans were 76 Gy (GD₇₆), 78 Gy (GD₇₈) and 80 Gy (GD₈₀) respectively. Details of the dose prescription for the four plans are listed in Table 4.2.

Table 4.2. List of prescribed dose to the targets in the four hypothetical plans

Plan	GTV		PTVH		PTVI		PTVL	
	Tol. dose (Gy)	Dose/F (Gy)	Tol. dose (Gy)	Dose/F (Gy)	Tol. dose (Gy)	Dose/F (Gy)	Tol.dose (Gy)	Dose/F (Gy)
GD ₇₀	70	2.12	70	2.12	60	1.82	54	1.64
GD ₇₆	76	2.30	70	2.12	60	1.82	54	1.64
GD ₇₈	78	2.36	70	2.12	60	1.82	54	1.64
GD ₈₀	80	2.42	70	2.12	60	1.82	54	1.64

GTV = gross tumour volume; PTVH = high risk planning target volume; PTVI = intermediate risk planning target volume; PTVL = low risk planning target volume; Tol. Dose = total dose; Dose/F = dose per fraction.

The OARs concerned in the treatment planning were included by following local planning guideline as listed in Table 4.3 (P. 74). Equally spaced beam arrangement using 9 beams, which was the clinical routine in local department, was used for the GD₇₀ plans, whereas the non-coplanar beam angle optimization (BAOnc) was used for the plan GD₇₆, GD₇₈, and GD₈₀. All treatment plans were planned with 6 MV photon and Millennium MLC. The Anisotropic Analytical Algorithm (Version 13.6.23) was used for volume dose calculation and the Photon Optimizer (Version 13.6.23) was used for optimization. The priorities of the objective functions for the structures were ranked, from the highest to the lowest, as follows: 1. Brain stem, spinal cord; 2. PTVs; 3. Other OARs. It is the local institutional practice to use higher priority in brain stem and spinal cord than PTVs as they are the critical OARs. Because the GTV dose escalated plans (GD₇₆, GD₇₈, GD₈₀) were compared with the original plan (GD₇₀) of the retrieved patients, it was intended

to use the same rationale of objective function setting for fair comparison. Otherwise, a significant increase in the dose of spinal cord and brain stem would be resulted.

Table 4.3. Dose parameters for OARs and the local OARs tolerances guideline

OAR	Dose parameter	Tolerance
Critical OAR		
Brain stem	D _{2%}	<54 Gy
Spinal cord	D _{2%}	<45 Gy
Other OAR		
Optic nerve	D _{2%}	<54 Gy
Optic chiasm	D _{2%}	<54 Gy
Eyeball	D _{2%}	< 45Gy
Lens	D _{2%}	< 10 Gy
Pituitary	D _{2%}	< 65 Gy
Temporal lobe	D _{2%}	< 67Gy
Parotid gland	D _{mean}	< 26 Gy
	D _{50%}	< 30 Gy
Cochlea	D _{2%}	< 58 Gy
Brachial plexus	D _{2%}	< 63 Gy

4.2.2 Plan Evaluation and Statistical Analysis

Plans were evaluated by the dose parameters generated from the dose volume histogram (DVH) of each structure. 95% of the PTVs and GTV should be covered by the prescribed dose. The

homogeneity index (HI) (Grégoire & Mackie, 2011) and conformation number (CN) (Riet et al., 1997) were generated in addition to the dose coverage. For the GTV in plan GD₇₀, because the prescription of the GTV is the same as the PTVH, the dose parameters were not separately evaluated and recorded. For the OARs, following the local planning guideline in Table 4.3 (P. 74), D_{2%} was used as the dose parameter for evaluation except the parotid gland, in which the D_{50%} and the D_{mean} were used.

The procedure of plan evaluation of statistical analysis is illustrated in Figure 4.1. The maximum deliverable dose was defined as the highest GTV dose that achieve acceptable PTVs and GTV dose coverage, HI and CN; with no significant increase in OARs dose. After plan evaluation, statistical analysis was performed using the SPSS version 20 (IBM Corp, Armonk, NY), with the aim to evaluate the maximum deliverable dose to the GTV. All the dose parameters were first tested for normality using the Shapiro-Wilk test. Paired sample t-test was used to analyze the differences of the mean dose parameters of all OARs between hypothetical plans and the original plan, except those for brain stem and spinal cord. Brain stem and spinal cord dose parameters were excluded as they were set as the highest priority in the optimization process, so their dose parameters were expected to be unaffected despite an increase in GTV dose. However, because of the proximity of the brain stem, spinal cord, PTVs and GTV in NPC cases, keeping the dose parameters of brain stem and spinal cord within tolerance might lead to sub-optimal dose coverage in PTVs and GTV. Therefore, it is important to evaluate whether the dose coverage, CN and HI of the PTVs and GTV achieved acceptable levels in the GTV dose escalated plans (GD₇₆, GD₇₈, GD₈₀).

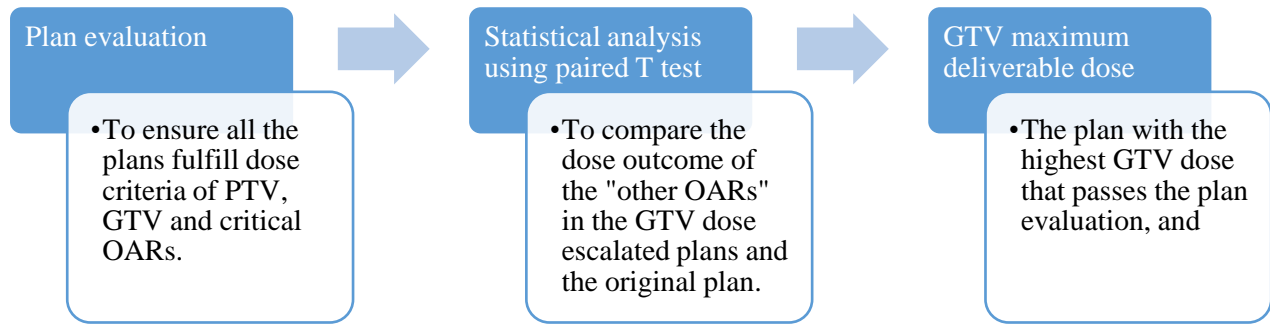


Figure 4.1. Plan evaluation and statistical analysis procedure

4.3 Results

4.3.1 Doses delivered to PTVs, GTV, spinal cord and brain stem

All the plans fulfilled dose coverage requirement of the PTV and GTV that 95% of the volume was covered with the prescribed dose. Table 4.4 (P. 78) shows the mean $D_{2\%}$, $D_{98\%}$, HI and CN for the PTVs and GTV. All the mean $D_{2\%}$ and $D_{98\%}$ were very close to the prescribed dose. For example, the mean $D_{2\%}$ of the GTV were 103.3%, 103.4% and 103.5% of the prescribed dose for the GD₇₆, GD₇₈ and GD₈₀ plans respectively. Whereas for the mean $D_{98\%}$, they accounted for 99.5%, 99.1% and 98.7% of the prescribed dose of the GD₇₆, GD₇₈ and GD₈₀ plans respectively. The values of $D_{98\%}$ and $D_{2\%}$ were used to calculate HI. The HI of all the 4 plans were very similar and it ranged from 0.037 to 0.048 in GTV. In addition, the conformity indices of PTV and GTV in all the plans were also very similar, with the range of 0.847 to 0.866 in PTVH.

Furthermore, Table 4.5 (P. 79) lists the dose parameters of the brain stem and spinal cord in the 4 plans. The mean $D_{2\%}$ of the brain stem in all the 4 plans were all close to 52 Gy. This was less than the dose tolerance of 54 Gy and there were no significant difference among the 4 plans. For the spinal cord, the mean $D_{2\%}$ in the 4 plans were around 41 Gy which were lower than the dose tolerance of 45 Gy.

Because the GTV volume of $\geq 3.5 \text{ cm}^3$ with less than 66.5 Gy was reported to be a prognostic factor of NPC IMRT (Ng et al., 2014), the minimum dose of the GTV in all the 25 patients is listed in Table 4.6 (P.80). There were 2 cases with GTV minimum dose less than 66.5 Gy, but the volumes of $< 66.5 \text{ Gy}$ were less than 0.1 cc.

4.3.2 Doses delivered to the other OARs

The mean dose parameters of the OARs are listed in Table 4.5 while the paired sample t-test comparison of the dose parameters of these OARs between the GTV dose escalated plans and the original plan are listed in Table 4.7 (P.81). The results showed that there was no significant difference in the GTV dose escalated plans compared with the original plan for the dose parameters of parotid gland, optic nerve, optic chiasm, cochlea and brachial plexus. However, there was statistically significant increase in the dose parameters for the lens, pituitary and temporal lobe in the GD₇₆, GD₇₈, and GD₈₀ plan compared with the original plan (GD₇₀). In these 3 OARs, there was a trend of progressively increasing dose parameters with the GTV dose prescription from 76 Gy to 80 Gy. For instance, the pituitary mean D_{2%} was increased by 1.520 Gy, 2.055 Gy and 2.538 Gy in the GD₇₆, GD₇₈ and GD₈₀ plans respectively.

On the other hand, the dose parameters of eyeball significantly decreased in the GTV dose escalated plans compared with the original plans. The magnitude of the decrease of eyeball dose reduced as the GTV dose increased.

Table 4.4 GTV and PTV coverage, HI and CN

Target volume		GD₇₀ (mean±SD)	GD₇₆ (mean±SD)	GD₇₈ (mean±SD)	GD₈₀ (mean±SD)
PTVH	D _{2%} (Gy)	72.4±0.3	73.0±0.7	73.5±0.9	74.0±1.2
	D _{98%} (Gy)	69.7±0.2	69.6±0.4	69.6±0.3	69.4±0.2
	HI	0.04±0.01	0.05±0.02	0.06±0.02	0.06±0.02
	CN	0.87±0.02	0.86±0.02	0.86±0.02	0.85±0.02
PTVI	D _{2%} (Gy)	65.7±0.3	65.8±0.4	65.8±0.4	65.9±0.4
	D _{98%} (Gy)	59.0±0.4	58.9±0.4	58.9±0.4	58.8±0.4
	HI	0.11±0.01	0.11±0.01	0.11±0.01	0.11±0.01
	CN	0.86±0.02	0.84±0.03	0.84±0.02	0.84±0.02
PTVL	D _{2%} (Gy)	57.6±0.4	57.3±0.3	57.3±0.2	57.2±0.05
	D _{98%} (Gy)	53.6±0.4	54.1±0.3	54.1±0.3	54.1±0.3
	HI	0.07±0.01	0.06±0.01	0.06±0.01	0.06±0.02
	CN	0.69±0.03	0.67±0.03	0.67±0.03	0.67±0.03
GTV	D _{2%} (Gy)		78.5±0.5	80.6±0.6	82.8±0.5
	D _{98%} (Gy)		75.6±0.2	77.3±0.2	78.9±0.3
	HI		0.04±0.01	0.04±0.01	0.05±0.01
	CN		0.78±0.04	0.79±0.04	0.78±0.04

Table 4.5. OARs dose parameters and integral dose between plans with different prescription

Structure	Dose parameter	GD₇₀ (mean±SD)	GD₇₆ (mean±SD)	GD₇₈ (mean±SD)	GD₈₀ (mean±SD)
Spinal cord	D _{2%} (Gy)	40.7±1.1	41.3±1.9	41.2±2.0	41.1±2.0
Brain stem	D _{2%} (Gy)	52.2±0.9	52.2±1.0	52.2±1.1	52.2±1.1
Parotid	D _{mean} (Gy)	34.0±3.8	33.9±3.9	33.8±3.9	33.9±3.9
	D _{50%} (Gy)	29.1±5.2	28.9±5.1	28.9±5.0	29.0±4.9
Optic nerve	D _{2%} (Gy)	55.4±5.0	55.8±4.5	55.8±4.2	55.7±4.5
Optic chiasm	D _{2%} (Gy)	55.5±5.7	56.0±4.4	56.1±4.5	56.1±5.6
Lens	D _{2%} (Gy)	6.6±3.6	8.1±4.9	8.2±4.8	8.4±4.7
Eyeball	D _{2%} (Gy)	27.7±10.9	22.2±10.6	22.4±10.6	22.7±10.5
Pituitary	D _{2%} (Gy)	65.2±6.5	66.7±8.0	67.3±8.5	67.8±9.1
Temporal lobe	D _{2%} (Gy)	63.7±5.0	64.4±5.9	64.6±6.2	64.8±6.6
Cochlea	D _{2%} (Gy)	59.1±7.2	58.7±9.4	59.1±8.7	59.6±8.3
Brachial plexus	D _{2%} (Gy)	60.8±1.5	61.0±1.6	61.0±1.6	61.0±1.6

Table 4.6 GTV minimum dose in all 25 recruited cases

Case ID	GD70		GD76		GD78		GD80	
	Minimum Dose (Gy)	Vol < 66.5 Gy (cc)	Minimum Dose (Gy)	Vol < 66.5 Gy (cc)	Minimum Dose (Gy)	Vol < 66.5 Gy (cc)	Minimum Dose (Gy)	Vol < 66.5 Gy (cc)
1	72.4	0	74.2	0	75.5	0	76.4	0
2	69.7	0	74.2	0	75.3	0	76.3	0
3	70.0	0	73.9	0	75.3	0	76.3	0
4	68.2	0	69.8	0	72.3	0	73.2	0
5	69.7	0	73.6	0	74.5	0	75.8	0
6	69.0	0	72.9	0	75.2	0	76.6	0
7	69.8	0	74.4	0	75.5	0	76.2	0
8	67.5	0	70.2	0	71.5	0	72.6	0
9	68.2	0	71.8	0	73.8	0	75.1	0
10	69.9	0	73.6	0	75.0	0	76.2	0
11	69.8	0	72.8	0	74.7	0	75.7	0
12	69.4	0	73.4	0	74.7	0	75.7	0
13	66.3	0.1	65.9	0.1	66.2	0.1	66.4	0.1
14	69.9	0	72.6	0	73.6	0	74.6	0
15	69.7	0	73.2	0	74.4	0	75.8	0
16	69.8	0	74.0	0	74.7	0	75.4	0
17	68.5	0	70.2	0	71.4	0	73.0	0
18	69.0	0	71.5	0	72.3	0	73.7	0
19	69.7	0	71.5	0	72.0	0	72.5	0
20	69.7	0	73.2	0	75.0	0	76.8	0
21	66.6	0	69.4	0	69.7	0	70.7	0
22	62.5	0.1	62.9	0.1	63.2	0.1	62.8	0.1
23	69.7	0	73.9	0	75.2	0	76.5	0
24	69.6	0	68.6	0	70.1	0	70.6	0
25	69.5	0	73.9	0	74.8	0	76.2	0

Table 4.7. Paired sample t-test results.

Structure	Dose parameter	Pair group					
		GD ₇₀ vs. GD ₇₆		GD ₇₀ vs. GD ₇₈		GD ₇₀ vs. GD ₈₀	
		Difference Mean±SD	p	Difference Mean±SD	p	Difference Mean±SD	p
Parotid	D _{mean} (Gy)	0.047±0.768	0.671	0.109±0.785	0.329	0.507±0.767	0.643
	D _{50%} (Gy)	0.104±0.814	0.373	0.162±0.834	0.176	0.506±0.823	0.630
Optic nerve	D _{2%} (Gy)	0.429±2.569	0.244	0.367±2.716	0.343	0.299±1.994	0.294
Optic chiasm	D _{2%} (Gy)	0.443±2.243	0.333	0.548±2.321	0.249	0.580±2.329	0.225
Lens	D _{2%} (Gy)	1.560±4.126	0.011	1.706±4.051	0.005	1.859±3.951	0.002
Eyeball	D _{2%} (Gy)	-5.407±7.209	<0.001	-5.243±7.281	<0.001	-4.969±7.168	<0.001
Pituitary	D _{2%} (Gy)	1.520±2.294	0.003	2.055±2.936	0.002	2.538±3.543	0.002
Temporal lobe	D _{2%} (Gy)	0.731±1.777	0.005	0.917±2.131	0.004	1.073±2.498	0.004
Cochlea	D _{2%} (Gy)	0.469±4.866	0.499	0.086±3.222	0.851	0.396±2.088	0.186
Brachial plexus	D _{2%} (Gy)	0.115±0.696	0.249	0.129±0.790	0.256	0.130±0.714	0.203

Bold font=result with statistical significant difference, negative sign (-) = dose parameters of the OAR decrease in the GTV dose escalated plans compared with the original plan, positive sign (+) = dose parameters of the OAR increase in the GTV dose escalated plans compared with the original plan

4.4 Discussion

The aim of this study is to investigate whether the use of BAOnc can keep the OARs doses below their tolerance in the GTV dose escalated plans compared with the original plans in IMRT of NPC. This in turn deduced the maximum deliverable dose to the GTV that would not increase the dose to the OARs when compared with the plan with original prescription. The results of this study suggested that BAOnc could generate plans that fulfilled the criteria to deliver conformal and homogeneous dose to the targets without overdose to the brain stem and spinal cord. In addition, there was no difference in the dose to parotid gland, optic nerve, optic chiasm, cochlea and brachial plexus, and even a statistical decrease in the dose to the eyeball when compared the original plan with the GTV dose escalated plans. However, the lens, pituitary gland and temporal lobe showed significant increase of dose when compared the original plan with the GTV dose escalated plans.

Although there were several OARs which showed no significant difference in the GTV dose escalated plans, some of the OARs, including the lens, pituitary gland and temporal lobe, showed significant increase in the dose parameters of the GTV dose escalated plans. Therefore, the plans with escalated GTV dose would inevitably impose unwanted clinical outcome to the corresponding OARs if the plans were to be delivered to real patients. Although the current study did not investigate the clinical outcome on real patients, the impact of the increase of dose in these three OARs can be discussed based on the dosimetric outcome. Firstly for the pituitary gland, the level of dose exceeded its tolerance might lead to radiation induced hypopituitarism and pituitary hormone deficiencies (K. S. L. Lam, Tse, Wang, Yeung, & Ho, 1991). However, this has already been a common late side effect for NPC patients treated with the original prescription of 70 Gy (Ratnasingam et al., 2015). It is because pituitary gland is situated close to the high dose region in

radiotherapy of NPC (Sze et al., 2019). These patients with post-radiotherapy endocrine disturbance due to hypopituitarism was manageable using hormone supplement (Lue, Huang, & Chen, 2008). In order to achieve good disease control by delivering enough dose to the targets, dose delivered to pituitary gland sometimes was allowed to exceed the tolerance (Ng et al., 2014). Secondly for the lens and the temporal lobe, although our results showed dose increase in these structures in the escalated plans, their mean $D_{2\%}$ did not exceed their tolerance doses, which were 10 Gy for the lens and 67 Gy for the temporal lobe. Therefore it was unlikely that they will develop complications such as cataract and temporal lobe necrosis respectively. In addition, a similar dose escalation study on NPC reported a mean $D_{2\%}$ of the temporal lobe greater than 68 Gy (Kwong et al., 2006), which was higher than that from our study (less than 65 Gy).

Furthermore, the eyeballs showed decrease dose in the GTV dose escalated plans compared with the original plan. The decrease could be attributed to the non-coplanar beam arrangement which had a greater freedom of beam angle choice to avoid beam entry on the eyeball compared with ESB. The eyeballs, alongside with the other OARs which showed no significant different dose parameters, revealed the superior ability of the use of BAOnc for the GTV dose escalation compared with ESB used in the reference plan. In a similar previous dose escalation study which utilized ESB-9 beam arrangement IMRT in head and neck cancers, the V_{30} of the parotid gland increased from 48% to 62% for the plans with the prescription of 68.1 Gy and 73.8 Gy (both over 30 fractions) respectively (Lauve et al., 2004). In contrast, the dosimetric result of the parotid in the current study did not show any statistical significant increase with an even higher escalated GTV dose of 80 Gy.

In summary, the major concern for GTV dose escalation is the dose to the pituitary gland. Dose escalation of the GTV should be cautious because the pituitary dose might exceed the tolerance. Although sacrificing the pituitary gland is sometimes justified for some advanced NPC cases for the purpose to deliver enough dose to the targets (Ng et al., 2014), it is not sure whether the benefit of GTV dose escalation outweigh the cost of pituitary gland overdose in all patients with locally advanced disease. Therefore, it is suggested a set of logical case selection criteria should be developed to get the maximum benefit of dose escalation. This will be discussed in section 6.4.2 in Chapter 6.

4.5 Conclusion

With the use of beam arrangement BA_{Onc}, it was able to produce GTV dose escalated IMRT plans in NPC cases up to 80 Gy with acceptable dose coverage, conformity and homogeneity for PTVs and GTV. Most of the OARs dose parameters did not show any significant increase when comparing the original plans and the GTV dose escalated plans. The results suggested that GTV dose escalation in NPC radiotherapy could be escalated to 80 Gy on condition that the pituitary gland is considered sacrificed and the lens and temporal lobe dose is kept within their tolerance.

Chapter 5

Study 3 - Development of Regression Model to Determine Reference OARs Doses from Anatomical Parameters in IMRT Treatment Planning of Nasopharyngeal Cancer

This study was conducted to develop a model to address the relationship between the OAR dose parameters and anatomical parameters in the IMRT of NPC, in correspondence to objective 3.

This study has been submitted for publication in the Journal of Medical Radiation Science and is under revision.

5.1 Introduction

Radiotherapy is the primary treatment for nasopharyngeal carcinoma (NPC). Sparing of organs at risk (OARs) from cancericidal radiation dose has been one of the major concerns in treatment planning because irradiation of the OARs may cause irreversible late side effects to the patients. These irreversible late side effects include xerostomia, ototoxicity and neurotoxicity (Chen et al., 2013; Tao et al., 2014). This concern has been increased with the advances in treatment technique using intensity modulated radiotherapy (IMRT) and the use of chemo-radiotherapy, which attribute to the increase of long-term survival in both early stages and loco-regional advanced NPC patients (M. L. K. Chua et al., 2016). As the life expectancy of post-radiotherapy patients becomes longer, their quality of life, which can be degraded by the irreversible late side effects, should be well addressed. OARs radiation dose sparing is therefore an important issue in radiotherapy (Hawkins, Kadam, Jackson, & Eisbruch, 2018).

Currently in radiotherapy planning of NPC, the doses to OARs are based on the guidelines of acceptable doses to individual organs (Sze et al., 2019). While the relationship of radiation dose and occurrence of OARs side effects has not been fully understood, these guidelines are based on the best understanding of a safe dose to be delivered from past clinical experience (Sze et al., 2019). However, the guidelines may not represent the optimal dose of the OARs to be delivered for individual patients because achieving lower OARs dose is often at the expense of adequate dose coverage of the planning target volumes (PTV). Therefore, although the guidelines represent the safe dose to the OARs, it does not necessarily tailor made for individual patients' conditions. With no other better option, the OARs dose in the routine clinical guidelines are often used during treatment planning and they are input as objective functions in initial optimization of IMRT plans (Chau et al., 2008). Planners can then adjust the objective functions for OARs for minimizing their doses, which may however compete with the aim to achieve adequate PTV dose coverage. Therefore, the generation of an optimal plan depends on the planners' experience, and the final OARs doses in the plan are therefore subject to variability among planners (Nelms et al., 2012).

Various models for OARs dose estimation in treatment planning have been proposed and their contributions in IMRT planning have been discussed (Appenzoller, Michalski, Thorstad, Mutic, & Moore, 2012; Moore, Brame, Low, & Mutic, 2011; B. Wu et al., 2009; Yuan et al., 2012). In general, some models correlated the OARs dose with the distance of the corresponding OARs to the PTV (Appenzoller et al., 2012) while the others correlated the OARs dose with the volume of the corresponding OARs overlapping with the PTV (Moore et al., 2011; B. Wu et al., 2009); and in addition there were models which incorporated both the corresponding distances and volumes (Yuan et al., 2012). In these studies, the effort was made with the aim to deduce the OARs dose

based on the corresponding distances and volumes based on past optimized plans. The current study is unique in a way that it uses a different model to establish the relationships between the OARs doses and the anatomical parameters using multiple regression algorithm. First, the model was based on specially generated IMRT plans with the aim to optimize the OARs dose. Second, the determined reference OARs dose was in the form of the dose metrics in OARs dose guidelines, such the $D_{2\%}$ for spinal cord (Sze et al., 2019). Furthermore, it was hypothesized that the OAR doses were related to the anatomical parameters including their volumes and respective distances from the PTV. The model is expected to be able to provide guidance for planners before the IMRT optimization as a reference dose and method for the assessment of optimal OARs doses after completion of plan optimization.

5.2 Materials and Methods

5.2.1 Subjects Selection and IMRT Plans Specifications

A total of 70 adult NPC patients previously treated by radical IMRT were randomly recruited. Among the 70 subjects, 45 of them were randomly selected as training dataset and the other 25 subjects were assigned as validation dataset. Using G*Power software (Heinrich Heine University, version 3.1.9.4) F-test with an effect size of 0.25 and an alpha value of 0.05, the power of 0.83 were calculated for a sample size 45 for training dataset. It showed that with the sample size, the statistical test had 83% chance to have a significant model of dosimetric and anatomical parameters relationship when it was true (Type II error), while there was a 5% chance to have a significant model where the relationships were untrue (Type I error). The demographics and distributions of the T and N stages of the patients are summarized in Table 5.1. Ethical approval was obtained from the Hong Kong Polytechnic University and the Princess Margaret

Hospital. To ensure confidentiality of the selected patients, the patient identifiers, such as name and registration number, were completely removed by an assigned study number and requirements of the Personal Data (Privacy) Ordinance was adhered to.

The prescription was 70 Gy in 33-35 fractions for high risk planning target volume (PTV) (PTVH) that encompassed the primary tumour and positive cervical nodal involvement. The other two PTVs were intermediate risk PTV (PTVI) and low risk PTV (PTVL) in the cervical nodal region and their prescribed doses were 60 Gy and 54 Gy respectively. All the PTVs were treated using simultaneously integrated boost. A hypothetical plan was computed for each patient using the Eclipse treatment planning system Version 13.6 (Varian Medical System, Palo Alto, US) by the same planner. The IMRT plans were generated with 6 MV photon and Millennium multi-leaf collimator (MLC). Each plan employed 9 equally spaced beams at 40° apart. The Anisotropic Analytical Algorithm (Version 13.6.23) was used for volume dose calculation and the Photon Optimizer (Version 13.6.23) was used for optimization. The training dataset was used to provide data for the multiple regression analysis and to establish the multiple regression model, while the validation dataset was used to provide data to validate the established model.

Table 5.1. Subjects characteristics

	Model Training Group (n=45)	Model Verification Group (n=25)
Gender		
Male	35	19
Female	10	6
Age		
0-34	1	0
35-64	32	21
65-84	12	2
>84	0	2
Tumour classification		
T1	5	0
T2	10	0
T3	22	19

T4	8	6
Lymph node status		
N0	19	18
N1	11	7
N2	15	0

5.2.2 Generation of IMRT plans

The same set of dose objective functions according to the institutional dose constraint protocol as listed in Table 5.2 were used in the initial optimization of all the plans. After the initial optimization and dose calculation, to ensure the OARs doses were optimized and tailor made according to different geometric relationship to the PTV in different patients, pseudo-structures were added to further reduce the OARs dose. These pseudo-structures were added with the aim to achieve the steep dose reduction gradient at the PTV-OARs interface at its maximum

Table 5.2. Dose constraint protocol of PTV and OAR dose for IMRT of NPC

Structure Name	1 st Goal	2 nd Goal
OAR		
Brain stem	Max 54 Gy	Max 60 Gy
Spinal cord	Max 45 Gy	Max 50 Gy
Optic chiasm	Max 54 Gy	Max 60 Gy
Optic nerve	Max 54Gy	Max 60 Gy
Temporal lobe	Max 67 Gy	Max 70 Gy
Parotid gland	Mean 26 Gy	50% volume (D_{50%}) 30 Gy
Cochlea	Max 58 Gy	
Lens	Max 6 Gy	Max 10 Gy
Eye ball	Max 45 Gy	

Brachial plexus	Max
	66 Gy
PTV	
95% volume (D ₉₅)	>= prescribed dose
20% volume (D ₂₀)	<= 110% of prescribed dose

Max = maximum

capability of 20 cGy/mm.(Moran, Radawski, & Fraass, 2005) This was done by converting the chosen isodose line into pseudo-structure at the PTV-OAR interface and then cropping the pseudo-structure with a respective distance from the PTV according to the maximum capable dose reduction gradient. The choice of isodose levels to be converted was based on the dose tolerance as stated in the OARs dose constraint protocol in Table 5.2. Taking the example of creating pseudo-structures for parotid glands as illustrated in Figure 5.1, 26 Gy isodose line was converted into pseudo-structures at the parotid-PTVI interface. Since the dose difference between PTVI (prescribed at 60 Gy) and the pseudo-structure (aim at restricting the 26 Gy) was 34 Gy, the isodose structure was cropped against PTVI with a distance of 17 mm (calculated by dividing 3400 cGy by 20 cGy/mm). The objective function of the pseudo-structures in the example would be to limit the maximum dose to less than 26 Gy. For the other OARs, the pseudo-structures were created using the same principle. As a result, the IMRT plans would be re-optimized to achieve better quality plans with more optimal OARs sparing.

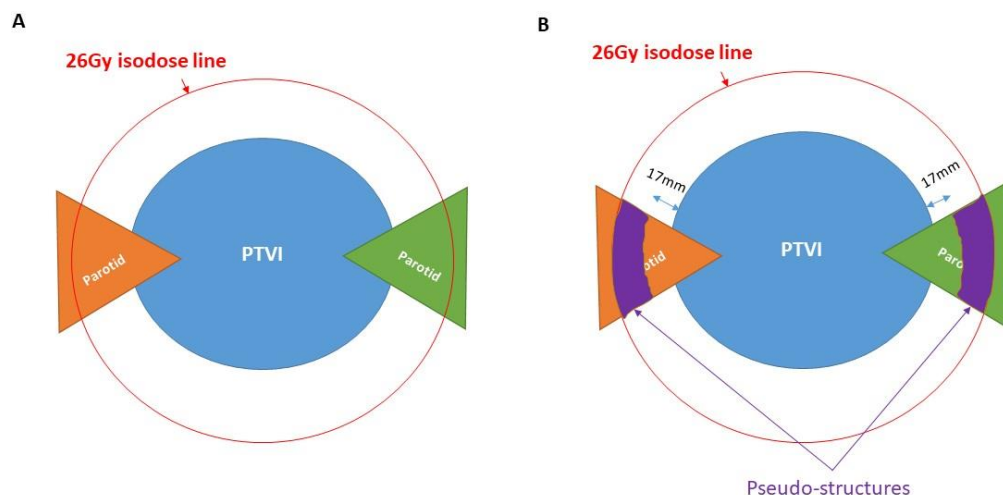


Figure 5.1 Schematic diagram of the creation of pseudo-structures to optimize the dose to parotid glands. (A) The dose distribution was calculated after initial optimization with the use of objective function according to the institutional dose constraint protocol. (B) The pseudo-structures were created by 2 steps: first, converting the 26 Gy isodose line into a structure at the PTV-parotid interface. Second, cropping the pseudo-structure by a distance with reference to the best achievable dose gradient steepness.

5.2.3 Data Acquisition

The proposed multiple regression model required the acquisition of two types of data, namely the dose parameters data and the anatomical parameters data. The dose parameters were the respective maximum dose (denoted as $D_{2\%}$ as recommended by ICRU report 83 ("Report 83," 2016)), mean dose (D_{mean}) and dose received by 50% volume ($D_{50\%}$) of OARs. They were chosen with reference to the OAR dose constraint protocol in the clinical practice as listed in Table 5.2. On the other hand, the anatomical parameters consisted of the volume measurement and distance measurement. The volume measurements included the OAR volume overlapping with PTV and the OAR volume outside PTV. The distance measurement referred to the distance between the OAR and the PTVs. The volumes were measured using the built-in volume measuring function of the Eclipse treatment planning system. The measurement of distance in 3-dimensional manner was carried out by expanding the volume of the OAR isotropically stepwise until it touched the

PTV. Then the magnitude of the OAR expansion was taken as the distance between the two structures. All the dose parameters and anatomical parameters acquired for the OARs are listed in Table 5.3. For the purpose of maximizing the sample size, in the paired organs, including the optic nerve, lens, eyeball, cochlea, temporal lobe and brachial plexus, each side of the pair in one subject was considered as an individual sample. As a result, the actual total sample size in the training dataset of the paired organs was 90. For the spinal cord, 5 samples were taken from each subject in which each sample represented the spinal cord in the first, second, third, fourth and fifth cervical vertebrae. Because of this, the total sample size in the training dataset of the spinal cord was 225.

Table 5.3 summarizes the dose parameters and anatomical parameters collected for the corresponding OARs. As the geometric relationships between various OARs and the PTVs were different, the anatomical parameters used for each OARs were not the same. For instance, the anatomical parameters related to volumes were only used for those OARs that had overlapping with the PTVs. Also, the OAR to PTV distance would be omitted if the distance was more than 5

Table 5.3. Dose parameters and anatomical parameters used for model training.

	OAR group 1	OAR group 2	OAR group 3
OAR	Brain stem	Temporal lobe	Parotid gland
	Spinal cord	Brachial plexus	
	Optic chiasm		
	Optic nerve		
	Lens		
	Eyeball		
	Cochlea		
Dose	D _{2%}	D _{2%}	D _{mean}
Parameters			D _{50%}

Anatomical	Distance from PTVH	Distance to PTVH	Distance to PTVH
Parameters	Distance from PTVI	Distance from PTVI	Distance from PTVI
	Distance from PTVH	Distance from PTVH	Distance from PTVH
	Distance from PTVI	Distance from PTVI	Distance from PTVI
	Distance from PTVH	Distance from PTVH	Distance from PTVH
	Distance from PTVI	Distance from PTVI	Distance from PTVI
		Percentage volume overlap PTVH	Percentage volume overlap PTVH
			Percentage volume outside PTVH

PTVH = High risk planning target volume, $D_{2\%}$ = maximum dose / dose received by 2% volume, D_{mean} = mean dose, $D_{50\%}$ = dose received by 50% volume

cm. It was because the dose fall-off at that distance was not likely to be affected by the pseudo-structures, therefore it was not likely to exhibit linear relationship. The OARs were classified into 3 groups. The first group were the spinal cord, brain stem, optic nerve, optic chiasm, eyeball, lens and cochlea. These were the OARs with no overlapping with the PTVs and the anatomical parameters used were only the distance from the PTVs. The second group of OARs included the temporal lobe and the brachial plexus. These were the OARs with some extent of overlapping with the PTVs, so the volume of overlapping was included in the anatomical parameter. The third group of OARs was the parotid gland. For this organ, apart from the presence of overlapping volume with PTVs, the assessment of D_{mean} and D_{50} were used instead of $D_{2\%}$ as in the first group according to the institutional dose constraint criteria listed in Table 5.2 (p.87). The reason for using D_{mean} and D_{50} was because they have been shown to be more representable for the functional preservation of the parotid gland instead of the $D_{2\%}$ (Eisbruch et al., 2001). Because the volume to receive lower dose would affect the overall D_{mean} and D_{50} , it was therefore reasonable to include an extra parameter which was the volume of parotid outside PTV.

5.2.4 Multiple Regression Modeling

The dose parameters were dependent variables whereas the anatomical parameters were the independent variables of the multiple regression model, which was used to evaluate how multiple anatomical parameters influenced the dose parameters of the OARs. SPSS (version 20.0. Armonk, NY: IBM Corp.) was used for the multiple regression analysis. The procedure in the modeling involved 3 steps: 1) checking for multicollinearity, 2) testing for assumption of linear relationship, and 3) the establishment of the model.

Multicollinearity referred to two independent variables that were highly correlated. If two independent variables were significantly correlated, one of them would be excluded from the modelling procedure. Variance inflation factors (VIF) were used to check for the multicollinearity of the anatomical parameters. One of the correlated anatomical variables would be removed if their VIF values were greater than 10. The removal would be selected by the Pearson correlation test in the next step, where the anatomical variable which showed weaker linear correlation would be removed. In addition, the Pearson correlation tested the linear relationships between all the dependent and independent variables. The anatomical variables which failed to show linear correlation with the dose parameters would be removed. Lastly, the regression model was established using the anatomical parameters that passed the tests for multicollinearity and linear relationship, stepwise-entering method would be used to fit them into the model. Stepwise-entering method was an automatic process through step-by-step consideration of each independent variable until all independent variables had gone through the process. During each step, independent variables were considered using the F-test. The independent variable would be added if the p-value of the F test <0.05 , while the other

independent variables added in the previous “step” would be removed if the p-value of the F test >0.10 . The process could eliminate the independent variables with the least contribution to the model, and therefore resulted in a simplified but valid model.

5.2.5 Residuals evaluation

A residual is the difference between an observed value in the training data set and the calculated value using the multiple regression models. To ensure the validity of the multiple regression models, the residuals were tested for the normality, homoscedasticity and independence because these were the assumptions of the regression analysis.(Jarque & Bera, 1980) Firstly, the normality of residuals were evaluated by normal probability plot to see whether the actual probability values would suit the pattern of normal distribution in the form a diagonal line.(Osbourne & Waters, 2002) Secondly, the homoscedasticity of residuals refers to the fact that the variance of errors should be the same across all the values of the anatomical parameters. If the homoscedasticity evaluation was passed, the error of the calculated dose parameters using the multiple regression model would be the same for all values of the anatomical parameters. It would be assessed by examining the scatterplot of regression standardized residual against regression standardized predicted value. The points of the scatterplot should be distributed evenly around the horizontal line at the level of zero to show that the error would not be increased as the anatomical parameters increased, or vice versa. Thirdly, the independence of residuals refers to whether the residuals of the regression model were correlated. It was evaluated using the Durbin-Watson test.(Parke, 2013) The value of Durbin-Watson statistic has a range of 0 to 4 and the value between 1.5 and 2.5 indicates no correlation detected.(Osbourne & Waters, 2002)

5.2.6 Model External validation

External validity of the multiple regression models was carried out using a group of another 25 subjects (validation dataset) after the training process. The validation aimed 1) to verify that the standard error of the estimates of the multiple regression models were reliable and not under-representing the error, and 2) to quantify the difference of the calculated dose parameters of the multiple regression models from the actual dose parameters in the plan of the validation dataset. This process helped to verify how well the models could be used in future cases. To start with, dose parameters of various OARs were calculated from the corresponding anatomical parameters using the multiple regression models. For the purpose of ensuring consistency in the measurement of anatomical parameters, the right side was chosen for all the paired organs, while the vertebral level which contained the maximum dose was chosen for the spinal cord.

Then, the calculated dose parameters and the actual dose parameters were used to calculate root mean squared prediction error (RMSPR). It was calculated by taking square root of mean squared prediction error (MSPR) calculated by $MSPR = \sum_{i=1}^n (Y_i - \hat{Y}_i)^2 / n$ where the actual OAR dose parameters were denoted as Y_i and calculated OAR dose parameters were denoted as \hat{Y}_i (Kutner, 2004). The RMSPR represented the deviations of the calculated dose parameters from the observed dose parameters in terms of the measurement units. The RMSPR was then compared to the standard error (SE) of the estimates of the model to see whether they were comparable.

Comparable RMSPR and standard error of the estimates would indicate that the model calculation error in the validation dataset was similar to the model error produced in the modeling process using the training dataset. An index of RMSPR:SE was calculated to quantify the comparison. The value of ≤ 1 would indicate that the standard error of the model did not

under-represent the error of the model, and it would be considered to have passed the validation. In addition, the value of RMSPR also quantified the difference of the calculated dose parameters and the actual parameters so that the true accuracy of the multiple regression model to determine the reference OARs dose could be examined.

5.3 Results

5.3.1 Analysis of the Anatomical Parameters

The anatomical parameters of the various OARs and their correlation results are shown in Table 5.4. Most anatomical parameters have shown statistically significant linear correlation with the dose parameters, except the lens distance from PTVL and the brachial plexus distance from the PTVH.

Table 5.4. Results of Pearson correlations between dose parameters and anatomical parameters

OARs	Anatomical parameters (unit)	Abbreviation	Pearson correlations results			
			D _{mean}		D _{50%}	
			r	p	r	p
Parotid Gland	Distance from PTVH (cm)	Dis _{PTVH}	-0.625	0.000	-0.540	0.000
	Distance from PTVI (cm)	Dis _{PTVI}	-0.394	0.000	-0.405	0.000
	Overlap volume with PTVH (cm ³)	OV _{PTVH}	0.622	0.000	0.558	0.000
	% Volume overlap with PTVH (%)	%OV _{PTVH}	0.616	0.000	0.591	0.000
	Overlap volume with PTVI (cm ³)	OV _{PTVI}	0.813	0.000	0.689	0.000
	% Volume overlap with PTVI (%)	%OV _{PTVI}	0.889	0.000	0.817	0.000
	Volume outside PTVI (cm ³)	outV _{PTVI}	-0.548	0.000	-0.370	0.000
	% Volume outside PTVI (%)	%outV _{PTVI}	-0.442	0.000	-0.247	0.019
			D _{2%}			
			r	p		
Spinal Cord	Distance from PTVH (cm)	Dis _{PTVH}	-0.518		0.000	
	Distance from PTVI (cm)	Dis _{PTVI}	-0.629		0.000	
Brain Stem	Distance from PTVH (cm)	Dis _{PTVH}	-0.896		0.000	
	Distance from PTVI (cm)	Dis _{PTVI}	-0.958		0.000	
Optic Nerve	Distance from PTVH (cm)	Dis _{PTVH}	-0.742		0.000	
	Distance from PTVI (cm)	Dis _{PTVI}	-0.751		0.000	
	Distance from PTVL (cm)	Dis _{PTVL}	-0.583		0.000	
Optic Chiasm	Distance from PTVH (cm)	Dis _{PTVH}	-0.745		0.000	
	Distance from PTVI (cm)	Dis _{PTVI}	-0.791		0.000	
	Distance from PTVL (cm)	Dis _{PTVL}	-0.602		0.000	
Eye	Distance from PTVH (cm)	Dis _{PTVH}	-0.679		0.000	
	Distance from PTVI (cm)	Dis _{PTVI}	-0.696		0.000	
	Distance from PTVL (cm)	Dis _{PTVL}	-0.371		0.000	
Lens	Distance from PTVH (cm)	Dis _{PTVH}	-0.501		0.000	
	Distance from PTVI (cm)	Dis _{PTVI}	-0.485		0.000	
	Distance from PTVL (cm)	Dis _{PTVL}	-0.078		0.474	
Temporal Lobe	Distance from PTVH (cm)	Dis _{PTVH}	-0.895		0.000	
	Distance from PTVI (cm)	Dis _{PTVI}	-0.916		0.000	
	Distance from PTVL (cm)	Dis _{PTVL}	-0.485		0.000	
	Overlap volume with PTVH (cm ³)	OV _{PTVH}	0.279		0.008	
	Percent overlap volume with PTVH	%OV _{PTVH}	0.27		0.01	
	Overlap volume with PTVI (cm ³)	OV _{PTVI}	0.445		0.000	
	Percent overlap volume with PTVI	%OV _{PTVI}	0.458		0.000	
Cochlea	Distance from PTVH (cm)	Dis _{PTVH}	-0.807		0.000	
	Distance from PTVI (cm)	Dis _{PTVI}	-0.915		0.000	
	Distance from PTVL (cm)	Dis _{PTVL}	-0.306		0.045	
Brachial Plexus	Distance from PTVH (cm)	Dis _{PTVH}	-0.188		0.076	
	Distance from PTVI (cm)	Dis _{PTVI}	-0.72		0.000	
	Distance from PTVL (cm)	Dis _{PTVL}	0.364		0.001	
	Overlap volume with PTVI (cm ³)	OV _{PTVI}	0.372		0.000	
	Percent overlap volume with PTVI (%)	%OV _{PTVI}	0.366		0.000	
	Overlap volume with PTVL (cm ³)	OV _{PTVL}	0.032		0.773	
	Percent overlap volume with PTVL(%)	%OV _{PTVL}	0.053		0.620	

5.3.2 Establishment of Multiple Regression Models

Multiple regression models of all the OARs generated from the above-mentioned process are summarized in Table 5.5. The models consist of 1 to 2 anatomical parameters and a constant variable as the model terms. All the model terms achieved p value < 0.05 . The standard error of the estimate is also listed in Table 5.5.

Table 5.5. Multiple Regression analysis

OAR	Dose Parameters	Model Terms	Coefficient	Standard Error	p value	Adjusted R Square	Standard Error of the Estimate	Model Equation
Parotid	D _{mean}	Constant	39.007	1.686	0.000	0.864	2.430	D _{mean} = 39.007 - 0.191 x %outV _{PTVI} + 0.376 x %OV _{PTVI}
		%outV _{PTVI}	-0.191	0.026	0.000			
		%OV _{PTVI}	0.376	0.056	0.000			
	D _{50%}	Constant	20.798	0.522	0.000	0.803	3.506	D _{50%} = 20.798 + 0.865 x %OV _{PTVI}
		%OV _{PTVI}	0.865	0.046	0.000			
Spinal Cord	D _{2%}	Constant	45.763	0.352	0.000	0.679	1.838	D _{2%} = 45.763 - 5.691 x Dis _{PTVI}
		Dis _{PTVI}	-5.691	0.261	0.000			
Brain Stem	D _{2%}	Constant	54.440	0.424	0.000	0.916	2.179	D _{2%} = 54.440 - 10.303 x Dis _{PTVI}
		Dis _{PTVI}	-10.303	0.470	0.000			
Optic Nerve	D _{2%}	Constant	54.898	1.937	0.000	0.582	13.081	D _{2%} = 54.898 - 4.936 x Dis _{PTVH} - 0.686 x Dis _{PTVL}
		Dis _{PTVH}	-4.936	0.690	0.000			
		Dis _{PTVL}	-0.686	0.229	0.004			
Optic Chiasm	D _{2%}	Constant	53.331	2.486	0.000	0.635	12.365	D _{2%} = 53.331 - 8.464 x Dis _{PTVI} - 0.796 x Dis _{PTVL}
		Dis _{PTVI}	-8.464	1.496	0.000			
		Dis _{PTVL}	-0.796	0.301	0.012			
Eye	D _{2%}	Constant	28.492	1.341	0.000	0.457	8.218	D _{2%} = 28.492 - 4.269 x Dis _{PTVI}
		Dis _{PTVI}	-4.269	0.502	0.000			
Lens	D _{2%}	Constant	7.444	0.369	0.000	0.436	1.520	D _{2%} = 7.444 - 0.799 x Dis _{PTVI}
		Dis _{PTVI}	-0.799	0.098	0.000			
Temp Lobe	D _{2%}	Constant	56.749	1.068	0.000	0.869	7.066	D _{2%} = 56.749 - 8.772 x Dis _{PTVI} - 4.215 x Dis _{PTVH}
		Dis _{PTVI}	-8.772	1.438	0.000			
		Dis _{PTVH}	-4.215	0.714	0.000			
Cochlea	D _{2%}	Constant	59.211	0.859	0.000	0.907	4.559	D _{2%} = 59.211 - 11.771 x Dis _{PTVI} - 2.008 x Dis _{PTVH}
		Dis _{PTVI}	-11.771	1.314	0.000			
		Dis _{PTVH}	-2.008	0.571	0.001			
Brachial Plexus	D _{2%}	Constant	60.088	0.283	0.000	0.450	1.887	D _{2%} = 60.088 + 0.156 x %OV _{PTVI} - 1.591 x Dis _{PTVI}
		%OV _{PTVI}	0.156	0.026	0.000			
		Dis _{PTVI}	-1.591	0.370	0.000			

PTVH = High risk planning target volume, PTVI = Intermediate risk planning target volume, D_{2%} = maximum dose / dose received by 2% volume, D_{mean} = mean dose, D_{50%} = dose received by 50% volume, %outV_{PTVI} = percentage volume outside PTVI, %OV_{PTVI} = percentage volume overlap PTVI, Dis_{PTVI} / Dis_{PTVH} = distance from PTVI / PTVH

5.3.3 Parotid Gland

The D_{mean} of the parotid decreased with the increase in % volume outside PTVI ($\% \text{outV}_{\text{PTVI}}$) and increased with the increase in % volume overlap with PTVI ($\% \text{OV}_{\text{PTVI}}$). The adjusted R square was 0.864 and the standard error of the estimate was 2.430. The model equation is shown in equation 1.

$$D_{\text{mean}} = 39.007 - 0.191 \times \% \text{outV}_{\text{PTVI}} + 0.376 \times \% \text{OV}_{\text{PTVI}} \quad (1)$$

On the other hand, the $D_{50\%}$ of the parotid increased with the increase in $\% \text{OV}_{\text{PTVI}}$. The adjusted R square was 0.803 and the standard error of the estimate was 3.506. The model equation is shown in equation 2.

$$D_{50\%} = 20.798 + 0.865 \times \% \text{OV}_{\text{PTVI}} \quad (2)$$

5.3.4 Spinal Cord

The model equation revealed that the spinal cord $D_{2\%}$ decreased with the increase of the distance from PTVI (Dis_{PTVI}). The adjusted R square was 0.679 and the standard error of the estimate was 1.838. The model equation is shown in equation 3.

$$D_{2\%} = 45.763 - 5.691 \times \text{Dis}_{\text{PTVI}} \quad (3)$$

5.3.5 Brain Stem

The mode for the calculation of $D_{2\%}$ of the brain stem resulted with the adjusted R square was as high as 0.916. The $D_{2\%}$ was found to be decreased with the increase in the Dis_{PTVI} as shown in equation 4.

$$D_{2\%} = 54.440 - 10.303 \times \text{Dis}_{\text{PTVI}} \quad (4)$$

5.3.6 Optic Nerve

Referring to equation 5, $D_{2\%}$ of the optic nerve yielded the adjusted R square of 0.582 and the standard error of the estimate of 13.081. The $D_{2\%}$ decreased with the increase in the distance from PTVH (Dis_{PTVH}) and Dis_{PTVI} .

$$D_{2\%} = 54.898 - 4.936 \times Dis_{PTVH} - 0.686 \times Dis_{PTVI} \quad (5)$$

5.3.7 Optic Chiasm

The adjusted R square of the model for optic chiasm was 0.635 and the standard error of the estimate was 12.365 as shown in equation 6. The $D_{2\%}$ decreased with the increase in Dis_{PTVI} and the distance from PTVL (Dis_{PTVL}).

$$D_{2\%} = 53.331 - 8.464 \times Dis_{PTVI} - 0.796 \times Dis_{PTVL} \quad (6)$$

5.3.8 Eyeball

$D_{2\%}$ of the eyeball decreased with the increase in Dis_{PTVI} . The adjusted R square of the model was 0.457 and the standard error of the estimate was 8.218. The model equation is shown in equation 7.

$$D_{2\%} = 28.492 - 4.269 \times Dis_{PTVI} \quad (7)$$

5.3.9 Lens

For the lens, $D_{2\%}$ was shown to decrease with the increase in Dis_{PTVI} . The adjusted R square was 0.436 and the standard error of the estimate was 1.520 as shown in equation 8.

$$D_{2\%} = 7.444 - 0.799 \times Dis_{PTVI} \quad (8)$$

5.3.10 Temporal Lobe

The adjusted R square for temporal lobe was 0.869 and the standard error of the estimate was 7.066. The model equation is shown in equation 9.

$$D_{2\%} = 56.749 - 8.772 \times \text{Dis}_{\text{PTVI}} - 4.215 \times \text{Dis}_{\text{PTVH}} \quad (9)$$

5.3.11 Cochlea

The adjusted R square for cochlea was 0.907 and the standard error of the estimate was 4.559. The model equation is shown in equation 10.

$$D_{2\%} = 59.211 - 11.771 \times \text{Dis}_{\text{PTVI}} - 2.008 \times \text{Dis}_{\text{PTVH}} \quad (10)$$

5.3.12 Brachial Plexus

The adjusted R square for brachial plexus was 0.450 and the standard error of the estimate was 1.887. The model equation is shown in equation 11.

$$D_{2\%} = 60.088 + 0.156 \times \% \text{OV}_{\text{PTVI}} - 1.591 \times \text{Dis}_{\text{PTVI}} \quad (11)$$

5.3.13 Residual Evaluations

Residuals evaluations for the independence of all the multiple regression models are summarized in Table 5.6. The independence evaluations using the Durbin-Watson test were satisfied for most models except the optic nerve, optic chiasm and eyeball, which displayed scores of below 1.5.

The results of normal probability plot is shown in Figure 5.2. The diagonal line on the plot represented the expected plot for an ideal normal distribution. Generally, it was observed that the actual probability values followed a diagonal line, despite there were some deviations from normality in some models as shown in optic nerve, optic chiasm, lens, temporal lobe and cochlea.

The homoscedasticity as shown in Figure 5.3 was seen to be violated in brain stem, optic nerve, optic chiasm, eyeball, lens, temporal lobe, cochlea and brachial plexus as the dots were not scattered randomly in a rectangular fashion.

Table 5.6. Residual Independence evaluation

OAR	Dose parameters	Durbin-Watson test
Parotid Gland	D_{mean}	1.840
	$D_{50\%}$	1.663
Spinal Cord	$D_{2\%}$	1.863
Brain Stem	$D_{2\%}$	1.617
Optic Nerve	$D_{2\%}$	1.362
Optic Chiasm	$D_{2\%}$	1.413
Eye	$D_{2\%}$	1.228
Lens	$D_{2\%}$	1.787
Temporal Lobe	$D_{2\%}$	2.273
Cochlea	$D_{2\%}$	2.475
Brachial Plexus	$D_{2\%}$	2.040

$D_{2\%}$ = maximum dose / dose received by 2% volume, D_{mean} = mean dose, $D_{50\%}$ = dose received by 50% volume

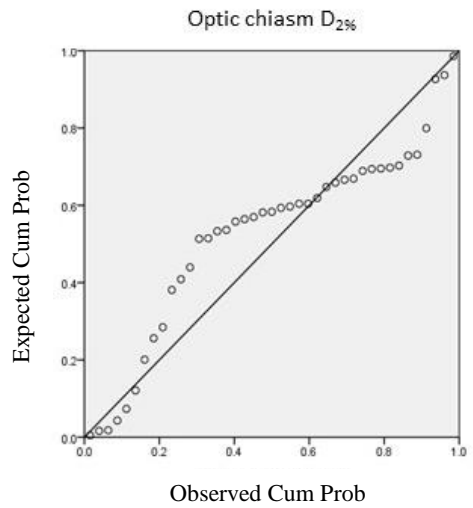
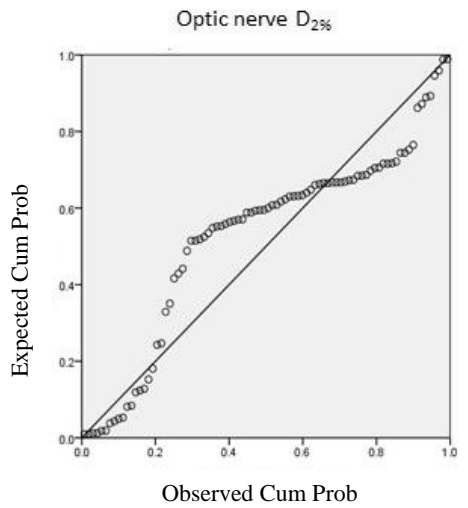
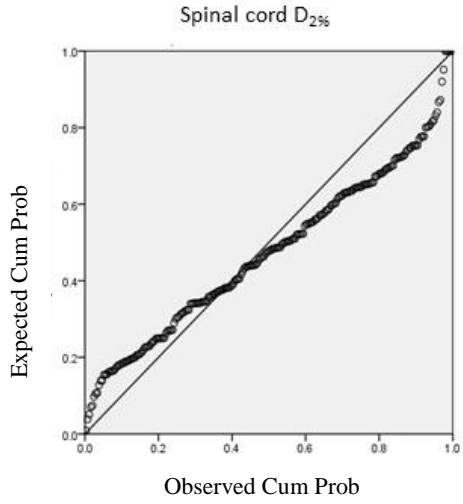
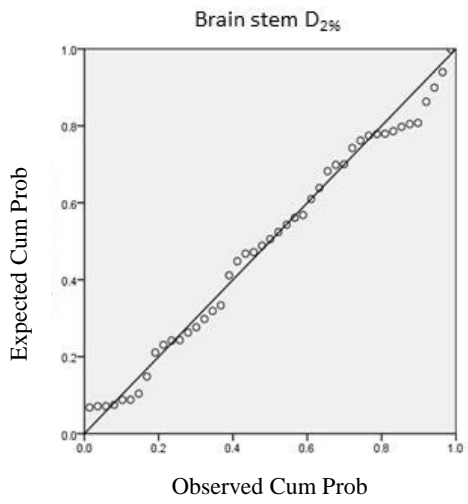
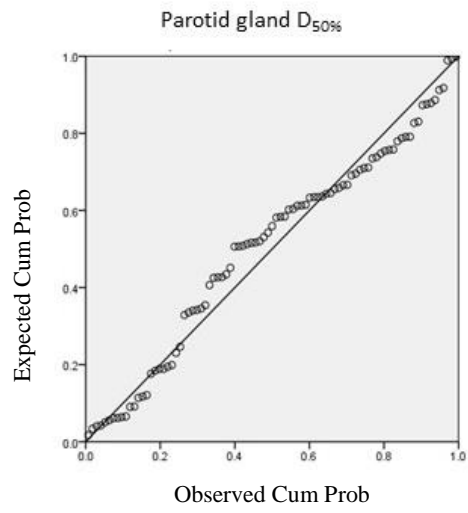
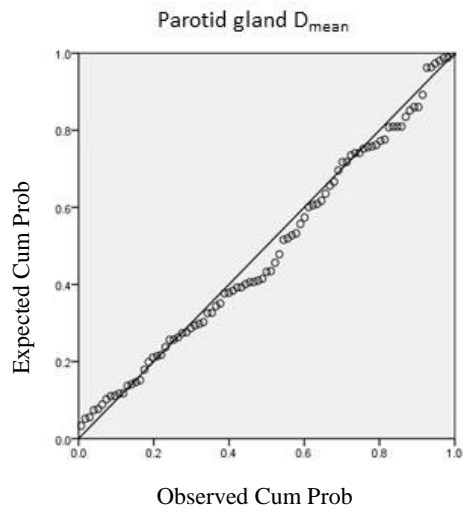


Fig. 5.2a. The normal probability plot for evaluation of residuals normality. The points that form a diagonal line represents the ideal normality of the residuals. Cum Prob = cumulative probability

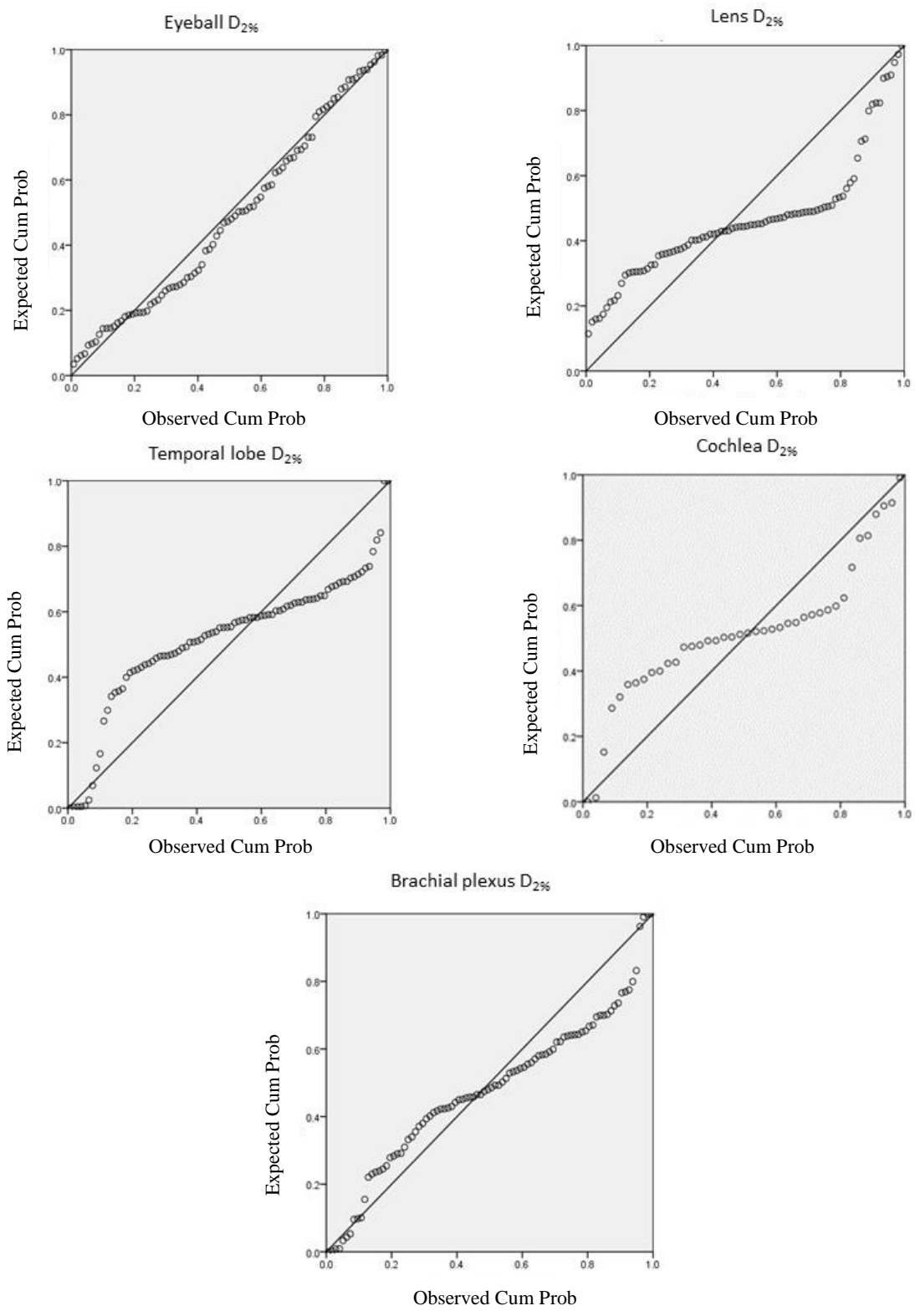


Fig. 5.2b. The normal probability plot for evaluation of residuals normality. The points that form a diagonal line represents the ideal normality of the residuals. Cum Prob = cumulative probability

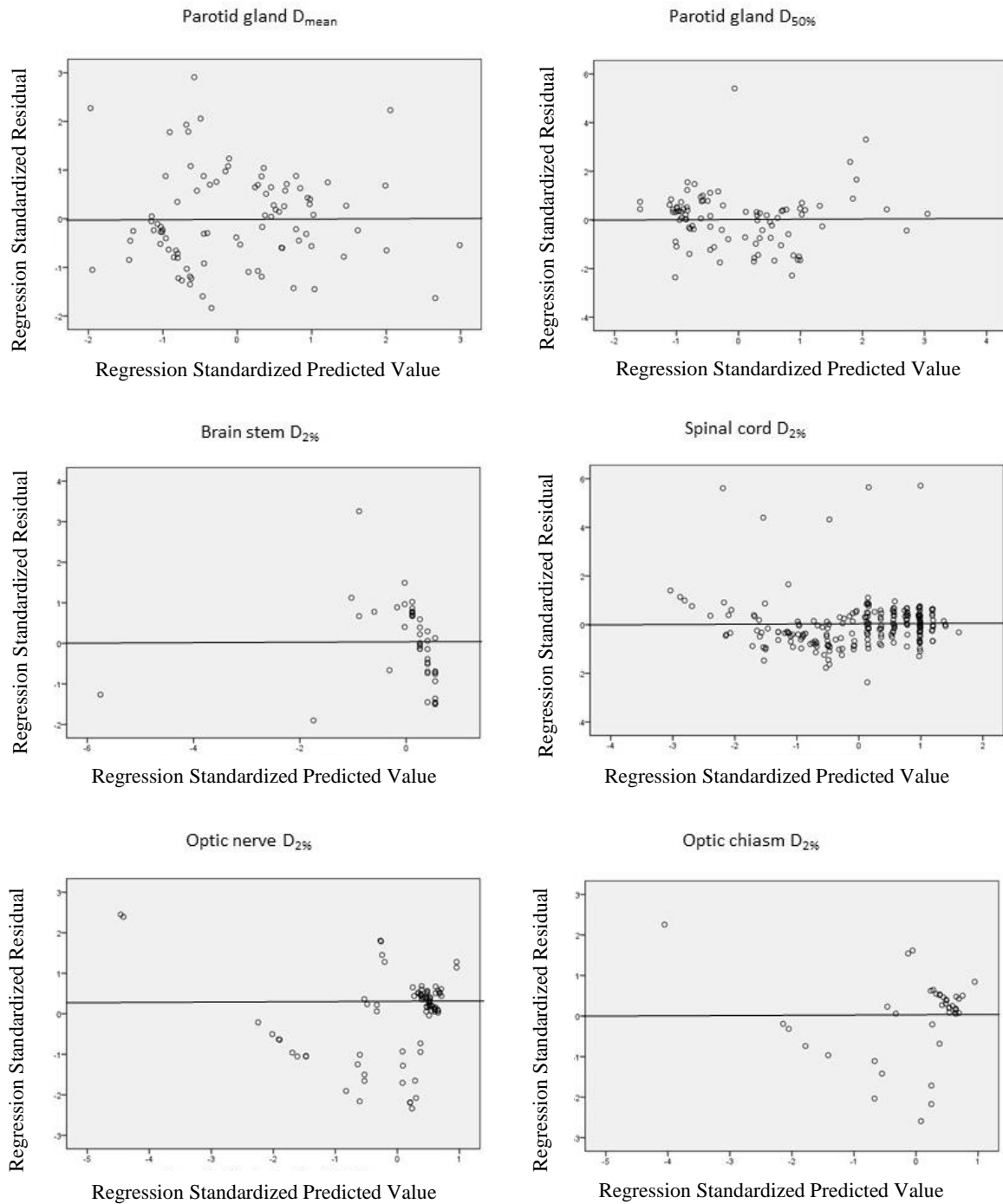


Fig. 5.3a. The scatterplot for evaluation of residuals homoscedasticity. The points that scattered randomly above and below the horizontal zero line represents the ideal homoscedasticity of the residuals.

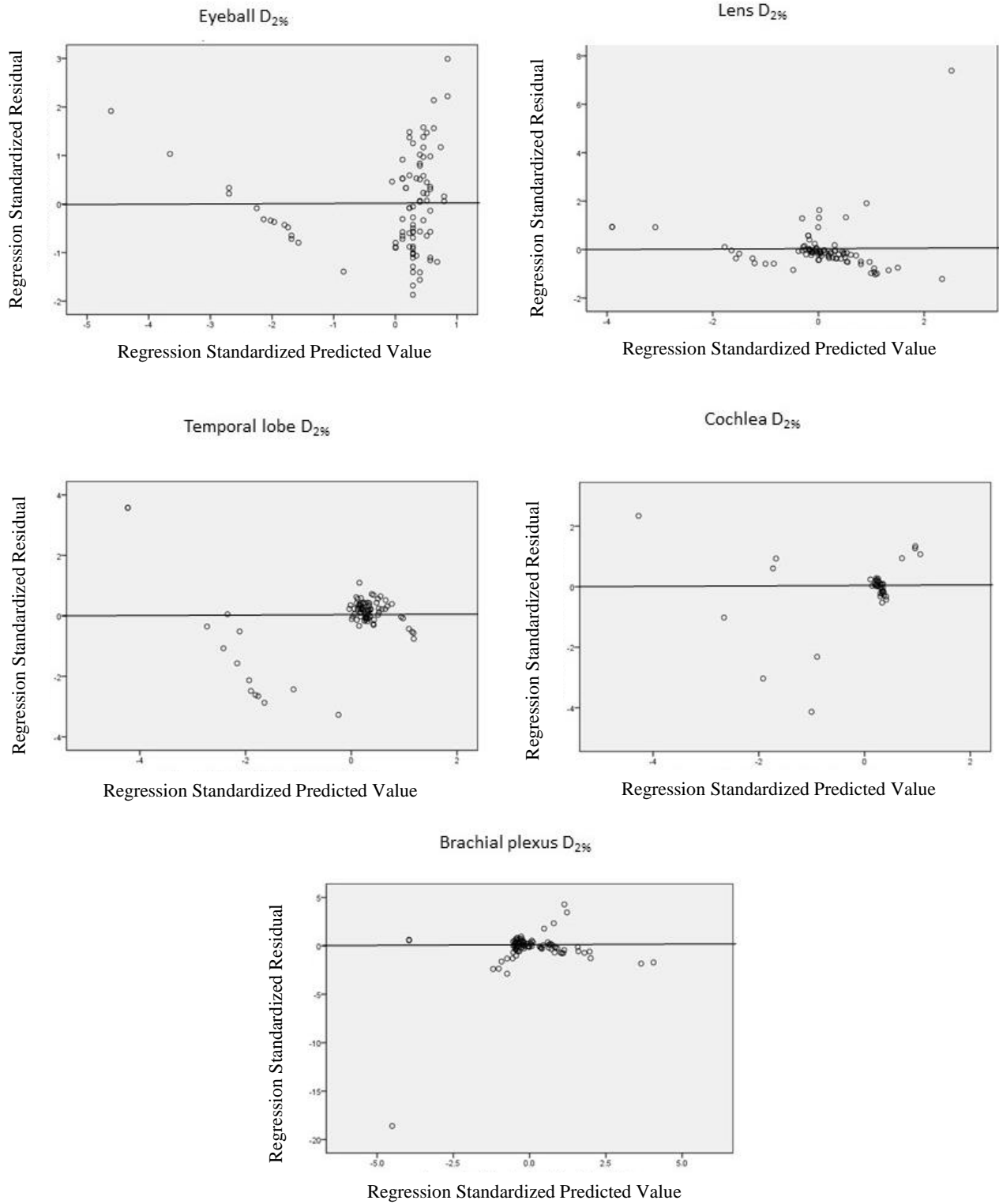


Fig. 5.3b. The scatterplot for evaluation of residuals homoscedasticity. The points that scattered randomly above and below the horizontal zero line represents the ideal homoscedasticity of the residuals.

5.3.14 Model Validation

Each of the formulated multiple regression models were validated using another set of subjects in the model verification group. The root mean squared error (RMSE) and the standard error (SE) of the estimate of each multiple regression models are summarized in Table 5.7. The ratios of RMSPR: SE was calculated. The ratios were less than or equal to one if the RMSPR value was less than SE as shown in the spinal cord, brain stem, optic nerve, optic chiasm, temporal lobe, cochlea and brachial plexus. Meanwhile, there were OARs which demonstrated a higher RMSPR values than the SE values. These included the parotid gland, eyeball, and lens.

Table 5.7. Model Validation

Models		Evaluation		
OAR	Dose parameters	Root Squared Error		RMSPR:SE Ratio
		RMSPR (Gy)	SE of the estimate (Gy)	
Parotid Gland	D _{mean}	3.322	2.430	1.38
	D _{50%}	4.180	3.506	1.19
Spinal cord	D _{2%}	0.780	1.838	0.42
Brain stem	D _{2%}	0.552	2.179	0.25
Optic nerve	D _{2%}	6.799	13.081	0.52
Optic chiasm	D _{2%}	5.598	12.365	0.45
Eyeball	D _{2%}	10.163	8.218	1.24
Lens	D _{2%}	2.474	1.520	1.63
Temporal lobe	D _{2%}	3.050	7.066	0.43
Cochlea	D _{2%}	3.440	4.559	0.75
Brachial plexus	D _{2%}	0.753	1.887	0.40

D_{2%} = maximum dose / dose received by 2% volume, D_{mean} = mean dose, D_{50%} = dose received by 50% volume, RMSPR = root mean squared prediction error, SE = standard error

5.4 Discussion

The goal of the current study was to model the effects on the dose parameters by the varying anatomical parameters. The derived model terms for each of the multiple regression models not only provided a new method to estimate the optimal OAR dose parameters, but also provided a better understanding on how the PTV-OAR geometrical relationship influenced the dose received by the OARs. It should be noted that the number of anatomical parameters included in the final model equation were less than those used in the model training. It was mainly due to two factors: the stepwise entering method in the formulation of the models and the assessment of multicollinearity of various anatomical parameters. The reduced number of anatomical parameters in the model would make the treatment planning easier and it would only require the planner to take just one to two measurements for the anatomical parameters to achieve optimal doses to the OARs during IMRT optimization.

The establishment of the multiple regression model was based on the data from the training dataset and the generation of IMRT plans with satisfactory OARs dose sparing and PTV dose conformity. This method helped to assess the optimal OAR dose before and after the treatment plan optimization, which were the aims of this study. Although it was difficult to deduce the absolute best plan in terms of OARs dose sparing, the approach adopted in this study allowed the generation of high-quality IMRT plans based on the prior knowledge of the physical properties of isodose distribution. Previous literatures have reported that the methods of OARs dose estimation using various models were usually based on past IMRT plans, in which they have established a model to correlate the PTV-OAR overlapping volume and the OAR dose. (Moore et al., 2011) However, the use of the past IMRT plans in the model training could not properly

estimate the OARs dose following their anatomical parameters. This was because planners tended to restrict the OARs doses according to their standard acceptable dose tolerance.(Chau et al., 2008) This practice is of particular concern in the spinal cord because it has variable distance from the PTVs in different vertebral levels while the acceptable dose tolerance guideline remains constant. Therefore, the variability of the spinal cord dose was not consistently correlated with their distance from PTV in different vertebral levels as reported in a study by Parashar et al.(2009). As discussed in section 5.2.2, our current study explicitly addressed this problem by generating the IMRT plans with pseudo-structures which aimed at optimizing the dose falloff at the rate of 20 cGy/mm at the PTV-OAR interface. This would help to create plans with more optimal OARs doses compared with past IMRT plans. The model established could be of higher clinical significance because it was not generated according to past sub-optimal plans based on standard acceptable dose tolerance only. Because of this, the calculated dose parameters using the multiple regression models could be used as references to assess the optimal OAR doses.

Although the multiple regression models of all the OARs were statistically significant, the applicability of the models, which was related to the error of the estimates, was determined by their standard error of the estimate and their validity. The SE of the estimate measured the accuracy of the calculated dose parameters. It had the advantage of expressing the error in terms of “Gy”, which was the same unit of the calculated dose parameters, making it to be easily interpreted. The validity test which compared the SE and the RMSPR was important as it could indicate whether the SE of the estimate could truly reflect the accuracy of the model in the new dataset. Therefore, the SE of the estimate should be small enough so that the calculated dose parameters were meaningful to planners while the validity should be passed so that the standard error of the estimate could reflect the accuracy of the models when it would be used in the future

plans. Although there is no guiding rule to determine how small the standard error of the estimate should be (C. H. Ellis, 2004), it is logical to deduce that the SE of the estimate as high as 12 – 13 Gy in the optic nerve model would not be as acceptable as that in the model for the parotid gland (2 – 3 Gy). For the validity, it was noted that most RMSPR (7 out of 11) showed similar or lower values compared with the SE, which were indicated by the RMSPR: SE ratios that were equal to or less than 1. These results showed that the multiple regression models calculated the OARs dose parameters with comparable or smaller error than those specified in the models' standard error of the estimate. Therefore these models were proven to have acceptable validity for use in cases other than the training dataset (Norton, Cormier, Smith, Jones, & Schubauer-Berigan, 2002). For the models with the RMSPR:SE ratios larger than 1, their performances might be inferior to those less than 1. It was because the calculated OARs dose parameter might encounter larger error than stated in the standard error of the estimate. As seen in Table 5.7 (p.108), the OARs regression models with RMSPR:SE ratio larger than 1 included the parotid gland, lens and eyeball. In light of their RMSPR:SE ratio, the determined OARs dose parameters by their regression models were expected to have larger error than those stated in the SE of the estimate. This implied that the models for determining lens and eyeball dose parameters are not recommended for clinical use. However, for the models of the parotid gland, they are considered to be fine for use because the differences of RMSPR and SE were only less than 1 Gy.

The reason for the less satisfactory model of the lens and the eyeball was largely due to the characteristics of multiple regression model. The current study used multiple regression analysis based on the linear relationship between the dose parameters and the anatomical parameters. The relationship was attributed by the planning techniques with the aim to achieve the maximum dose reduction gradient from the PTV prescribed dose to the OARs planning goals dose at the PTV-

OAR interface. However, the maximum dose reduction gradient might not be achieved in some parts across the field because the multi-leaf collimator (MLC) responsible for the intensity modulation had a maximum speed (Kerns, Childress, & Kry, 2014). In those parts where the maximum dose reduction gradient was not achieved, the relationship between the dose parameters and the anatomical parameters could not be completely explained by the current model based on the linear relationship. More complicated model, such as the method suggested by Yuan et al., (Yuan et al., 2012) could be better in determining non-linear relationship in those parts. However, with the aim to establish a simple and clinically applicable method, the model provided by the current study would be easier to implement by planners.

Since the models developed in this study were based on the distance and overlapping volume of the corresponding OARs to the PTV, it was not recommended to extend the results of this study to other head and neck cancers. It was because application of the models in other head and neck cancers, which express different range of OAR-PTV distances and overlapping volumes from NPC, would lead to extrapolation of the models and increase in inaccuracy in the determined OARs dose parameters (Montgomery, 2012). Nevertheless, the methodology of this study can be applied in other head and neck cancers to develop other their own models for the same purpose, so that other head and neck cancers patients can also be benefited.

5.5 Conclusion

The multiple regression models for the calculation of the OARs doses in the treatment planning of NPC IMRT achieved statistically significant results. The models served as an easily accessible tool for planners to obtain reference OARs dose before treatment planning, and to assess the OARs dose after the IMRT plan optimization. Therefore, the developed models could improve

the efficiency of the IMRT optimization process because planners could use the calculated OARs dose to decide the appropriate objective function more quickly. Also, the models can be used as a tool to evaluate the OARs dose in IMRT plans which can better address individual patients' difference when compared to the evaluation using the general OARs acceptable dose guidelines.

Chapter 6 Discussion

There were three studies in this thesis. There is a common purpose among these three studies which serves a general aim to provide guidance in treatment planning of head and neck using intensity modulated radiotherapy (IMRT). Chapters 3 to 5 present the three studies in correspond to the hypotheses and research questions listed in section 2.4. This chapter discusses how the three studies can be integrated to support the treatment planning of head and neck cancers.

6.1 Relationship and Novelty of the Studies

Radiotherapy is an important component in the treatment of head and neck cancers as discussed in Chapter 1. IMRT improves the treatment outcome, delivers less dose to OARs and allows the possibility for dose escalation, as compared with conventional and 3D conformal radiotherapy (Gomez-Millan et al., 2013). Treatment planning is an important step for IMRT to exercise its benefits. However, as discussed in Chapter 2, the choice of beam arrangement in head and neck IMRT has largely been depended on personal preference and the potential advantage of the use of different field arrangement has not been comprehensively addressed. The study 1 in this thesis presents a thorough comparison of the commonly used beam arrangement of IMRT across 5 different types of head and neck cancers, which has not been published before in terms of the comprehensiveness of the cases included except that there is a recent published article investigating dosimetric comparison of beam arrangement in glioblastoma multiforme (GBM) (Hou et al., 2019). Dosimetric parameters of the PTVs and OARs of plans using ESB and VMAT has been presented over a sample size of 13 patients. Their results showed marginal benefit of VMAT in OAR sparing, but failed to draw any overall recommendation of the beam arrangement

for GBM patients. In contrast, our study has the merit of larger sample size and inclusion of more cancer types. Because of this, we believe that our results were more reliable and clinically relevant. Also, in our study through the application of a figure-of-merit, the optimal beam arrangement can be established based on a single quantitative index, which can serve as useful reference for planners working on IMRT plans. In contrast, similar studies which mainly compared various dose parameters among beam arrangement methods could not arrive at an optimal beam arrangement in a quantitative way (Hou et al., 2019; Vanetti et al., 2009).

Results of study 1 showed that non-coplanar beam angle optimization (BAOnc) produced the optimal plans for NPC in terms of OARs sparing. Study 2 applied this result and worked on the dose escalation in IMRT of NPC using this beam arrangement. Although similar clinical and dosimetric studies have been conducted before and reported the feasibility of dose escalation to the GTV in NPC treated with IMRT (Kwong et al., 2006; Lauve et al., 2004), results of the study 2 was unique in a way that it proved IMRT in NPC using BAOnc could further increase the GTV dose safely in dosimetric perspective. The study by Kwong et al examined the clinical results of NPC dose escalation (Kwong et al., 2006) and suggested a maximum GTV dose of 76 Gy over 35 fractions. In contrast, we suggested a higher maximum deliverable GTV dose of 80 Gy over 33 fractions under specified condition in study 2 (Chapter 4). Based on the calculation using the equation of biological equivalent dose (BED) and the alpha beta ratio of 10, the increase in maximum deliverable dose in our study would result in an increase of the biological equivalent GTV dose of over 7% (92.5 Gy vs 99.4 Gy), which is seen as an improvement in terms of dose escalation outcome. It is logical to expect that the local tumour control would be further improved.

Study 3 focuses on the dose to the OARs, in which a simple and valid method using regression models to estimate the optimal OARs dose has been developed. Compared with previous studies which established models to determine OARs dose based on past IMRT plans (Moore et al., 2011; Yuan et al., 2012), the uniqueness of the current study is that the pursuit of optimal OARs dose is quantified by the suggested dose reduction gradient (Moran et al., 2005) instead of direct adoption of past plans. This quantitatively ensures the quality of the IMRT used for the generation of the multiple regression, and hence more indicative of the optimal estimated OARs dose. Knowledge based radiotherapy planning has recently emerged as rapidly developing area with the aim to improve the IMRT planning process (Ge & Wu, 2019). Knowledge-based planning refers to the strategy to incorporate past plans data (known as knowledge) into the treatment planning process. 6 different categories of purpose in knowledge-based planning have been summarised in a review article, which includes 1) the determination of DVH, 2) specific dose metrics, 3) voxel-level doses, 4) objective function weights, 5) beam parameters and 6) quality assurance metrics (Ge & Wu, 2019). Study 3 in the current thesis contributes to the second category in knowledge-based planning in the determining specific dose metrics of OARs in IMRT of head and neck cancers. It is believed that the results of study 3 can effectively guide the planners during the plan optimization and the decision-making processes regarding the OARs doses.

6.2 Clinical Impacts and Practical Challenges in Implementation

In general, this thesis provides evidence in the choice of beam arrangement method, GTV dose escalation and optimal OARs dose, which will collectively improve the IMRT treatment planning

of head and neck cancers and particularly in NPC. It will benefit the department as the efficiency of treatment planning is expected to be improved because the time used for deciding beam angle arrangement and optimal OARs dose will be saved, especially for new planners who are undergoing training practices. It also brings benefit to head and neck cancer patients because they can receive treatment by the beam arrangement with optimal dosimetric advantages. Also, NPC patients will be benefited by the potential improvement of local control by GTV dose escalation up to 80 Gy, as well as the improvement of plan quality using multiple regression model guided OARs dose determination instead of plans generated purely based on individual planners' experience.

The practical challenges for the implementation of the optimal beam arrangement as suggested in study 1 are expected to be minimal. It is because the suggested choice of beam arrangement, VMAT and static coplanar beam IMRT using BAO, are available in the Eclipse treatment planning systems. Furthermore, it is expected that the implementation of the results can be extended to other treatment planning systems, such as the Monaco system (Elekta, Maryland Heights, MO, USA) that supports VMAT using linear accelerators from Elekta, because previous study has reported that the dosimetric differences between the systems were minimal (Kumar, Holla, Sukumar, Padmanaban, & Vivekanandan, 2013). However, for studies 2 and 3, their applications in clinical setting are more challenging. Because the results of study 2 have only investigated the dosimetric feasibility of GTV dose escalation of NPC, the relationship of the dose escalation to the actual clinical outcome including the benefits in local control and the related toxicities has to be confirmed through randomized controlled clinical trials. Moreover, the use of non-coplanar beam arrangement is currently not common because it involves rotation of couch that increases the treatment time in each fraction. This disadvantage with non-coplanar

beam arrangement can be overcome with the use of 4pi radiotherapy technology in which automated movement of linear accelerator components including the couch is possible. A study by Yu et al (Yu et al., 2015) has reported the development of collision prediction model, which was a major step to facilitate the machine motion automation for non-coplanar beams. With the 4pi radiotherapy becomes commercially available in the near future, the implementation of GTV dose escalation using non-coplanar beams would be more feasible. For the development of multiple regression models for determination of reference OARs dose (study 3), the challenge would be to overcome the additional steps in measuring the necessary anatomical parameters, which may affect the original planning workflow. It is common to see resistance towards changes in working practice among medical staff (Gollop, Whitby, Buchanan, & Ketley, 2004), and better support is crucial to engage staff in the change for improvement. The support can be provided by the development of automated workflow of the anatomical parameters measurement using application programming interface (API) in the Eclipse treatment planning system (Olsen et al., 2014). The API allows user to access the treatment plans information by writing scripts, which are then are integrated into the treatment planning system for planners to use.

6.3 Limitations of the Study

6.3.1 Exclusion of Partial-arc VMAT in the Beam Angle Arrangement Comparison

In the treatment planning of head and neck cancers with tumours situated on one side, such as the parotid gland and the maxillary sinus, partial arcs may be used instead of 2 – 3 full arcs (Pursley et al., 2017). However, it was not used in the study 1 despite it could be a potential choice of beam angle arrangement. Therefore, it was unable to compare the partial-arc VMAT with the

other beam arrangement methods, and unable to address its pros and cons in the perspective of dosimetric evaluation in our study for planners' reference. The reason for the exclusion of partial-arc VMAT is because the design of the study was to compare the selected beam arrangement method across 5 types of head and neck cancers. Partial-arc VMAT, although being used in parotid and maxillary sinus cancers, is seldom used for centrally situated cancers including NPC, oral cavity and larynx. Also, the length and start / end gantry angle of partial arc is often adjusted according to the shape and extend of the PTV (Yang, Yan, & Tyagi, 2012). For the purpose of more coherent and fair comparison, and unstandardized factors which may affect the result of the dosimetric comparison, partial-arc VMAT were not included in the study.

6.3.2 Lack of Clinical Results to Support the Suggested Dose Escalation

Dosimetric study was conducted to evaluate the maximum deliverable dose to the GTV of locally advanced NPC. The limitation of dosimetric study is that the association of the results with clinical outcome cannot be confirmed. All the OARs which were suggested to be unaffected in the GTV escalated plans were only based on computer dose calculation. The results of study 2 therefore cannot be viewed as the evidence for the safe delivery of dose escalation in the NPC patients. Instead, it should be regarded as the supporting evidence to carry out clinical studies to investigate the clinical outcome and to measure the side effects of the patients.

6.3.3 Clustering Feature in the Residuals of Multiple Regression

In the scatterplot of the residuals in the results of study 3, it is best to have the scatterplot evenly distributed in the chart to show that the variance of error of the regression model is the same regardless of the value of the anatomical parameters (Osbourne & Waters, 2002). In other words, the expected error of the estimated OARs dose should be the same with all range of the

calculated values. The results of the study 3 shows that the multiple regression models, although resulted in good adjusted R^2 value and passed the validation, may not have stable accuracy in the estimation.

6.4 Future Directions

6.4.1 Evaluation of the Dosimetric Effect of 4pi VMAT in Head and Neck Radiotherapy

Dose Escalation

The technology of delivering 4pi VMAT is emerging. 4pi radiotherapy refers to the incorporation of beams distributed on the imaginary isotropically expanded spherical surface around the iso-centre during plan optimization (Tran et al., 2017). 4pi VMAT can be delivered by non-coplanar arc beams using static couch or synchronising the arc rotation of the gantry with a rotating couch (Lyu et al., 2018; Wild, Bangert, Nill, & Oelfke, 2015) . It has been shown that 4pi VMAT has the potential to further decrease the dose to OARs compared with coplanar VMAT. For example, a study on head and neck cancers reported that the mean D_{max} to the brain stem and spinal were decreased by 6 Gy and 3.8 Gy respectively using 4pi VMAT (Subramanian et al., 2017). In addition, the method of delivering 4pi VMAT with synchronised gantry and couch rotation enabled more sophisticated arc trajectories compared with the static couch method. It was expected to deliver highly conformed dose to the PTV with reduction of OARs dose and 50% isodose volume in patient body (Lyu et al., 2018). It is worthwhile to further evaluate the dosimetric effect of the use of 4pi VMAT so that a comprehensive comparison of the optimal beam arrangement can be done; and to investigate its capability in the NPC GTV dose escalation. Although the treatment time will increase by 30% in current linear accelerators compared with coplanar VMAT (Wild et al., 2015), the potential of 4pi VMAT can be unleashed with the

advancement of the future linear accelerators with automatic couch and gantry motion capabilities for faster 4pi VMAT delivery (Khan et al., 2016).

6.4.2 Application of Radiomics to Selection of NPC Cases for Dose Escalation

Radiomics refers to the extraction of features in the regions of interest (ROI) from medical images (Larue, Defraene, Ruyscher, Lambin, & Elmpt, 2017). The extracted features can be the image voxel intensity, ROI texture and shape features, etc. (Hugo et al., 2014). These extracted radiomics features can be used to correlate with clinical data such as recurrence and metastasis status of patients, so as to develop tools for prediction of treatment outcome in future patients based on individual patients' image radiomics features. Research articles have been published to evaluate the chance of local recurrence in NPC patients, and it was reported that local recurrence can be predicted using pre-treatment imaging with concordance index of over 0.8 (L.-L. Zhang et al., 2019; L. Zhang et al., 2019). Chapter 5 of this thesis presents a method to escalate GTV dose in locally advanced NPC patients, with the selection of patients according to the clinical stage of T3-4 N0-1. The future direction could be to incorporate radiomics study for more accurate and individualized patient selection instead of based on their staging. With the attempt to generate own local recurrence prediction model based on radiomics features, NPC patients indicated for GTV dose escalation could be more accurately identified. With the proposed dosimetric study (in section 6.4.1) using 4pi VMAT for dose escalation in the identified patients, it will be able to evaluate its ability to deliver highly conformed escalated dose to PTV and GTV. In addition, clinical studies can also be conducted with the introduction of linear accelerator with automated gantry and couch motion.

6.4.3 Refinement of Models by LASSO Regression and Integration with Knowledge-based Radiotherapy Planning

Multiple regression with stepwise selection has been used in the current study to determine OARs dose parameters because it can appropriately serve the research aim as discussed in the chapter 5. However, it has been reported that this method is inherited with the drawback of incapability in selecting the most significant independent variables, making the final model less accurate when applied to samples other than the training dataset (Smith, 2018). This drawback will become significant when the sample size and the number of independent variables increase (Ranstam & Cook, 2018). For future study with the aim to improve the model accuracy and to increase the number of samples and independent variables, models can be generated by the least absolute shrinkage and selection operator (LASSO) regression. In general, LASSO regression requires the setting of λ which shrinks the model coefficients of the independent variables, and to exclude the corresponding independent variable if the coefficient is shrunk to zero during model training. Also, users need to set the value of k which defines the number of cross-validation and the number of division from the pool of sample into groups of sub-samples. During model training, one of the sub-sample group acts as validation dataset to check the model developed by the other sum-sample groups. This model training process will be repeated by k times, in which the role of various sub-sample groups will be switched between training and validation, so that an appropriate value of λ is determined. The determined λ can then be used for the generation of the final model (F. Li, Yang, & Xing, 2005; Ranstam & Cook, 2018). LASSO regression allows better independent variables selection and coefficient determination, and hence improving model accuracy in future studies (Rancati & Fiorino, 2019; Ranstam & Cook, 2018).

Chapter 7 Conclusion

Treatment planning of radiotherapy is one of the key procedures in radiotherapy treatment, the process involves a lot of decision-making steps which are largely dependent on planners' preference. The aim of this thesis was to provide evidence-based guidance in the decision of beam arrangement, GTV dose and OARs doses in IMRT treatment planning of head and neck cancers; so as to enhance the quality and efficiency of IMRT treatment planning. Based on the dosimetric evaluation results and the development of multiple regression model, the general aims of this thesis are achieved. By evaluating the dosimetric parameters of IMRT plans, this thesis has suggested the optimum beam arrangement method for various head and neck cancers and the dosimetric feasibility to escalate the GTV dose of NPC. In addition, the development of regression models has provided a reliable method to determine reference OARs doses to guide IMRT plan optimization for NPC patients.

The research in this thesis started with the dosimetric evaluation to determine the suggested beam arrangement among the available choices in the Eclipse treatment planning system for 5 types of head and neck cancers. The use of the UTCI score to rank the plans was essential for the determination because it summarised the overall quality of plans into a single quantitative metric. Hence, despite all beam arrangement methods were able to produce clinically acceptable plans, VMAT was suggested for centrally located head and neck cancers and BAOc was suggested for ipsilateral head and neck cancers. Notwithstanding VMAT was suggested for NPC, BAOnc was found to be better sparing of OARs. Because of this, BAOnc was used to determine its ability to further escalate the GTV dose in locally advanced NPC while keeping the doses to OARs within the clinically acceptable levels. Although certain OARs dose parameters increased in the GTV

dose escalated plans, this study provided the feasibility of further escalating the GTV dose to 80 Gy on condition that the pituitary gland was considered sacrificed because of the extent of the disease. Furthermore, the research clearly illustrated the correlation of OARs dose parameters and their corresponding anatomical parameters using multiple regression models. The models can be used as an easily accessible tool for planners to obtain reference OARs dose before treatment planning, and to assess the OARs dose after the IMRT plan optimization.

Based on these results, planners can consider follow the recommendations of beam arrangements in the treatment planning of various head and neck cancers. For the implementation of dose escalation in NPC, the selection of suitable candidates is important, future studies that can examine the ways for more individualized and accurate patient selection by the prediction of clinical outcome using radiomics features in the pre-treatment images are suggested. Also, studies that evaluate the capability of 4pi VMAT in dose escalation are suggested when more advanced linear accelerators become available. Furthermore, the regression models for determination of reference OARs dose are recommended for clinical use. Future research is suggested to improve the accuracy of the models by incorporating more samples and independent variables, as well as the use of LASSO regression.

This thesis presented studies to enhance the quality and efficiency of IMRT plans in head and neck cancers including NPC. From the perspective of the clinical departments, by the implementation of the results in clinical practice, the procedure in IMRT planning will be more efficient because the time for the decision making on beam arrangement and OARs dose can be saved. The training of new planners will be more effective because of the clear evidence based suggestion and the components of knowledge-based radiotherapy planning. In addition, patients

will be benefited by the high quality treatment planning and escalation of GTV dose that can bring about better local control.

REFERENCES

- Adams, S., Baum, R. P., Stuckensen, T., Bitter, K., & Hör, G. (1998). Prospective comparison of 18 F-FDG PET with conventional imaging modalities (CT, MRI, US) in lymph node staging of head and neck cancer. *Eur J Nucl Med*, 25(9), 1255-1260. doi:10.1007/s002590050293
- Adelstein, D. J., Koyfman, S. A., El-Naggar, A. K., & Hanna, E. Y. (2012). Biology and management of salivary gland cancers. *Semin Radiat Oncol*, 22(3), 245-253. doi:10.1016/j.semradonc.2012.03.009
- Ahmed, M., Hansen, V. N., Harrington, K. J., & Nutting, C. M. (2009). Reducing the risk of xerostomia and mandibular osteoradionecrosis: the potential benefits of intensity modulated radiotherapy in advanced oral cavity carcinoma. *Med Dosim*, 34(3), 217-224. doi:10.1016/j.meddos.2008.08.008
- American Joint Committee on, C. (2017). *AJCC cancer staging manual* (Eighth edition ed.). New York]: Springer.
- Anonymous. (1991). Induction Chemotherapy plus Radiation Compared with Surgery plus Radiation in Patients with Advanced Laryngeal Cancer. *New England Journal of Medicine*, 324(24), 1685-1690. doi:10.1056/nejm199106133242402
- Antolak, J. A., & Rosen, I. I. (1999). Planning target volumes for radiotherapy: how much margin is needed? *International Journal of Radiation Oncology, Biology, Physics*, 44(5), 1165-1170. doi:10.1016/S0360-3016(99)00117-0
- Aoyama, H., Westerly, D. C., Mackie, T. R., Olivera, G. H., Bentzen, S. M., Patel, R. R., . . . Mehta, M. P. (2006). Integral radiation dose to normal structures with conformal external beam radiation. *International Journal of Radiation Oncology, Biology, Physics*, 64(3), 962-967. doi:10.1016/j.ijrobp.2005.11.005
- Appenzoller, L. M., Michalski, J. M., Thorstad, W. L., Mutic, S., & Moore, K. L. (2012). Predicting dose-volume histograms for organs-at-risk in IMRT planning. *Med Phys*, 39(12), 7446-7461. doi:10.1118/1.4761864
- Banaei, A., Hashemi, B., Bakhshandeh, M., & Mofid, B. (2019). Trade-off between the conflicting planning goals in correlation with patient's anatomical parameters for intensity-modulated radiotherapy of prostate cancer patients. *Journal of Radiotherapy in Practice*, 18(3), 232-238. doi:10.1017/S1460396919000025
- Barrett, A., & Dobbs, J. (2009). *Practical radiotherapy planning* (4th ed. / Ann Barrett ... [et al.].. ed.). London: Hodder Arnold.
- Berger, A. (2003). How does it work? Positron emission tomography. *BMJ (Clinical research ed.)*, 326(7404), 1449-1449. doi:10.1136/bmj.326.7404.1449
- Bhalavat, R. L., Fakih, A. R., Mistry, R. C., & Mahantshetty, U. (2003). Radical radiation vs surgery plus post-operative radiation in advanced (resectable) supraglottic larynx and pyriform sinus cancers: a prospective randomized study. *European Journal of Surgical Oncology (EJSO)*, 29(9), 750-756. doi:10.1016/s0748-7983(03)00072-6
- Bitar, R., Leung, G., Perng, R., Tadros, S., Moody, A. R., Sarrazin, J., . . . Roberts, T. P. (2006). MR pulse sequences: what every radiologist wants to know but is afraid to ask. *Radiographics : a review publication of the Radiological Society of North America, Inc*, 26(2), 513-537. doi:10.1148/rg.262055063
- Bohsung, J., Gillis, S., Arrans, R., Bakai, A., De Wagter, C., Knoos, T., . . . Williams, P. (2005). IMRT treatment planning:- a comparative inter-system and inter-centre planning exercise of the ESTRO QUASIMODO group. *Radiother Oncol*, 76(3), 354-361. doi:10.1016/j.radonc.2005.08.003
- Brahme, A. (1982). Solution of an integral equation encountered in rotation therapy. *Physics in Medicine and Biology*, 27(10), 1221-1229. doi:10.1088/0031-9155/27/10/002

- Brahme, A. (1988). Optimization of stationary and moving beam radiation therapy techniques. *Radiotherapy and Oncology*, 12(2), 129-140. doi:10.1016/0167-8140(88)90167-3
- Bristol, I. J., Ahamad, A., Garden, A. S., Morrison, W. H., Hanna, E. Y., Papadimitrakopoulou, V. A., . . . Ang, K. K. (2007). Postoperative radiotherapy for maxillary sinus cancer: long-term outcomes and toxicities of treatment. *Int J Radiat Oncol Biol Phys*, 68(3), 719-730. doi:10.1016/j.ijrobp.2007.01.032
- Brockstein, B., & Masters, G. (2003). *Head and Neck Cancer*. Boston: Springer.
- Brodin, N. P., & Tome, W. A. (2018). Revisiting the dose constraints for head and neck OARs in the current era of IMRT. *Oral Oncol*, 86, 8-18. doi:10.1016/j.oraloncology.2018.08.018
- Brouwer, C. L., Steenbakkers, R. J., Bourhis, J., Budach, W., Grau, C., Gregoire, V., . . . Langendijk, J. A. (2015). CT-based delineation of organs at risk in the head and neck region: DAHANCA, EORTC, GORTEC, HKNPCSG, NCIC CTG, NCRI, NRG Oncology and TROG consensus guidelines. *Radiother Oncol*, 117(1), 83-90. doi:10.1016/j.radonc.2015.07.041
- Budach, W., Bolke, E., Kammers, K., Gerber, P. A., Orth, K., Gripp, S., & Matuschek, C. (2016). Induction chemotherapy followed by concurrent radio-chemotherapy versus concurrent radio-chemotherapy alone as treatment of locally advanced squamous cell carcinoma of the head and neck (HNSCC): A meta-analysis of randomized trials. *Radiother Oncol*, 118(2), 238-243. doi:10.1016/j.radonc.2015.10.014
- Budrukkar, A. N., Hope, G., Cramb, J., Corry, J., & Peters, L. J. (2004). Dosimetric study of optimal beam number and arrangement for treatment of nasopharyngeal carcinoma with intensity-modulated radiation therapy. *Australasian Radiology*, 48(1), 45-50. doi:10.1111/j.1440-1673.2004.01241.x
- Burnet, N. G., Thomas, S. J., Burton, K. E., & Jefferies, S. J. (2004). Defining the tumour and target volumes for radiotherapy. *Cancer Imaging*, 4(2), 153-161. doi:10.1102/1470-7330.2004.0054
- Chan, A. T., Felip, E., & Group, E. G. W. (2008). Nasopharyngeal cancer: ESMO clinical recommendations for diagnosis, treatment and follow-up. *Ann Oncol*, 19 Suppl 2, ii81-82. doi:10.1093/annonc/mdn098
- Chan, A. T., Gregoire, V., Lefebvre, J. L., Licitra, L., Hui, E. P., Leung, S. F., . . . Group, E.-E.-E. G. W. (2012). Nasopharyngeal cancer: EHNS-ESMO-ESTRO Clinical Practice Guidelines for diagnosis, treatment and follow-up. *Ann Oncol*, 23 Suppl 7, vii83-85. doi:10.1093/annonc/mds266
- Chao, H. L., Liu, S. C., Tsao, C. C., Lin, K. T., Lee, S. P., Lo, C. H., . . . Lin, C. S. (2017). Dose escalation via brachytherapy boost for nasopharyngeal carcinoma in the era of intensity-modulated radiation therapy and combined chemotherapy. *J Radiat Res*, 58(5), 654-660. doi:10.1093/jrr/rrx034
- Chau, R. M., Leung, S. F., Kam, M. K., Cheung, K. Y., Kwan, W. H., Yu, K. H., . . . Chan, A. T. (2008). A split-organ delineation approach for dose optimisation for intensity-modulated radiotherapy for advanced T-stage nasopharyngeal carcinoma. *Clin Oncol (R Coll Radiol)*, 20(2), 134-141. doi:10.1016/j.clon.2007.10.006
- Chen, Y., Sun, Y., Liang, S. B., Zong, J. F., Li, W. F., Chen, M., . . . Ma, J. (2013). Progress report of a randomized trial comparing long-term survival and late toxicity of concurrent chemoradiotherapy with adjuvant chemotherapy versus radiotherapy alone in patients with stage III to IVB nasopharyngeal carcinoma from endemic regions of China. *Cancer*, 119(12), 2230-2238. doi:10.1002/cncr.28049
- Cheung, W. K., Lee, K. H., Cheng, H. C., Cheung, C. H., Chan, C. L., & Ngan, K. C. (2010). Comparison of RapidArc and static gantry intensity-modulated radiotherapy for nasopharyngeal carcinoma. *Journal of the Hong Kong College of Radiologists*, 13(3), 125-132.
- Cho, B. (2018). Intensity-modulated radiation therapy: a review with a physics perspective. *Radiation oncology journal*, 36(1), 1-10. doi:10.3857/roj.2018.00122
- Chua, D. T. T., Sham, J. S. T., Wei, W. I., Ho, W. K., & Au, G. K. H. (2001). The predictive value of the 1997 American Joint Committee on Cancer stage classification in determining failure patterns in

- nasopharyngeal carcinoma. *Cancer*, 92(11), 2845-2855. doi:10.1002/1097-0142(20011201)92:11<2845::AID-CNCR10133>3.0.CO;2-7
- Chua, M. L. K., Wee, J. T. S., Hui, E. P., & Chan, A. T. C. (2016). Nasopharyngeal carcinoma. *The Lancet*, 387(10022), 1012-1024. doi:10.1016/s0140-6736(15)00055-0
- Chui, C.-S., & Spirou, S. V. (2001). Inverse planning algorithms for external beam radiation therapy. *Medical Dosimetry*, 26(2), 189-197. doi:10.1016/S0958-3947(01)00069-3
- Clivio, A., Fogliata, A., Franzetti-Pellanda, A., Nicolini, G., Vanetti, E., Wytenbach, R., & Cozzi, L. (2009). Volumetric-modulated arc radiotherapy for carcinomas of the anal canal: A treatment planning comparison with fixed field IMRT. *Radiotherapy and Oncology*, 92(1), 118-124. doi:10.1016/j.radonc.2008.12.020
- Craft, D. L., Hong, T. S., Shih, H. A., & Bortfeld, T. R. (2012). Improved Planning Time and Plan Quality Through Multicriteria Optimization for Intensity-Modulated Radiotherapy. *International Journal of Radiation Oncology, Biology, Physics*, 82(1), e83-e90. doi:10.1016/j.ijrobp.2010.12.007
- Daly, M. E., Le, Q. T., Jain, A. K., Maxim, P. G., Hsu, A., Loo, B. W., Jr., . . . Chang, D. T. (2011). Intensity-modulated radiotherapy for locally advanced cancers of the larynx and hypopharynx. *Head Neck*, 33(1), 103-111. doi:10.1002/hed.21406
- Damodaran, O., Rizk, E., Rodriguez, J., & Lee, G. (2014). Cranial nerve assessment: a concise guide to clinical examination. *Clin Anat*, 27(1), 25-30. doi:10.1002/ca.22336
- Das, I. J., Cheng, C.-W., Fein, D. A., Coia, L. R., Curran, W. J., & Fowble, B. (1997). Dose estimation to critical organs from vertex field treatment of brain tumors. *International Journal of Radiation Oncology*Biological*Physics*, 37(5), 1023-1029. doi:[https://doi.org/10.1016/S0360-3016\(96\)00567-6](https://doi.org/10.1016/S0360-3016(96)00567-6)
- Dawson, L. A., Anzai, Y., Marsh, L., Martel, M. K., Paulino, A., Ship, J. A., & Eisbruch, A. (2000a). Patterns of local-regional recurrence following parotid-sparing conformal and segmental intensity-modulated radiotherapy for head and neck cancer. *International Journal of Radiation Oncology, Biology, Physics*, 46(5), 1117-1126. doi:10.1016/S0360-3016(99)00550-7
- Dawson, L. A., Anzai, Y., Marsh, L., Martel, M. K., Paulino, A., Ship, J. A., & Eisbruch, A. (2000b). Patterns of local-regional recurrence following parotid-sparing conformal and segmental intensity-modulated radiotherapy for head and neck cancer. *International Journal of Radiation Oncology*Biological*Physics*, 46(5), 1117-1126. doi:10.1016/S0360-3016(99)00550-7
- Dijkstra, P. U., Kalk, W. W. I., & Roodenburg, J. L. N. (2004). Trismus in head and neck oncology: a systematic review. *Oral Oncology*, 40(9), 879-889. doi:10.1016/j.oraloncology.2004.04.003
- Earl, M. A., Shepard, D. M., Li, X. A., & Yu, C. X. (2001). Inverse planning for intensity modulated arc therapy using direct aperture optimization. *International Journal of Radiation Oncology, Biology, Physics*, 51(3), 405-406. doi:10.1016/S0360-3016(01)02570-6
- Eisbruch, A., Foote, R. L., O'Sullivan, B., Beitler, J. J., & Vikram, B. (2002). Intensity-modulated radiation therapy for head and neck cancer: Emphasis on the selection and delineation of the targets. *Seminars in Radiation Oncology*, 12(3), 238-249. doi:10.1053/srao.2002.32435
- Eisbruch, A., Kim, H. M., Terrell, J. E., Marsh, L. H., Dawson, L. A., & Ship, J. A. (2001). Xerostomia and its predictors following parotid-sparing irradiation of head-and-neck cancer. *International Journal of Radiation Oncology, Biology, Physics*, 50(3), 695-704. doi:10.1016/S0360-3016(01)01512-7
- Elicin, O., Terribilini, D., Shelan, M., Volken, W., Mathier, E., Dal Pra, A., . . . Manser, P. (2017). Primary tumor volume delineation in head and neck cancer: missing the tip of the iceberg? *Radiat Oncol*, 12(1), 102. doi:10.1186/s13014-017-0838-4
- Ellis, C. H. (2004). Standard error of the estimate. In *The SAGE Encyclopedia of Social Science Research Methods*. Thousand Oaks: SAGE Publications. Retrieved from <http://sk.sagepub.com/reference/socialscience>. doi:10.4135/9781412950589

- Ellis, M. A., Graboyes, E. M., Wahlquist, A. E., Neskey, D. M., Kaczmar, J. M., Schopper, H. K., . . . Day, T. A. (2018). Primary Surgery vs Radiotherapy for Early Stage Oral Cavity Cancer. *Otolaryngology–Head and Neck Surgery*, *158*(4), 649-659. doi:10.1177/0194599817746909
- Eversole, L. R., & Silverman, S. (2001). Swellings and tumors of the oral cavity and face. In *Essentials of Oral Medicine* (pp. 228-243). Hamilton-London: BC Decker.
- Ezzell, G. A., Galvin, J. M., Low, D., Palta, J. R., Rosen, I., Sharpe, M. B., . . . committee, A. R. T. (2003). Guidance document on delivery, treatment planning, and clinical implementation of IMRT: report of the IMRT Subcommittee of the AAPM Radiation Therapy Committee. *Med Phys*, *30*(8), 2089-2115. doi:10.1118/1.1591194
- Farrar, D. E. (1967). Multicollinearity in regression analysis: the problem revisited. *The review of economics and statistics*, *49*(1), 92-107.
- Ferlay, J., Ervik, M., Lam, F., Colombet, M., Mery, L., Pineros, M., . . . Soerjomataram, I. (2018). Nasopharynx fact sheet: GLOBOCAN 2018. Retrieved from gco.iarc.fr/today/data/factsheets/cancers/4-Nasopharynx-fact-sheet.pdf
- Fitzgerald, R., Owen, R., Barry, T., Hargrave, C., Pryor, D., Bernard, A., . . . Fielding, A. (2016). The effect of beam arrangements and the impact of non-coplanar beams on the treatment planning of stereotactic ablative radiation therapy for early stage lung cancer. *Journal of Medical Radiation Sciences*, *63*(1), 31-40. doi:10.1002/jmrs.118
- Fridman, E., Na'ara, S., Agarwal, J., Amit, M., Bachar, G., Villaret, A. B., . . . Neck, C. (2018). The role of adjuvant treatment in early-stage oral cavity squamous cell carcinoma: An international collaborative study. *Cancer*, *124*(14), 2948-2955. doi:10.1002/cncr.31531
- Fu, Y., Deng, M., Zhou, X., Lin, Q., Du, B., Tian, X., . . . Gong, Y. (2017). Dosimetric effect of beam arrangement for intensity-modulated radiation therapy in the treatment of upper thoracic esophageal carcinoma. *Medical Dosimetry*, *42*(1), 47-52. doi:10.1016/j.meddos.2016.11.002
- Funk, R. K., Stockham, A. L., & Laack, N. N. I. (2016). Basics of Radiation Therapy. In *Clinical Cardio-Oncology* (pp. 39-60).
- Gao, Y., Liu, J. J., Zhu, S. Y., & Yi, X. (2014). The diagnostic accuracy of ultrasonography versus endoscopy for primary nasopharyngeal carcinoma. *PLoS One*, *9*(3), e90412. doi:10.1371/journal.pone.0090412
- Ge, Y., & Wu, Q. J. (2019). Knowledge-based planning for intensity-modulated radiation therapy: A review of data-driven approaches. *Med Phys*, *46*(6), 2760-2775. doi:10.1002/mp.13526
- Gollop, R., Whitby, E., Buchanan, D., & Ketley, D. (2004). Influencing sceptical staff to become supporters of service improvement: a qualitative study of doctors' and managers' views. *Quality and Safety in Health Care*, *13*(2), 108. doi:10.1136/qshc.2003.007450
- Gomez-Millan, J., Fernandez, J. R., & Medina Carmona, J. A. (2013). Current status of IMRT in head and neck cancer. *Rep Pract Oncol Radiother*, *18*(6), 371-375. doi:10.1016/j.rpor.2013.09.008
- Gomez, D. R., Zhung, J. E., Gomez, J., Chan, K., Wu, A. J., Wolden, S. L., . . . Lee, N. Y. (2009). Intensity-Modulated Radiotherapy in Postoperative Treatment of Oral Cavity Cancers. *International Journal of Radiation Oncology, Biology, Physics*, *73*(4), 1096-1103. doi:10.1016/j.ijrobp.2008.05.024
- Gregoire, V., Ang, K., Budach, W., Grau, C., Hamoir, M., Langendijk, J. A., . . . Lengele, B. (2014). Delineation of the neck node levels for head and neck tumors: a 2013 update. DAHANCA, EORTC, HKNPCSG, NCIC CTG, NCRI, RTOG, TROG consensus guidelines. *Radiother Oncol*, *110*(1), 172-181. doi:10.1016/j.radonc.2013.10.010
- Gregoire, V., Evans, M., Le, Q. T., Bourhis, J., Budach, V., Chen, A., . . . Grau, C. (2018). Delineation of the primary tumour Clinical Target Volumes (CTV-P) in laryngeal, hypopharyngeal, oropharyngeal and oral cavity squamous cell carcinoma: AIRO, CACA, DAHANCA, EORTC, GEORCC, GORTEC, HKNPCSG, HNCIG, IAG-KHT, LPRHHT, NCIC CTG, NCRI, NRG Oncology, PHNS, SBRT, SOMERA, SRO, SSHNO, TROG consensus guidelines. *Radiother Oncol*, *126*(1), 3-24. doi:10.1016/j.radonc.2017.10.016

- Grégoire, V., & Mackie, T. R. (2011). State of the art on dose prescription, reporting and recording in Intensity-Modulated Radiation Therapy (ICRU report No. 83). *Cancer/Radiothérapie*, 15(6), 555-559. doi:10.1016/j.canrad.2011.04.003
- Grover, V. P., Tognarelli, J. M., Crossey, M. M., Cox, I. J., Taylor-Robinson, S. D., & McPhail, M. J. (2015). Magnetic Resonance Imaging: Principles and Techniques: Lessons for Clinicians. *J Clin Exp Hepatol*, 5(3), 246-255. doi:10.1016/j.jceh.2015.08.001
- Gupta, T., Agarwal, J., Jain, S., Phurailatpam, R., Kannan, S., Ghosh-Laskar, S., . . . D'cruz, A. (2012). Three-dimensional conformal radiotherapy (3D-CRT) versus intensity modulated radiation therapy (IMRT) in squamous cell carcinoma of the head and neck: A randomized controlled trial. *Radiotherapy and Oncology*, 104(3), 343-348. doi:10.1016/j.radonc.2012.07.001
- Hawkins, P. G., Kadam, A. S., Jackson, W. C., & Eisbruch, A. (2018). Organ-Sparing in Radiotherapy for Head-and-Neck Cancer: Improving Quality of Life. *Semin Radiat Oncol*, 28(1), 46-52. doi:10.1016/j.semradonc.2017.08.002
- Higby, C., Khafaga, Y., Al-Shabanah, M., Mousa, A., Ilyas, M., Nazer, G., & Khalil, E. M. (2016). Volumetric-modulated arc therapy (VMAT) versus 3D-conformal radiation therapy in supra-diaphragmatic Hodgkin's Lymphoma with mediastinal involvement: A dosimetric comparison. *Journal of the Egyptian National Cancer Institute*, 28(3), 163-168. doi:10.1016/j.jnci.2016.04.007
- Hong Kong Cancer Registry. (2016). Nasopharyngeal Cancer in 2016. Retrieved from <http://www3.ha.org.hk/cancereg/facts.html>
- Hornig, J. D., Malin, B. T., & Oconnell, B. (2014). Clinical evaluation of the head and neck cancer patient. In *Head and neck cancer: a multidisciplinary approach* (Fourth ed.). Philadelphia: Lippincott Williams & Wilkins.
- Hou, Y., Zhang, Y., Liu, Z., Yv, L., Liu, K., Tian, X., & Lv, Y. (2019). Intensity-modulated radiotherapy, coplanar volumetric-modulated arc, therapy, and noncoplanar volumetric-modulated arc therapy in, glioblastoma: A dosimetric comparison. *Clinical neurology and neurosurgery*, 187, 105573. doi:10.1016/j.clineuro.2019.105573
- Huang, D., Xia, P., Akazawa, P., Akazawa, C., Quivey, J. M., Verhey, L. J., . . . Lee, N. (2003). Comparison of treatment plans using intensity-modulated radiotherapy and three-dimensional conformal radiotherapy for paranasal sinus carcinoma. *International Journal of Radiation Oncology*Biophysics*, 56(1), 158-168. doi:10.1016/s0360-3016(03)00080-4
- Huang, S. H., & O'Sullivan, B. (2013). Oral cancer: Current role of radiotherapy and chemotherapy. *Med Oral Patol Oral Cir Bucal*, 18(2), e233-240. doi:10.4317/medoral.18772
- Hugo, J. W. L. A., Emmanuel Rios, V., Ralph, T. H. L., Chintan, P., Patrick, G., Sara, C., . . . Philippe, L. (2014). Decoding tumour phenotype by noninvasive imaging using a quantitative radiomics approach. *Nature Communications*, 5(1). doi:10.1038/ncomms5006
- Hunt, M. A., & Burman, C. M. (2003). Treatment planning considerations using IMRT. In *Memorial Sloan-Kettering Cancer Center (eds: Z. Fuks, SA Leibel, CC Ling). A Practical Guide to Intensity-Modulated Radiation Therapy* (pp. 103-121). Madison, Wisconsin: Medical Physics Pub.
- Hurley, K. F. (2011). *OSCE and clinical skills handbook* (2nd ed. ed.). Toronto: Elsevier/Saunders.
- Jain, N. L., & Kahn, M. G. (1992). Ranking radiotherapy treatment plans using decision-analytic and heuristic techniques. *Computers and Biomedical Research*, 25(4), 374-383. doi:10.1016/0010-4809(92)90027-8
- Jarque, C. M., & Bera, A. K. (1980). Efficient tests for normality, homoscedasticity and serial independence of regression residuals. *Economics Letters*, 6(3), 255-259. doi:[https://doi.org/10.1016/0165-1765\(80\)90024-5](https://doi.org/10.1016/0165-1765(80)90024-5)
- Johnston, M., Clifford, S., Bromley, R., Back, M., Oliver, L., & Eade, T. (2011). Volumetric-modulated arc therapy in head and neck radiotherapy: a planning comparison using simultaneous integrated boost for nasopharynx and oropharynx carcinoma. *Clin Oncol (R Coll Radiol)*, 23(8), 503-511. doi:10.1016/j.clon.2011.02.002

- Jones, A. D., Mendenhall, M. C., Kirwan, G. J., Morris, J. C., Donnan, R. A., Holwerda, M. S., . . . Mendenhall, M. W. (2010). Radiation Therapy for Management of T1–T2 Glottic Cancer at a Private Practice. *American Journal of Clinical Oncology*, 33(6), 587-590. doi:10.1097/COC.0b013e3181beaab0
- Kam, M. K., Leung, S. F., Zee, B., Choi, P. H. K., Chau, R. M. C., Cheung, K. Y., . . . Chan, A. T. C. (2005). Impact of intensity-modulated radiotherapy (IMRT) on salivary gland function in early-stage nasopharyngeal carcinoma (NPC) patients: A prospective randomized study. *Journal of Clinical Oncology*, 23(16_suppl), 5501-5501. doi:10.1200/jco.2005.23.16_suppl.5501
- Kam, M. K., Teo, P. M., Chau, R. M., Cheung, K. Y., Choi, P. H., Kwan, W. H., . . . Chan, A. T. (2004). Treatment of nasopharyngeal carcinoma with intensity-modulated radiotherapy: the Hong Kong experience. *Int J Radiat Oncol Biol Phys*, 60(5), 1440-1450. doi:10.1016/j.ijrobp.2004.05.022
- Katz, T. S., Mendenhall, W. M., Morris, C. G., Amdur, R. J., Hinerman, R. W., & Villaret, D. B. (2002). Malignant tumors of the nasal cavity and paranasal sinuses. *Head Neck*, 24(9), 821-829. doi:10.1002/hed.10143
- Kerns, J. R., Childress, N., & Kry, S. F. (2014). A multi-institution evaluation of MLC log files and performance in IMRT delivery. *Radiation Oncology*, 9(1), 176. doi:10.1186/1748-717X-9-176
- Khan, S. J., Chin, E., Otto, K., Hristov, D. H., Xing, L., & Fahimian, B. P. (2016). Beyond VMAT—Assessing the Potential of Noncoplanar Arc Delivery Trajectories Incorporating Dynamic Couch Motion in Intracranial Radiation Therapy. *International Journal of Radiation Oncology, Biology, Physics*, 96(2), S80-S81. doi:10.1016/j.ijrobp.2016.06.204
- Kumar, S. A. S., Holla, R., Sukumar, P., Padmanaban, S., & Vivekanandan, N. (2013). Treatment planning and dosimetric comparison study on two different volumetric modulated arc therapy delivery techniques. *Reports of Practical Oncology & Radiotherapy*, 18(2), 87-94. doi:10.1016/j.rpor.2012.07.008
- Kutner, M. H. (2004). *Applied linear regression models* (4th ed. / Michael H. Kutner, Christopher J. Nachtsheim, John Neter.. ed.). Boston: McGraw-Hill/Irwin.
- Kwee, T., & Kwee, R. (2009). Combined FDG-PET/CT for the detection of unknown primary tumors: systematic review and meta-analysis. *Eur Radiol*, 19(3), 731-744. doi:10.1007/s00330-008-1194-4
- Kwong, D. L., Sham, J. S., Leung, L. H., Cheng, A. C., Ng, W. M., Kwong, P. W., . . . Au, G. (2006). Preliminary results of radiation dose escalation for locally advanced nasopharyngeal carcinoma. *Int J Radiat Oncol Biol Phys*, 64(2), 374-381. doi:10.1016/j.ijrobp.2005.07.968
- Lam, K. S. L., Tse, V. K. C., Wang, C., Yeung, R. T. T., & Ho, J. H. C. (1991). Effects of Cranial Irradiation on Hypothalamic—Pituitary Function—a 5-Year Longitudinal Study in Patients with Nasopharyngeal Carcinoma. *QJM: An International Journal of Medicine*, 78(2), 165-176. doi:10.1093/oxfordjournals.qjmed.a068535
- Lam, P., Au-Yeung, K. M., Cheng, P. W., Wei, W. I., Yuen, A. P.-W., Trendell-Smith, N., . . . Li, R. (2004). Correlating MRI and histologic tumor thickness in the assessment of oral tongue cancer. *AJR. American journal of roentgenology*, 182(3), 803-808. doi:10.2214/ajr.182.3.1820803
- Larue, R. T. H. M., Defraene, G., Ruysscher, D. D., Lambin, P., & Elmt, W. v. (2017). Quantitative radiomics studies for tissue characterization: a review of technology and methodological procedures. *90(1070)*, 20160665. doi:10.1259/bjr.20160665
- Lauve, A., Morris, M., Schmidt-Ullrich, R., Wu, Q., Mohan, R., Abayomi, O., . . . Reiter, E. (2004). Simultaneous integrated boost intensity-modulated radiotherapy for locally advanced head-and-neck squamous cell carcinomas: II—clinical results. *Int J Radiat Oncol Biol Phys*, 60(2), 374-387. doi:10.1016/j.ijrobp.2004.03.010
- Lee, A. W., Ngan, R. K., Tung, S. Y., Cheng, A., Kwong, D. L., Lu, T. X., . . . Chappell, R. (2015). Preliminary results of trial NPC-0501 evaluating the therapeutic gain by changing from concurrent-adjuvant to induction-concurrent chemoradiotherapy, changing from fluorouracil to capecitabine, and changing from conventional to accelerated radiotherapy fractionation in patients

- with locoregionally advanced nasopharyngeal carcinoma. *Cancer*, 121(8), 1328-1338.
doi:10.1002/cncr.29208
- Lee, A. W. M., Ng, W. T., Chan, L. L. K., Hung, W. M., Chan, C. C. C., Sze, H. C. K., . . . Yeung, R. M. W. (2014). Evolution of treatment for nasopharyngeal cancer – Success and setback in the intensity-modulated radiotherapy era. *Radiotherapy and Oncology*, 110(3), 377-384.
doi:10.1016/j.radonc.2014.02.003
- Leung, L. H., Kan, M. W., Cheng, A. C., Wong, W. K., & Yau, C. C. (2007). A new dose-volume-based Plan Quality Index for IMRT plan comparison. *Radiother Oncol*, 85(3), 407-417.
doi:10.1016/j.radonc.2007.10.018
- Leung, S. F., Tsao, S. Y., Teo, P., & Foo, W. (1990). Cranial nerve involvement by nasopharyngeal carcinoma: Response to treatment and clinical significance. *Clinical Oncology*, 2(3), 138-141.
doi:10.1016/S0936-6555(05)80146-3
- Li, F., Yang, Y., & Xing, E. P. (2005). From Lasso regression to Feature Vector Machine. In (pp. 779-786).
- Li, J.-C., Mayr, N. A., Yuh, W. T. C., Wang, J. Z., & Jiang, G.-L. (2006). Cranial Nerve Involvement in Nasopharyngeal Carcinoma: Response to Radiotherapy and its Clinical Impact. *Annals of Otolaryngology, Rhinology & Laryngology*, 115(5), 340-345. doi:10.1177/000348940611500504
- Li, M., Qu, S., Qin, Y., Lu, J., Yu, S., Lan, G., . . . Si, Y. (2017). Diagnosis of nonexophytic nasopharyngeal lesion with endoscopy-guided core needle biopsy after narrow band imaging. *Oncotarget*, 8(44), 76069-76075. doi:10.18632/oncotarget.18475
- Lomax, N. J., & Scheib, S. G. (2003). Quantifying the degree of conformity in radiosurgery treatment planning. *International Journal of Radiation Oncology*Biophysics*, 55(5), 1409-1419.
doi:10.1016/S0360-3016(02)04599-6
- Lomax, R. G. (2012). *An introduction to statistical concepts* (3rd ed., ed.). New York: Routledge.
- Low, D. A., Moran, J. M., Dempsey, J. F., Dong, L., & Oldham, M. (2011). Dosimetry tools and techniques for IMRT. *Med Phys*, 38(3), 1313-1338. doi:10.1118/1.3514120
- Lue, B.-H., Huang, T.-S., & Chen, H.-J. (2008). Physical Distress, Emotional Status, and Quality of Life in Patients With Nasopharyngeal Cancer Complicated by Post-Radiotherapy Endocrinopathy. *International Journal of Radiation Oncology, Biology, Physics*, 70(1), 28-34.
doi:10.1016/j.ijrobp.2007.06.053
- Lyu, Q., Yu, V. Y., Ruan, D., Neph, R., O'connor, D., & Sheng, K. (2018). A novel optimization framework for VMAT with dynamic gantry couch rotation. *Physics in Medicine and Biology (Online)*, 63(12). doi:10.1088/1361-6560/aac704
- Mackenzie, M. A., & Robinson, D. M. (2002). Intensity modulated arc deliveries approximated by a large number of fixed gantry position sliding window dynamic multileaf collimator fields. *Medical Physics*, 29(10), 2359-2365. doi:10.1118/1.1508110
- Mayles, P., Nahum, A., & Rosenwald, J. C. (2007). *Handbook of Radiotherapy Physics* (1 ed.).
- Mazon, J. J., Ardiet, J. M., Haie-Meder, C., Kovacs, G., Levendag, P., Peiffert, D., . . . Strnad, V. (2009). GEC-ESTRO recommendations for brachytherapy for head and neck squamous cell carcinomas. *Radiother Oncol*, 91(2), 150-156. doi:10.1016/j.radonc.2009.01.005
- Mendenhall, W. M., Amdur, R. J., & Palta, J. R. (2006). Head and Neck Cancer. In *Technical Basis of Radiation Therapy: Practical Clinical Applications* (4th Revised Edition ed., pp. 453-484). Berlin, Heidelberg.
- Menhel, J., Levin, D., Alezra, D., Symon, Z., & Pfeffer, R. (2006). Assessing the quality of conformal treatment planning: a new tool for quantitative comparison. *Phys Med Biol*, 51(20), 5363-5375.
doi:10.1088/0031-9155/51/20/019
- Meyer, R. R., Zhang, H. H., Goadrich, L., Nazareth, D. P., Shi, L., & D'Souza, W. D. (2007). A multiplan treatment-planning framework: a paradigm shift for intensity-modulated radiotherapy. *Int J Radiat Oncol Biol Phys*, 68(4), 1178-1189. doi:10.1016/j.ijrobp.2007.02.051

- Miften, M. M., Das, S. K., Su, M., & Marks, L. B. (2004). A dose-volume-based tool for evaluating and ranking IMRT treatment plans. *Journal of Applied Clinical Medical Physics*, 5(4), 1-14. doi:10.1120/jacmp.v5i4.1981
- Montgomery, D. C. (2012). *Introduction to linear regression analysis* (Fifth edition. ed.). Hoboken, New Jersey: Wiley.
- Moore, K. L., Brame, R. S., Low, D. A., & Mutic, S. (2011). Experience-based quality control of clinical intensity-modulated radiotherapy planning. *Int J Radiat Oncol Biol Phys*, 81(2), 545-551. doi:10.1016/j.ijrobp.2010.11.030
- Moran, J. M., Radawski, J., & Fraass, B. A. (2005). A dose-gradient analysis tool for IMRT QA. *Journal of Applied Clinical Medical Physics*, 6(2), 62-73. doi:10.1120/jacmp.v6i2.2006
- Mukherji, S. K., Isaacs, D. L., Creager, A., Shockley, W., Weissler, M., & Armao, D. (2001). CT detection of mandibular invasion by squamous cell carcinoma of the oral cavity. *AJR. American journal of roentgenology*, 177(1), 237. doi:10.2214/ajr.177.1.1770237
- Napier, S. S., & Speight, P. M. (2008). Natural history of potentially malignant oral lesions and conditions: an overview of the literature. *J Oral Pathol Med*, 37(1), 1-10. doi:10.1111/j.1600-0714.2007.00579.x
- Nelms, B. E., Robinson, G., Markham, J., Velasco, K., Boyd, S., Narayan, S., . . . Sobczak, M. L. (2012). Variation in external beam treatment plan quality: An inter-institutional study of planners and planning systems. *Practical Radiation Oncology*, 2(4), 296-305. doi:<https://doi.org/10.1016/j.prro.2011.11.012>
- Ng, W. T., Lee, M. C., Chang, A. T., Chan, O. S., Chan, L. L., Cheung, F. Y., . . . Lee, A. W. (2014). The impact of dosimetric inadequacy on treatment outcome of nasopharyngeal carcinoma with IMRT. *Oral Oncol*, 50(5), 506-512. doi:10.1016/j.oraloncology.2014.01.017
- Ng, W. T., Wong, E. C. Y., Lee, V. H. F., Chan, J. Y. W., & Lee, A. W. M. (2017). Head and neck cancer in Hong Kong. *Japanese Journal of Clinical Oncology*, 48(1), 13-21. doi:10.1093/jjco/hyx151
- Niu, X., Chang, X., Gao, Y., Hu, C., & Kong, L. (2013). Using neoadjuvant chemotherapy and replanning intensity-modulated radiotherapy for nasopharyngeal carcinoma with intracranial invasion to protect critical normal tissue. *Radiat Oncol*, 8(1), 226-226. doi:10.1186/1748-717x-8-226
- Norton, S. B., Cormier, S. M., Smith, M., Jones, R. C., & Schubauer-Berigan, M. (2002). Predicting levels of stress from biological assessment data: empirical models from the Eastern Corn Belt Plains, Ohio, USA. *Environmental toxicology and chemistry*, 21(6), 1168-1175. doi:10.1002/etc.5620210608
- O'Donnell, W. E. (1962). Physical examination of head and neck. In *Early detection and diagnosis of cancer*. St. Louis: The C. V. Mosby Company.
- Olsen, L. A., Robinson, C. G., He, G. R., Wooten, H. O., Yaddanapudi, S., Mutic, S., . . . Moore, K. L. (2014). Automated radiation therapy treatment plan workflow using a commercial application programming interface. *Practical Radiation Oncology*, 4(6), 358-367. doi:<https://doi.org/10.1016/j.prro.2013.11.007>
- Omami, G., Tamimi, D., & Branstetter, B. F. (2014). Basic principles and applications of (18)F-FDG-PET/CT in oral and maxillofacial imaging: A pictorial essay. *Imaging science in dentistry*, 44(4), 325-332. doi:10.5624/isd.2014.44.4.325
- Ortholan, C., Benezery, K., & Bensadoun, R. J. (2010). Normal tissue tolerance to external beam radiation therapy: Salivary glands.(Report). *Cancer / Radiotherapie*, 14(4-5), 290. doi:10.1016/j.canrad.2010.03.007
- Osbourne, J. W., & Waters, E. (2002). Four Assumptions of Multiple Regression That Researchers Should Always Test. *Practical Assessment, Research & Evaluation*, 8(2).
- Pan, C. C., Eisbruch, A., Lee, J. S., Snorrason, R. M., Ten Haken, R. K., & Kileny, P. R. (2005). Prospective study of inner ear radiation dose and hearing loss in head-and-neck cancer patients. *International Journal of Radiation Oncology, Biology, Physics*, 61(5), 1393-1402. doi:10.1016/j.ijrobp.2004.08.019

- Parashar, B., Kuo, C., Kutler, D., Kuhel, W., Sabbas, A., Wernicke, G., & Nori, D. (2009). Importance of contouring the cervical spine levels in initial intensity-modulated radiation therapy radiation for head and neck cancers: Implications for re-irradiation. *Journal of Cancer Research and Therapeutics*, 5(1), 36-40. doi:10.4103/0973-1482.48767
- Pardoe, I. (2012). *Applied regression modeling: A business approach*. Hoboken: John Wiley & Sons.
- Parke, C. S. (2013). *Essential first steps to data analysis : scenario-based examples using SPSS*. Thousand Oaks: SAGE Publications.
- Parker, R. P. (1979). The direct use of ct numbers in radiotherapy dosage calculations for inhomogeneous media. *Physics in Medicine and Biology*, 24(4), 802-809. doi:10.1088/0031-9155/24/4/011
- Parker, W., & Patrocínio, H. (2005). Clinical treatment planning in external photon beam radiotherapy. In *Radiation oncology physics: A handbook for teachers and students*. Vienna: IAEA (pp. 219). Vienna: IAEA.
- Pfister, D. G., Laurie, S. A., Weinstein, G. S., Mendenhall, W. M., Adelstein, D. J., Ang, K. K., . . . Wolf, G. T. (2006). American Society of Clinical Oncology clinical practice guideline for the use of larynx-preservation strategies in the treatment of laryngeal cancer. *J Clin Oncol*, 24(22), 3693-3704. doi:10.1200/JCO.2006.07.4559
- Pursley, J., Damato, A. L., Czerminska, M. A., Margalit, D. N., Sher, D. J., & Tishler, R. B. (2017). A comparative study of standard intensity-modulated radiotherapy and RapidArc planning techniques for ipsilateral and bilateral head and neck irradiation. *Medical Dosimetry*, 42(1), 31-36. doi:<https://doi.org/10.1016/j.meddos.2016.10.004>
- Qiuwen, W. (2003). Intensity-modulated radiotherapy optimization with geud-guided dosevolume objectives. *IMRT optimizations with gEUD and DV*, 48(3), 279-291. doi:10.1088/0031-9155/48/3/301
- Rancati, T., & Fiorino, C. (2019). *Modelling Radiotherapy Side Effects: Practical Applications for Planning Optimisation*: CRC Press.
- Ranstam, J., & Cook, J. A. (2018). LASSO regression. *British Journal of Surgery*, 105(10), 1348-1348. doi:10.1002/bjs.10895
- Ratnasingam, J., Karim, N., Paramasivam, S., Ibrahim, L., Lim, L., Tan, A., . . . Chan, S. (2015). Hypothalamic pituitary dysfunction amongst nasopharyngeal cancer survivors. *Pituitary*, 18(4), 448-455. doi:10.1007/s11102-014-0593-6
- Rehman, J. u., Zahra, Ahmad, N., Khalid, M., Noor ul Huda Khan Asghar, H. M., Gilani, Z. A., . . . Usmani, M. N. (2019). Intensity modulated radiation therapy: A review of current practice and future outlooks. *Journal of Radiation Research and Applied Sciences*, 11(4), 361-367. doi:10.1016/j.jrras.2018.07.006
- Report 83. (2016). *Journal of the International Commission on Radiation Units and Measurements*, 10(1), NP-NP. doi:10.1093/jicru/10.1.Report83
- Riet, A. v. t., Mak, A. C. A., Moerland, M. A., Elders, L. H., & van der Zee, W. (1997). A conformation number to quantify the degree of conformality in brachytherapy and external beam irradiation: Application to the prostate. *International Journal of Radiation Oncology*Biophysics*, 37(3), 731-736. doi:[https://doi.org/10.1016/S0360-3016\(96\)00601-3](https://doi.org/10.1016/S0360-3016(96)00601-3)
- Rowbottom, C. G., Nutting, C. M., & Webb, S. (2001). Beam-orientation optimization of intensity-modulated radiotherapy: clinical application to parotid gland tumours. *Radiotherapy and Oncology*, 59(2), 169-177. doi:10.1016/S0167-8140(00)00321-2
- Rumboldt, Z., Castillo, M., & Smith, J. K. (2002). The palatovaginal canal: can it be identified on routine CT and MR imaging? *AJR. American journal of roentgenology*, 179(1), 267. doi:10.2214/ajr.179.1.1790267
- Rumboldt, Z., Gordon, L., Bonsall, R., & Ackermann, S. (2006). Imaging in head and neck cancer. *Curr. Treat. Options in Oncol.*, 7(1), 23-34. doi:10.1007/s11864-006-0029-2
- Rwigema, J.-C. M., Nguyen, D., Heron, D. E., Chen, A. M., Lee, P., Wang, P.-C., . . . Sheng, K. (2015). 4π Noncoplanar Stereotactic Body Radiation Therapy for Head-and-Neck Cancer: Potential to

- Improve Tumor Control and Late Toxicity. *International Journal of Radiation Oncology, Biology, Physics*, 91(2), 401-409. doi:10.1016/j.ijrobp.2014.09.043
- Sakata, K.-I., Hareyama, M., Tamakawa, M., Oouchi, A., Sido, M., Nagakura, H., . . . Asakura, K. (1999). Prognostic factors of nasopharynx tumors investigated by MR imaging and the value of MR imaging in the newly published TNM staging. *International Journal of Radiation Oncology, Biology, Physics*, 43(2), 273-278. doi:10.1016/S0360-3016(98)00417-9
- Schoenfeld, J. D., Sher, D. J., Norris, C. M., Jr., Haddad, R. I., Posner, M. R., Balboni, T. A., & Tishler, R. B. (2012). Salivary gland tumors treated with adjuvant intensity-modulated radiotherapy with or without concurrent chemotherapy. *Int J Radiat Oncol Biol Phys*, 82(1), 308-314. doi:10.1016/j.ijrobp.2010.09.042
- Seeram, E. (1994). *Computed tomography : physical principles, clinical applications & quality control*. Philadelphia [Pa.]: W.B. Saunders.
- Shield, K. D., Ferlay, J., Jemal, A., Sankaranarayanan, R., Chaturvedi, A. K., Bray, F., & Soerjomataram, I. (2017). The global incidence of lip, oral cavity, and pharyngeal cancers by subsite in 2012. *CA Cancer J Clin*, 67(1), 51-64. doi:10.3322/caac.21384
- Shukla, A., Kumar, S., Sandhu, I., Oinam, A., Singh, R., & Kapoor, R. (2016). Dosimetric study of beam angle optimization in intensity-modulated radiation therapy planning. *Journal of Cancer Research and Therapeutics*, 12(2), 1045-1049. doi:10.4103/0973-1482.157324
- Skora, T., Nowak-Sadzikowska, J., Mucha-Malecka, A., Szyszka-Charewicz, B., Jakubowicz, J., & Glinski, B. (2015). Postoperative irradiation in patients with pT3-4N0 laryngeal cancer: results and prognostic factors. *Eur Arch Otorhinolaryngol*, 272(3), 673-679. doi:10.1007/s00405-014-3333-7
- Smith, G. (2018). Step away from stepwise. *Journal of Big Data*, 5(1). doi:10.1186/s40537-018-0143-6
- Soyfer, V., Meir, Y., Corn, B. W., Schifter, D., Gez, E., Tempelhoff, H., & Shtraus, N. (2012). AP-PA field orientation followed by IMRT reduces lung exposure in comparison to conventional 3D conformal and sole IMRT in centrally located lung tumors. *Radiat Oncol*, 7, 23. doi:10.1186/1748-717X-7-23
- Spratt, D. E., Salgado, L. R., Riaz, N., Doran, M. G., Tam, M., Wolden, S., . . . Lee, N. Y. (2014). Results of photon radiotherapy for unresectable salivary gland tumors: is neutron radiotherapy's local control superior? *Radiol Oncol*, 48(1), 56-61. doi:10.2478/raon-2013-0046
- Srivastava, S. P., Das, I. J., Kumar, A., & Johnstone, P. A. S. (2011). Dosimetric Comparison of Manual and Beam Angle Optimization of Gantry Angles in IMRT. *Medical Dosimetry*, 36(3), 313-316. doi:10.1016/j.meddos.2010.07.001
- Stein, J., Mohan, R., Wang, X. H., Bortfeld, T., Wu, Q., Preiser, K., . . . Schlegel, W. (1997). Number and orientations of beams in intensity-modulated radiation treatments. *Medical Physics*, 24(2), 149-160. doi:10.1118/1.597923
- Studer, G., Zwahlen, R. A., Graetz, K. W., Davis, B. J., & Glanzmann, C. (2007). IMRT in oral cavity cancer. *Radiation oncology (London, England)*, 2, 16-16.
- Subramanian, V. S., Subramani, V., Chilukuri, S., Kathirvel, M., Arun, G., Swamy, S. T., . . . Cozzi, L. (2017). Multi-isocentric 4π volumetric-modulated arc therapy approach for head and neck cancer. *18(5)*, 293-300. doi:10.1002/acm2.12164
- Sze, H. C. K., Ng, A. W. Y., Yuen, K. T., Lai, J. W. Y., & Ng, W. T. (2019). International Consensus on Delineation of Target Volumes and Organs at Risk. In *Nasopharyngeal Carcinoma* (pp. 239-261).
- Tanaka, Y., Fujimoto, K. i., & Yoshinaga, T. (2015). Dose-volume constrained optimization in intensity-modulated radiation therapy treatment planning. *Journal of Inequalities and Applications*, 2015(1). doi:10.1186/s13660-015-0643-2
- Tao, C.-J., Lin, L., Zhou, G.-Q., Tang, L.-L., Chen, L., Mao, Y.-P., . . . Sun, Y. (2014). Comparison of Long-Term Survival and Toxicity of Cisplatin Delivered Weekly versus Every Three Weeks Concurrently with Intensity-Modulated Radiotherapy in Nasopharyngeal Carcinoma (Weekly vs. Three Weekly Cisplatin CCRT in NPC). 9(10), e110765. doi:10.1371/journal.pone.0110765

- Teo, P. M. L., Leung, S. F., Lee, W. Y., & Zee, B. (2000). Intracavitary brachytherapy significantly enhances local control of early T-stage nasopharyngeal carcinoma: the existence of a dose–tumor-control relationship above conventional tumoricidal dose. *International Journal of Radiation Oncology*Biophysics*, *46*(2), 445-458. doi:[https://doi.org/10.1016/S0360-3016\(99\)00326-0](https://doi.org/10.1016/S0360-3016(99)00326-0)
- Timme, D. W., Jonnalagadda, S., Patel, R., Rao, K., & Robbins, K. T. (2015). Treatment Selection for T3/T4a Laryngeal Cancer: Chemoradiation Versus Primary Surgery. *Ann Otol Rhinol Laryngol*, *124*(11), 845-851. doi:10.1177/0003489415588130
- Tran, A., Zhang, J., Woods, K., Yu, V., Nguyen, D., Gustafson, G., . . . Sheng, K. (2017). Treatment planning comparison of IMPT, VMAT and 4[pi] radiotherapy for prostate cases. *Radiation Oncology*, *12*(1). doi:10.1186/s13014-016-0761-0
- Tsai, C.-L., Wu, J.-K., Chao, H.-L., Tsai, Y.-C., & Cheng, J. C.-H. (2011). Treatment and Dosimetric Advantages Between VMAT, IMRT, and Helical TomoTherapy in Prostate Cancer. *Medical Dosimetry*, *36*(3), 264-271. doi:10.1016/j.meddos.2010.05.001
- Turgut, M., Ertürk, Ö., Saygi, S., & Özcan, O. (1998). Importance of cranial nerve involvement in nasopharyngeal carcinoma. A clinical study comprising 124 cases with special reference to clinical presentation and prognosis. *Neurosurg. Rev.*, *21*(4), 243-248. doi:10.1007/BF01105779
- Vanetti, E., Clivio, A., Nicolini, G., Fogliata, A., Ghosh-Laskar, S., Agarwal, J. P., . . . Cozzi, L. (2009). Volumetric modulated arc radiotherapy for carcinomas of the oro-pharynx, hypo-pharynx and larynx: a treatment planning comparison with fixed field IMRT. *Radiother Oncol*, *92*(1), 111-117. doi:10.1016/j.radonc.2008.12.008
- Vanetti, E., Nicolini, G., Nord, J., Peltola, J., Clivio, A., Fogliata, A., & Cozzi, L. (2011). On the role of the optimization algorithm of RapidArc(R) volumetric modulated arc therapy on plan quality and efficiency. *Med Phys*, *38*(11), 5844-5856. doi:10.1118/1.3641866
- Verbakel, W. F. A. R., Cuijpers, J. P., Hoffmans, D., Bieker, M., Slotman, B. J., & Senan, S. (2009). Volumetric Intensity-Modulated Arc Therapy Vs. Conventional IMRT in Head-and-Neck Cancer: A Comparative Planning and Dosimetric Study. *International Journal of Radiation Oncology, Biology, Physics*, *74*(1), 252-259. doi:10.1016/j.ijrobp.2008.12.033
- Vlachaki, M. T., Teslow, T. N., Amosson, C., Uy, N. W., & Ahmad, S. (2005). IMRT versus conventional 3DCRT on prostate and normal tissue dosimetry using an endorectal balloon for prostate immobilization. *Medical Dosimetry*, *30*(2), 69-75. doi:10.1016/j.meddos.2005.01.002
- Wang, K. H., Austin, S. A., Chen, S. H., Sonne, D. C., & Gurushanthaiah, D. (2017). Nasopharyngeal Carcinoma Diagnostic Challenge in a Nonendemic Setting: Our Experience with 101 Patients. *Perm J*, *21*, 16-180. doi:10.7812/TPP/16-180
- Wang, X., Zhang, X., Dong, L., Liu, H., Gillin, M., Ahamad, A., . . . Mohan, R. (2005). Effectiveness of noncoplanar IMRT planning using a parallelized multiresolution beam angle optimization method for paranasal sinus carcinoma. *Int J Radiat Oncol Biol Phys*, *63*(2), 594-601. doi:10.1016/j.ijrobp.2005.06.006
- Webb, S. (1994). Optimizing the planning of intensity-modulated radiotherapy. *Physics in Medicine and Biology*, *39*(12), 2229-2246. doi:10.1088/0031-9155/39/12/007
- Westbrook, C. (2019). *MRI in practice* (Fifth edition.. ed.). Hoboken, NJ: Wiley Blackwell.
- Wild, E., Bangert, M., Nill, S., & Oelfke, U. (2015). Noncoplanar VMAT for nasopharyngeal tumors: Plan quality versus treatment time. *Medical Physics*, *42*(5), 2157-2168. doi:10.1118/1.4914863
- Won, H. S., Chun, S. H., Kim, B. S., Chung, S. R., Yoo Ie, R., Jung, C. K., . . . Kang, J. H. (2009). Treatment outcome of maxillary sinus cancer. *Rare Tumors*, *1*(2), e36. doi:10.4081/rt.2009.e36
- Wu, B., Ricchetti, F., Sanguineti, G., Kazhdan, M., Simari, P., Chuang, M., . . . McNutt, T. (2009). Patient geometry-driven information retrieval for IMRT treatment plan quality control. *Med Phys*, *36*(12), 5497-5505. doi:10.1118/1.3253464
- Wu, Q., Manning, M., Schmidt-Ullrich, R., & Mohan, R. (2000). The potential for sparing of parotids and escalation of biologically effective dose with intensity-modulated radiation treatments of head and

- neck cancers: a treatment design study. *International Journal of Radiation Oncology, Biology, Physics*, 46(1), 195-205. doi:10.1016/S0360-3016(99)00304-1
- Xu, G. Z., Guan, D. J., & He, Z. Y. (2011). (18)FDG-PET/CT for detecting distant metastases and second primary cancers in patients with head and neck cancer. A meta-analysis. *Oral Oncol*, 47(7), 560-565. doi:10.1016/j.oraloncology.2011.04.021
- Yang, K., Yan, D., & Tyagi, N. (2012). Sensitivity analysis of physics and planning SmartArc parameters for single and partial arc VMAT planning. *13(6)*, 34-45. doi:10.1120/jacmp.v13i6.3760
- Yirmibesoglu, E., Kostich, M., Fried, D., Rosenman, J., Shockley, W., Weissler, M., . . . Chera, B. (2011). Dosimetric Evaluation of an Ipsilateral Intensity Modulated Radiotherapy Beam Arrangement for Parotid Malignancies. *International Journal of Radiation Oncology, Biology, Physics*, 81(2), S527-S528. doi:10.1016/j.ijrobp.2011.06.816
- Yu, V. Y., Tran, A., Nguyen, D., Cao, M., Ruan, D., Low, D. A., & Sheng, K. (2015). The development and verification of a highly accurate collision prediction model for automated noncoplanar plan delivery. *Medical Physics*, 42(11), 6457-6467. doi:10.1118/1.4932631
- Yuan, L., Ge, Y., Lee, W. R., Yin, F. F., Kirkpatrick, J. P., & Wu, Q. J. (2012). Quantitative analysis of the factors which affect the interpatient organ-at-risk dose sparing variation in IMRT plans. *Med Phys*, 39(11), 6868-6878. doi:10.1118/1.4757927
- Zhang, B., Mo, Z., Du, W., Wang, Y., Liu, L., & Wei, Y. (2015). Intensity-modulated radiation therapy versus 2D-RT or 3D-CRT for the treatment of nasopharyngeal carcinoma: A systematic review and meta-analysis. *Oral Oncol*, 51(11), 1041-1046. doi:10.1016/j.oraloncology.2015.08.005
- Zhang, L.-L., Huang, M.-Y., Li, Y., Liang, J.-H., Gao, T.-S., Deng, B., . . . Sun, Y. (2019). Pretreatment MRI radiomics analysis allows for reliable prediction of local recurrence in non-metastatic T4 nasopharyngeal carcinoma. *EBioMedicine*, 42, 270-280. doi:<https://doi.org/10.1016/j.ebiom.2019.03.050>
- Zhang, L., Zhou, H., Gu, D., Tian, J., Zhang, B., Dong, D., . . . Zhang, S. (2019). Radiomic Nomogram: Pretreatment Evaluation of Local Recurrence in Nasopharyngeal Carcinoma based on MR Imaging. *Journal of Cancer*, 10(18), 4217-4225. doi:10.7150/jca.33345
- Zhao, W., Lei, H., Zhu, X., Li, L., Qu, S., & Liang, X. (2016). Investigation of long-term survival outcomes and failure patterns of patients with nasopharyngeal carcinoma receiving intensity-modulated radiotherapy: a retrospective analysis. *Oncotarget*, 7(52), 86914-86925. doi:10.18632/oncotarget.13564

APPENDICES

1. Ethics approval from the Hong Kong Polytechnic University



THE HONG KONG
POLYTECHNIC UNIVERSITY
香港理工大學

To	WU Wing Cheung Vincent (Department of Health Technology and Informatics)		
From	LEUNG Hang Mei Polly, Chair, Departmental Research Committee		
Email	htpolly@	Date	11-May-2012

Application for Ethical Review for Teaching/Research Involving Human Subjects

I write to inform you that approval has been given to your application for human subjects ethics review of the following project for a period from 14-May-2012 to 13-May-2015:

Project Title: A study to evaluate the effect of beam arrangements in intensity modulated radiation therapy of head and neck cancers.

Department: Department of Health Technology and Informatics

Principal Investigator: WU Wing Cheung Vincent

Please note that you will be held responsible for the ethical approval granted for the project and the ethical conduct of the personnel involved in the project. In the case of the Co-PI, if any, has also obtained ethical approval for the project, the Co-PI will also assume the responsibility in respect of the ethical approval (in relation to the areas of expertise of respective Co-PI in accordance with the stipulations given by the approving authority).

You are responsible for informing the Departmental Research Committee in advance of any changes in the proposal or procedures which may affect the validity of this ethical approval.

You will receive separate email notification should you be required to obtain fresh approval.

LEUNG Hang Mei Polly

Chair

Departmental Research Committee

2. Ethics approval from Princess Margaret Hospital, Kowloon West Cluster



醫院管理局
HOSPITAL
AUTHORITY

Mr LEUNG Wan Shun,
Radiation Therapist II,
Department of Oncology,
Princess Margaret Hospital

29 October, 2012

Dear Mr LEUNG,

KWC-REC Reference: KW/EX-12-091 (55-13)

Title: A study to evaluate the effect of beam arrangements in intensity modulated radiation therapy of head and neck cancers.

The Kowloon West Cluster Research Ethics Committee (KWC-REC) is authorized by the Cluster Chief Executive to review and monitor clinical research. It serves to ensure that research complies with the Declaration of Helsinki, ICH GCP Guidelines, local regulations and HA policy. It has the authority to approve, require modifications in (to secure approval), or disapprove research. This Committee has power to terminate / suspend a research at any time if there is evidence to indicate that the above principles and requirements have been violated.

KWC-REC has approved your research application on 25 October, 2012 by expedited review process, and reached the following decision on the documents submitted as shown below. You are required to adhere to the attached conditions.

Study site(s)	Princess Margaret Hospital
Document(s) approved	I. Clinical Research Ethics Review Application Form (revised on 20 September 2012) II. One-Page Summary Form (received 20 July 2012) III. Research Degree Proposal, Version 1, 10.7.2012
Document(s) reviewed	I. Academia issued by The Hong Kong Polytechnic University dated 2 May 2012 II. CV of Principal Investigator, Version 1, 10.7.2012
Conditions	1. Do not deviate from, or make changes to the study protocol without prior written REC approval, except when it is necessary to eliminate immediate hazards to research subjects or when the change involves only logistical or administrative issues. 2. Apply a clinical trial certificate from Department of Health if indicated. 3. Report the followings to KWC-REC* : (i) study protocol or consent document changes, (ii) serious adverse event, (iii) study progress (iv) new information that may be relevant to a subject's willingness to continue participation in the study. 4. Report first study progress to KWC-REC at <u>12-monthly intervals</u> until study closure. [*Forms are available from KWC-REC intranet webpage]

Please quote the REC Reference KW/EX-12-091 (55-13) in all your future correspondence with the KWC-REC, including submission of progress reports and requesting for amendments to the research protocol.

If you have any inquiry, please feel free to contact Ms Catherine CHENG, Secretary of the KWC-REC, at 2990 Thank you for your attention.

Yours sincerely,

Secretary of
Research Ethics Committee,
Kowloon West Cluster

Room 838, 6/F, Block J,
Princess Margaret Hospital,
Lai Chi Kok, Kowloon,
Hong Kong
Tel: (852) 2990 3749
Fax: (852) 2990 3486

Princess Margaret Hospital
7-10 Princess Margaret
Hospital Road, NT
Tel: (852) 2990 1111
Fax: (852) 2766 3929

傳真查詢
新界東醫院管理局2-105號
電話: (852) 2990 1111
傳真: (852) 2796 3629

c.c. COS(Oncology), PMH

(Dr Patrick WONG)
Deputizing Chairperson
Research Ethics Committee
Kowloon West Cluster



HA(G)1 (Rev.03/2012)

Ms LIU Yuen Wai,
Senior Radiation Therapist,
Department of Oncology,
Princess Margaret Hospital

25 February 2019

Dear Ms LIU,

KWC-REC Reference: KW/EX-19-019(131-07)

Title: A study to evaluate the effect of beam arrangements in intensity modulated radiation therapy of head and neck cancers.

The Kowloon West Cluster Research Ethics Committee (KWC-REC) is authorized by the Cluster Chief Executive to review and monitor clinical research. It serves to ensure that research complies with the Declaration of Helsinki, ICH GCP Guidelines, local regulations and HA policy. It has the authority to approve, require modifications in (to secure approval), or disapprove research. This Committee has power to terminate / suspend a research at any time if there is evidence to indicate that the above principles and requirements have been violated.

KWC-REC has approved your research application on 25 February 2019 by an expedited review process, and reached the following decision on the documents submitted as shown below. You are required to adhere to the attached conditions.

Study site(s)	Princess Margaret Hospital
Document(s) approved	I. Clinical Research Ethics Review Application Form (revised on 03 January 2019) II. Protocol Version 02 dated 02 January 2019
Document(s) reviewed	I. CV of all Investigators II. Academia issued by The Hong Kong Polytechnic University dated 23 December 2013 for Co-investigator: Mr LEUNG Wan Shun
Conditions	<ol style="list-style-type: none"> 1. Observe and comply with all applicable requirements under our Standard Operating Procedures (SOP), the Declaration of Helsinki and the ICH-GCP (if applicable). 2. Do not implement any amendment/change to any approved study document/material without our written approval, except where necessary to eliminate any immediate hazard to the subjects or if an amendment/change is only of an administrative or logistical nature. 3. Submit safety reports to the KWC-REC on all Serious Adverse Events (SAEs) observed from any subject recruited at your study site or Suspected Unexpected Serious Adverse Reactions (SUSARs) reported from outside your study site in accordance with the requirements set out in Appendix 8 of our SOP by using the REC's specified form. 4. Report the followings to KWC-REC* : (i) changes in study protocol, consent document or source of funding, (ii) protocol deviation or breach of privacy, (iii) new information that may be relevant to a subject's willingness to continue participation in the study. 5. Submit first Research Progress Report Form to KWC-REC by 25 February 2020 and at yearly intervals until study closure#. 6. Submit Research Final Report Form to KWC-REC by 31 March 2021#. 7. Apply a clinical trial certificate from Department of Health if applicable. 8. Report any adverse events to hospital management through Advanced Incidents Reporting System (AIRS) in a timely manner if applicable and state the AIRS number on the SAE form to KWC-REC. <p>[*Forms are available from KWC-REC intranet webpage.] [#Failure to comply with point 5 and 6 may result in non-acceptance of any future research application as Principal Investigator or Co-investigator.]</p>

Secretary of Research Ethics Committee,
Kowloon West Cluster
Room 530, 5/F, Block J,
Princess Margaret Hospital
Tel: (852) 29901017 / 26301047
Fax: (852) 26903436

Princess Margaret Hospital
2-10 Princess Margaret
Hospital Road, NT
Tel: (852) 2990 1111
Fax: (852) 2786 3629

瑪嘉烈醫院
新界葵涌醫院道2-10號
電話：(852) 2990 1111
傳真：(852) 2786 3629



醫院管理局
HOSPITAL
AUTHORITY

Please quote the REC Reference **KW/EX-19-019(131-07)** in all your future correspondence with the KWC-REC, including submission of progress reports and requesting for amendments to the research protocol.

Yours sincerely,

(Dr Ashley CHENG)
Chairperson
Research Ethics Committee
Kowloon West Cluster

c.c. COS(ONC), KWC

Secretary of
Research Ethics Committee,
Kowloon West Cluster
Room 553, 5/F, Block J,
Princess Margaret Hospital
Tel: (852) 29901017 / 29901047
Fax: (852) 29903438

Princess Margaret Hospital
2-10 Princess Margaret
Hospital Road, KT
Tel: (852) 2990 1111
Fax: (852) 2786 3629

新加坡醫院
新加坡醫院2-10號
電話：(852) 2990 1111
傳真：(852) 2786 3629

Page 2 of 2

HA(G)1 (Rev.03/2012)

144

